Precambrian Research 414 (2024) 107589

Contents lists available at ScienceDirect

Precambrian Research

journal homepage: www.elsevier.com/locate/precamres

50th Anniversary Invited Review

Precambrian Earth: Co-evolution of life and geodynamics

Frances Westall [a,*], Shuhai Xiao [b]

[a] CNRS-Centre de Biophysique Moléculaire, Rue Charles Sadron, CS 85001, 45,701 Orléans, France
[b] Department of Geosciences, 4044 Derring Hall, Virginia Tech, 926 West Campus Drive, Blacksburg, VA 24061, USA

ARTICLE INFO

Keywords:
Early Earth geology
Early evolution of life
Microbialites
Eukaryotes
Geodynamics

ABSTRACT

The Precambrian covers 80% of the history the Earth. In this timespan, the Earth developed from an anaerobic planet to the oxygenic planet dominated by Wilson-style plate tectonics that we know today. Concomitant with geological evolution, life emerged and evolved, gradually colonising all known aqueous habitats. Until the Palaeoarchaean, life was largely dominated by its geological environment. However, as of the Mesoarchaean, when there were major changes in geodynamics leading to continental erosion and runoff of essential nutrients, the effects of life started to impinge on the geological environment. The interaction of life and Earth was and is reciprocal, hence the term biogeodynamics. In this review, we trace the evolution of geology and life in parallel, thus highlighting the gradual buildup of the importance of life on terrestrial processes, and the importance of changes in the geological environment on the evolution of life. We do not attempt to make an exhaustive review of all the occurrences of life in the Precambrian but use selected examples to illustrate key events and changes. We conclude by addressing certain aspects of the evolution of life that require more in-depth study and show how the finding of extra-terrestrial life would advance our understanding of life on Earth.

1. Introduction

The Precambrian comprises more than 80 % of Earth's history. It witnessed many important milestones in the evolution of life on Earth that included: (1) the emergence of life probably in the Hadean (4.56–4.0 Ga); (2) the appearance of anaerobic prokaryotes including chemotrophs and photosynthesisers in the Eo-Palaeoarchaean (4.0–3.2 Ga); (3) the evolution of oxygenic photosynthesisers possibly already in the Meso-Neoarchaean (3.2–2.4 Ga); (4) eukaryotes and multicellular organisms in the Palaeo-Mesoproterozoic (2.4–1.0 Ga, and possibly before); (5) and, at its terminal stage, during the Neoproterozoic Era (1.0–0.539 Ga), the initial evolution of skeletal organisms and rapid diversification of eukaryotes, including animals toward the end of this era.

All of these events were accompanied by changes and evolution in geological and environmental processes, from the geosphere through the hydrosphere to the atmosphere (e.g., Fig. 1), the whole influenced by conditions in the Solar System, such as solar insolation, UV radiation, and meteorite/asteroid influx. The geosphere saw the consolidation of the planet Earth from primordial materials at about 4.56 Ga, collision with a Mars-sized planet (named Theia by Halliday, 2000) that led to the formation of the Moon, condensation of water on the rapidly re-cooled surface to form oceans, the emergence of protocontinents, and transition in geodynamic regime from plume tectonics to horizontal tectonics. The Palaeoproterozoic is typically defined as the period when modern-style plate tectonics was initiated (e.g., François et al., 2018). Note, however, that it has been suggested that Wilson-style tectonics only appeared in the Neoproterozoic (Hawkesworth et al., 2020) and, critically, was associated with major changes in the environment, such as global glaciation, and an increase in atmospheric oxygen levels (Grosch and Hazen, 2015; Lyons et al., 2014, 2021).

These large-scale geological changes were accompanied by major hydrospheric and atmospheric evolutionary events. The Hadean-Archaean oceans may have been slightly more acidic than today (Knauth, 2005) but were globally anoxic (Catling and Zahnle, 2020), with low levels of sulphate (an important electron acceptor in microbial respiration) and phosphate (an essential element for life). The Hadean to Mesoarchaean atmosphere comprised CO_2 and N_2 probably with CH_4 as a major greenhouse gas (Catling and Zahnle, 2020). Molecular oxygen started to accumulate in the atmosphere well after the emergence of oxygenic phototrophs in the Mesoarchaean (Sánchez-Baracaldo et al., 2014; Planavsky et al., 2014) or even earlier (Buick, 2008; Robbins et al., 2023), culminating in the Great Oxidation Event at ca. 2.4 Ga (Lyons et al., 2014, 2021). Nevertheless, for much of the Palaeo-

* Corresponding author.
E-mail address: frances.westall@cnrs.fr (F. Westall).

https://doi.org/10.1016/j.precamres.2024.107589
Received 12 July 2024; Received in revised form 14 October 2024; Accepted 15 October 2024

Mesoproterozoic, only the surface seawater was oxygenated, although there is evidence of local, transient oxygenation of the deep oceans of the Mesoproterozoic (e.g., Stüeken et al., 2021). Oxygenation of the deep ocean through enhanced organic carbon burial and deep-water overturn may have driven the Neoproterozoic Oxygenation Event (NEO) and Cryogenian glaciations (Banerjee et al., 2022).

Within the framework of these large-scale events, life emerged locally and then colonised available biomes according to its existential needs and preferences. Early non-phototrophic microorganisms took advantage of the volcanic and hydrothermal habitats available, shunning exposure to harmful UV radiation. With the advent of phototrophy, early anoxygenic phototrophs with their UV-protecting pigments could invade shallow water, sunlit environments, either in coastal regions or in the planktonic realm and, as some believe, eventually moving up rivers. As they emerged, oxygenic phototrophs resulted in the consequent slow but relentless oxygenation of the geosphere, hydrosphere and atmosphere. The availability of molecular oxygen primed the surface environment for the rise of eukaryotes and multicellular organisms. Thus, by the end of the Proterozoic, all possible habitats, including exposed landmasses, were inhabited.

However, it was not only geological processes that contributed to the well-being of Precambrian life. The very fact that life played a major role in the production of carbonate (for example, the huge stromatolitic platforms that characterised the Precambrian oceans from the Neoarchaean and, particularly, during the Proterozoic) and in the production of organic carbon, both of which were partially removed to the mantle through subduction, helped to regulate CO_2 and O_2 in the atmosphere and had a mitigating effect on the climate and the surface environment of the Earth (Catling and Zahnle, 2020). These feedbacks helped to maintain liquid water at Earth's surface and lubricated tectonic recycling – which contributed to recycling of essential bionutrients back to the surface of the Earth.

In view of these interconnected events and processes, in this review of Precambrian life, we aim to place key events in the evolution of life and their associated biosignatures within the framework of the geological evolution of the Earth. This is not an exhaustive review of early geological and biological processes, nor do we aim to provide a complete list of all the fossil occurrences that are described in the literature. Rather, our objective is to highlight a few key examples that best illustrate a particular evolutionary phenomenon on a global scale. Our ultimate aim is to emphasise the reciprocal influence and interaction between the geological environment and evolution of life. Moreover, since the main geological phases and steps in the evolution of life fall along the general divisions of geological time, we subdivide our discussion into the following time intervals: Hadean (4.56–4.0 Ga), Eo-Palaeoarchaean (4.0–3.2 Ga), Mesoarchaean (3.2–2.8 Ga) to Neoarchaean (2.8–2.4 Ga), and Proterozoic (Palaeo- (2.4–1.6 Ga), Meso- (1.6–1.0 Ga) and Neoproterozoic (1.0 – 0.541 Ga)).

However, considering that we are dealing with the fossilised remains of life, we first provide information on how microorganisms are preserved in the rock record and on the principles of biogenicity and syngenicity.

2. Taphonomy and the principles of biogenicity and syngenicity

The Precambrian is unique in that most organisms that lived in this era are characterised by a lack of hard parts. This complicates their potential for preservation and interpretation of morphological and

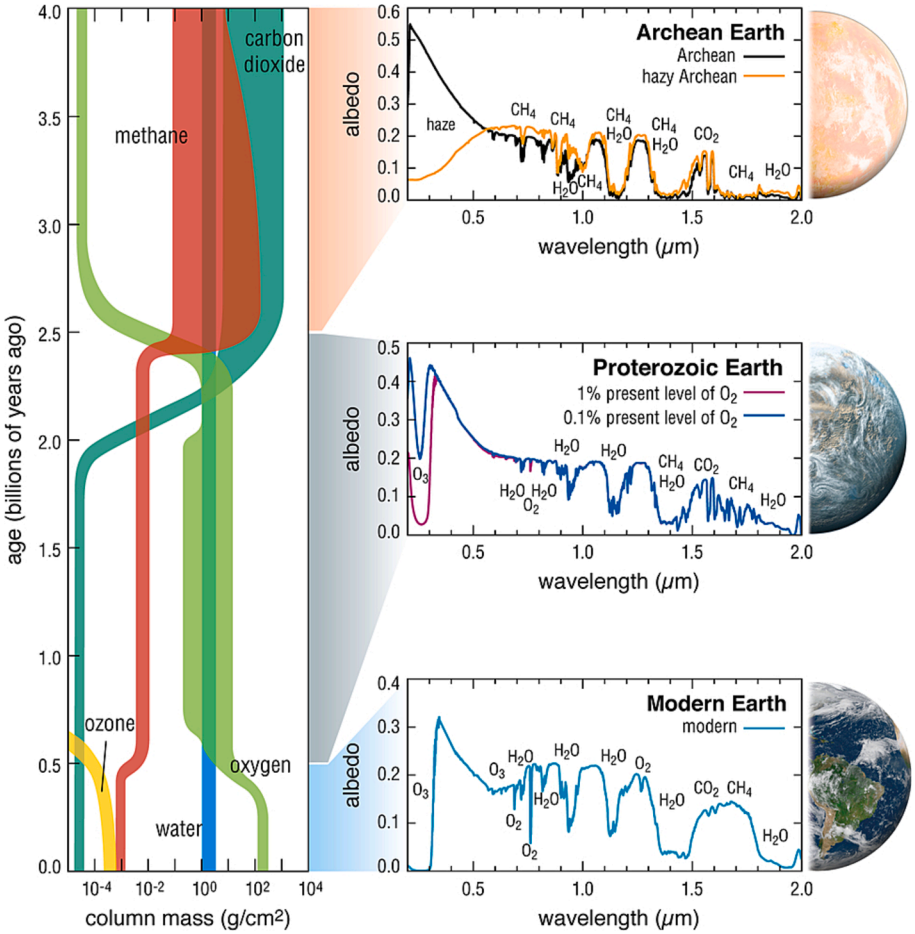

Fig. 1. Evolution of Earth's atmosphere through time (Roberge et al., 2019).

chemical remains that are frequently enigmatic. Efremov (1940) was the first to use the term taphonomy to describe the study of the transition of remains, parts, or products of organisms from the biosphere to the lithosphere. Understanding of the process of degradation of organism soft parts with time is aided by laboratory experiments (e.g., Butterfield, 1990; Briggs, 1995). Behrensmeyer et al. (2000) summarise the factors affecting the preservation of soft, organic remains. While many organisms are not preserved as physical structures in the rock record, unless they are rapidly mineralised (see Westall and Cavalazzi, 2001; Westall and Hickman-Lewis, 2018), their degraded organic remains may be preserved, as well as some evidence of their metabolic processes (for example, isotopic signatures of C, N, S, Fe, trace element concentrations, or microbially mediated precipitates, such as carbonates or oxides). The controls on the preservation of biological remains are wide ranging, including the initial amount of biological remains in a given environment; the physical parameters of that environment, *i.e.,* modification by local physical, chemical and biological agents; the rate and permanency of burial; diagenetic conditions and post burial modification. Finally, the preservation of the larger sedimentary body comes into play, related to tectonic processes, burial and metamorphism.

Experimental fossilisation of microorganisms has demonstrated different parameters that affect variability in their preservation. For example, Orange et al. (2009) showed that two, *a priori* similar microorganisms, the thermophilic Archaea *Pyrococcus abyssi* and *Methanocaldococcus jannaschii*, reacted very differently to the same fossilising solution (silica). The former resulted in a silica crust templated onto the surfaces of the cells, while the latter disintegrated (lysed) and only the associated polymer (extracellular polymeric substances or EPS) was mineralised. In the right conditions, the cells of *P. abyssi* would be fossilised but not those of *M. janaschii*, although the EPS of the latter could be recorded in the rock record. In a similar manner, Westall et al. (1995) demonstrated in a mixture of marine microorganisms that some microorganisms were susceptible to rapid encasement and fossilisation whereas others resisted chelation of the fossilising medium (silica) to their cells for many months. Furthermore, the effects of time on the degradation of specific organic components has been evaluated experimentally. Orange et al. (2013) investigated changes with time (1 year) in the composition and quantity of amino acids, monosaccharides and fatty acids of the hyperthermophilic Archaea *M. jannaschii*, documenting that amino acids and fatty acids were the best-preserved compounds. Significantly, this study demonstrated the importance of very rapid (within 24 h) polymerisation of silica on EPS dissolved in the medium, leading to the precipitation of silica and EPS. Orange et al. (2009) had previously noted the lack of cellular preservation of *M. jannaschii* but the significant preservation of its EPS. Obviously, fossilisation of biological remains, whether physical or organic (*i.e.,* as diffuse molecules) by minerals or fine-grained anoxic sediments, is an important step in the early and long-term preservation of microbial remains.

While identification of the remains of complex life forms is generally non-controversial, identification of the oldest traces of very simple life requires a considered, stepwise approach that takes into account the environment in which the purported biosignature formed and various other aspects of the lifeform, including its morphology, organic composition, metabolic processes, associations, and interactions with its immediate environment. There are many proposals of biogenicity criteria (see for example, Westall and Cavalazzi, 2011; Summons et al., 2011; Neveu et al., 2018) but all are predicated on the basic principles noted above. Ideally, evidence of all the basic criteria would be needed to establish the biogenicity of a particular feature, but this is not always possible. For example, in certain circumstances, the organic components of a microbial community may be completely oxidised, either because the environment is oxidising or, in an anoxic environment, because the organic matter of the primary producers is subsequently used as a substrate by chemoorganotrophic microorganisms that oxidise it to produce energy. For example, Dodd et al. (2017) suggest that remnant carbonaceous matter associated with carbonate and apatite globules in the Nuvvuagittuq jasperlites represents the degraded remains of the organic components of the Fe-oxidisers that are purported to have formed the hematite tubes and filaments. In other situations, only the carbonaceous remains of former microbial colonies may be preserved in fine-grained, anoxic sediments, while morphological microbial features, such as cells or colonies, are not.

Evidence for biogenicity according to Neveu et al. (2018) includes evidence of Darwinian evolution, growth and reproduction, molecules and structures conferring function, potential biomolecule components and biofabrics. All of these features should occur in an environmental context conducive to habitability. However, the above-listed attributes are more related to living organisms than their fossilised remains. In the rock record they would translate into morphology, isotopic fractionations, mineralogical evidence (*i.e.*, biomediated precipitates), large enantiomeric excess (chiral excess), and complex organics and patterns in the organic molecular signatures. Of importance in determining biogenicity is the necessity of demonstrating that more than one criterion has been satisfied, and preferably a number of criteria. For example, although carbon isotopic fractionations may be indicative of microbial activity, the wide, overlapping ranges of abiotic carbon isotopic signatures in meteoritic material, for instance, mean that further biogenicity criteria are required (Summons et al., 2011). However, a number of the above described criteria for biogenicity may, in fact, individually have an abiotic origin. Indeed, it is now recognised that the frontier between geomicrobiology and mineralogy is not clear-cut (Templeton and Benzerara, 2015; McMahon, 2019; McMahon et al., 2021). Thus, even with supposed evidence of all biogenicity criteria, interpretations may still be erroneous.

Importantly, interpretations of data related to biogenicity, especially of the microbial world, are inherently dependent on our own understanding of the natural world, which has vastly improved over the last couple of decades. While comparisons with modern microbes and the modern microbial world are often very enlightening, they may also lead to misunderstandings because the anoxic early Earth was not like oxygenated modern Earth. Biogenicity, especially related to early traces of life on Earth or on extra-terrestrial objects, should be considered in terms of likelihood, rather than certainty.

Equally important, with respect to ancient traces of life, is determining the syngenicity of a purported biosignature. Was the feature formed at the same time as its host rock or was it introduced at a later stage? This is demonstrated, for example, by the presence of the fossilised remains of endolithic cyanobacteria occurring in a banded iron formation (BIF) from the 3.75–3.8 Ga Isua Greenstone Belt in Greenland (Westall and Folk, 2003). In this case, in the summer period when ice and snow melted, thermal disequilibria between the magnetite-rich layers and the translucent quartz rich layers of the BIF created fractures in which endolithic microorganisms could take refuge. Since the originally ice-covered area only became exposed about 8000 years ago, the cyanobacterial endoliths are much younger than the host rock. Another example is provided by what was originally described as the oldest known biomarker molecules (*i.e.*, degraded molecules that have distinctive structures and compositions that can be traced back to specific molecules of biological origin, especially for example those associated with the lipid membranes of certain prokaryotes, Summons and Lincoln, 2012) that supposedly documented the early rise of oxygenic phototrophs and eukaryotes in 2.7 Ga rocks from the Pilbara (Brocks et al., 1999). Subsequent studies demonstrated that the biomarker molecules represented later contamination (French et al., 2015).

3. Hadean (4.56–4.0 Ga)

3.1. Geological environment

The Hadean Earth is characterised by a lack of preserved rocks but inherited geochemical signals in Hadean-age zircon crystals and in younger rocks (c.f. Kamber, 2015). Nevertheless, it was during this eon

that life probably first emerged (Sleep, 2010; Westall et al., 2023a). After the consolidation of the Earth at 4.56 Ga (Halla et al., 2024) and its re-consolidation after the Moon-forming impact, estimated to have occurred between 4.36 Ga (Borg and Carlson, 2023) and 4.44–4.50 (Jacobson et al., 2014), there was still a significant flux of extra-terrestrial materials (late veneer) to the Earth (Marchi et al., 2021). The ca. 30 % less luminous Sun (Fig. 2) (Sagan and Mullen, 1972; Bahcall et al., 2001) emitted more high energy radiation (Tehrany et al., 2002), with high UV fluxes to the surface of the Earth (especially the more detrimental UVB and UVC, reaching DNA-weighted values of 10 W/m^2 (and up to 1000 W/m^2 in a worst case scenario), compared to 1 W/m^2 today (Cockell, 2000; Ranjan and Sasselov, 2017)) because of extremely low levels of oxygen and ozone in the early atmosphere. The initial, post Moon-forming impact atmosphere comprised hydrogen, helium, water vapour, methane, and ammonia but a secondary atmosphere rich in carbon dioxide, molecular nitrogen, water vapour was rapidly outgassed (Sleep et al., 2014). Atmospheric water could start condensing at an approximate 100 bars of CO_2 atmosphere, but only when it decreased to about 25 bars and surface temperatures reached ca. 122 °C could significant, life-producing, prebiotic chemistry initiate (Sleep et al., 2014; Zahnle et al., 2015).

The importance of CO_2 in the early atmosphere likely led to a slightly acidic global ocean (Sleep, 2010), although local variations would have occurred at the rock/water interface owing to aqueous alteration of ultramafic rocks, as well as being related to exhalation of alkaline to acidic hydrothermal effluent. The generally anoxic environment meant that there was little dissolved sulphate or nitrate, two limiting nutrients that became more available as the seawaters became oxidised during the Proterozoic. It is possible that oxygen was produced in very small quantities at a local scale by abiotic processes, including radiolysis of seawater by EUV, photo dissociation of water vapour in the atmosphere (Kasting et al. 1979), or by dissociation of pressurised water vapour exiting shallow hydrothermal vents (Westall et al., 2023b).

On the other hand, the early seawater was enriched in transition metals, such as soluble Fe^{2+}, Ni^{2+}, Co^{2+} and Mn^{2+} that were important for various microbial metabolisms (Rickaby et al., 2015; Hickman-Lewis et al., 2020a). Early salinities have been estimated as either being similar to those of the present-day Earth (Marty et al., 2018) or higher (Knauth 2005; Catling and Zahnle 2020). The early Earth was volcanically and hydrothermally active, with hydrothermal fluids having a significant influence on the early seawater composition (Hofmann and Harris, 2008; Westall et al., 2018, 2023a). The latter authors inferred relatively high water-temperatures immediately adjacent to the volcanic crust and the thin layers of volcanic sediments owing to higher heat flow from the early mantle (Arndt and Nisbet, 2012; Ruiz 2017; Korenaga 2018). Other proxies of early water temperatures (oxygen, silicon, and hydrogen isotopic signatures) provide estimates that range from a lower value of 26 °C (Hren et al., 2006; Blake et al. 2010) up to between 50 and 70 °C (Robert and Chaussidon 2006; Van den Boorn et al. 2010; Marin-Carbonne et al. 2012; Tartèse et al. 2017). While it is likely that rock/water temperatures in the ocean (deep or shallow) were above freezing and possibly relatively high, it has been questioned whether the surface of the Earth could have been frozen because of the lower solar luminosity (Cartier, 2022). High CO_2 partial pressures and the presence of greenhouse gases may have precluded global glaciation. High oxygen isotope values, quartz and aluminosilicate inclusions, as well as other geochemical proxies, indicate that some of Hadean zircons formed in crust that had been altered by water (Harrison, 2009).

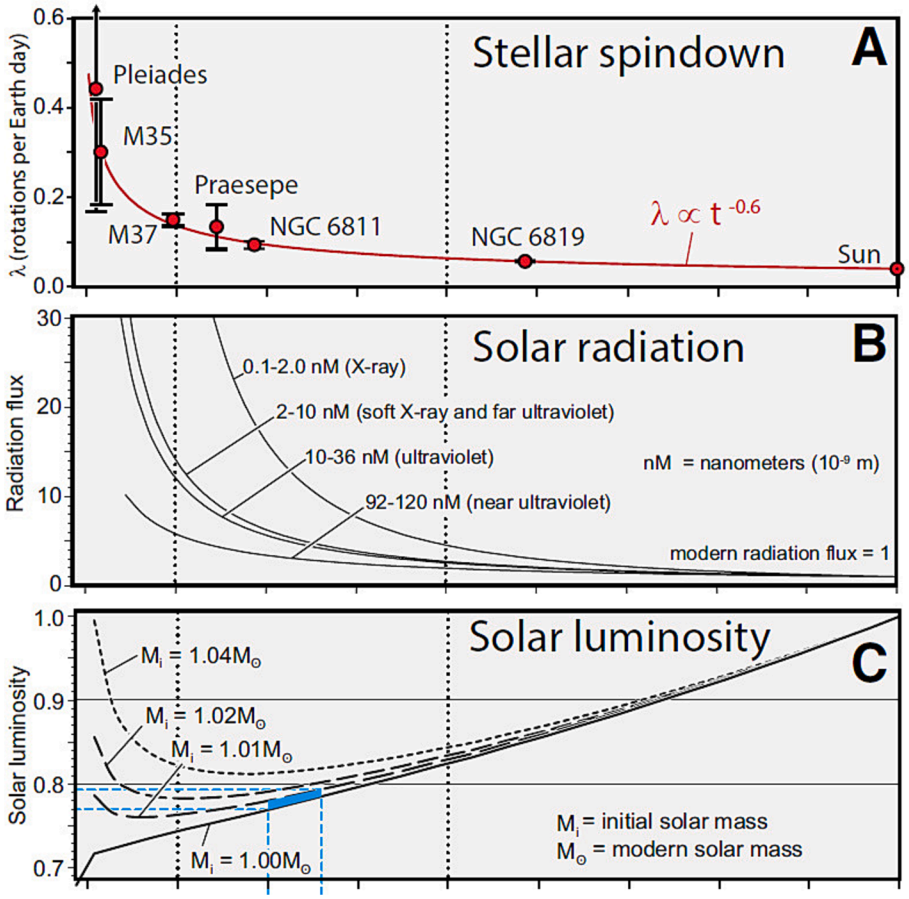

Fig. 2. Changes in solar parameters through geological time. (A) Stellar spindown, (B) Solar radiation, and (C) solar luminosity. (D) Significant events in Earth's history that reflect climate and atmospheric composition (see Spencer, 2019 for details).

A critical question with potentially significant bearing on some emergence of life scenarios during the Hadean is whether there was emergent land. This question is related to the style of tectonic regime, vertical (plume tectonics) and/or horizontal tectonics, with some suggesting an early initiation of horizontal tectonics during the Hadean (see recent reviews by Korenaga, 2021 and references therein), while others consider its emergence during the Palaeo-Mesoarchaean (see reviews by Hawkesworth et al., 2020; Roberts et al., 2024 and references in both). In the model proposed by Hawkesworth et al (2020), the Hadean would have been characterised by stagnant lid and mantle drip tectonics. A recent review concludes that Hadean/Palaeoarchaean plate tectonics was shallower than today owing to the thicker, hotter, more buoyant crust, and that plates were smaller (Roberts et al., 2024).

Continental crust is formed by differentiation of initially basaltic crust to produce a stratified ensemble comprising underlying cumulates, mid crustal intrusions, and an upper crust of volcanic rocks and intrusions (Roberts et al., 2024). It is during the collision of oceanic arcs and continental (primitive or not) blocks that fractionated, more felsic magma is produced. The early granites were of the type tonalite-trondjehmite granitoids (TTGs) that were formed predominantly through intracrustal melting. This crustal fractionation in the Hadean is documented by a few inherited zircons that have been reworked into younger crust (Wilde et al., 2001; Harrison, 2009).

The importance of all of this is the resulting topography of the surface of the Earth and the availability of emergent land as opposed to ocean, and therefore the environments in which life may potentially have arisen. The earlier, hotter crust would not have been able to support modern continents and high mountains as do modern continents, and it has been suggested that exposed landmasses on the early Earth rather resembled volcanic islands and their surficial sediments on top of mainly submerged protocontinents above mantle plumes (Korenaga, 2021; Westall et al., 2023a,b; Roberts et al., 2024).

3.2. Emergence of life

There is significant evidence for the widespread existence of diversified life (chemotrophs and phototrophs) by 3.5 Ga and, as we will see below, probably even earlier. For this reason, we infer life to have emerged during the Hadean. Previously it had been proposed that the emergence of life or its early existence would have been limited by a cataclysmic cycle of impacts around 3.9 Ga (the late heavy bombardment, Maher and Stevenson, 1988). However, more recent models (Mojzsis et al., 2019; Marchi et al., 2021) suggest a gradual decline in the flux of extra-terrestrial material reaching the Earth (late veneer), estimating that the last planet-sterilising impact occurred at about 4.3 Ga, effectively placing the likely emergence of life after this date.

Westall et al. (2018, 2023a,b) and Rodriguez et al. (2024) reviewed, from different perspectives, the context of the emergence of life, starting with the formation of the Earth, through to the development of important environmental parameters and the availability of ingredients (cf. also Hazen, 2005; Grosch and Hazen, 2015). These publications also considered the different kinds of environments that have been suggested as locations for the emergence of life. Briefly, early considerations concentrated on deep sea hydrothermal environments (Baross and Hoffman, 1985; Russell and Hall, 1997; Martin et al., 2008). Later, other kinds of environments were considered, including pumice rafts (Brasier et al., 2012), nuclear-enriched coastal sands (Adam, 2007), and deep-seated faults (Schreiber et al., 2012). More recently, subaerial hydrothermal springs were proposed by Damer and Deamer (2020) and van Kranendonk et al. (2021), while Sasselov et al. (2020), for example, also envisaged life emerging in a constrained series of steps in a subaerial setting. The existence of exposed landmasses is therefore important for the latter theories. In some scenarios, it is considered to be essential that, at some point during abiogenesis, the products are frozen, *i.e.*, that the Hadean Earth was frozen in order to enable all of the steps from nucleotide synthesis to RNA copying (Zhang et al., 2021). We note, however, that, in certain abiogenesis hypotheses, high UV radiation is essential at least during the initial stages of prebiotic chemistry (e.g., Pascal et al., 2013; Damer and Deamer, 2020), while in others it is not (e.g., Martin et al., 2008).

An alternative theory of "panspermia", the insemination of the Earth by viable cells originating from another body in the Solar System, was first proposed by Arrhenius (1908) and revisited by Crock and Orgel (1973), who counselled that "infective theories for the origins of life" do not explain the biochemistry or biology of terrestrial life, a point of view echoed by Di Giulio (2010).

3.3. Hadean traces of life?

Despite the fact that life must have emerged during the Hadean, the overall lack of rock preservation makes the detection of potential traces of life difficult. Nevertheless, Bell et al. (2015) determined a —24 ‰ carbon isotope signature for graphite inclusions in a 4.1 Ga zircon crystal and concluded that it may be an indication of biological fractionation. Also, there has been a suggestion of biological remains in a jasperlite from the Nuvvuagittuq terrane of disputed age (dates ranging from 4.3 Ga or 3.7 Ga to 2.5 Ga, Dodd et al., 2017; Papineau et al., 2022; Lan et al., 2022). These remains comprise filamentous and tubular objects outlined by hematite that are described as strongly resembling similar structures formed by Fe-oxidising microorganisms in hydrothermal vents (Fig. 3A). These structures occur in carbonate and apatitic diagenetic deposits with which carbonaceous matter is associated. Dodd et al. (2015) and Papineau et al. (2022) suggest that the carbonaceous matter may be the remains of chemoorganotrophs that oxidised the original chemolithotrophic biomass. For the context, these chemical sediments are interpreted to have formed part of an ancient, basaltic seafloor crust, the rocks of which were subsequently subjected to upper amphibolite-grade metamorphism. Alternative, abiotic explanations have been proposed for these hematite rods (e.g., McMahon, 2019; Lan

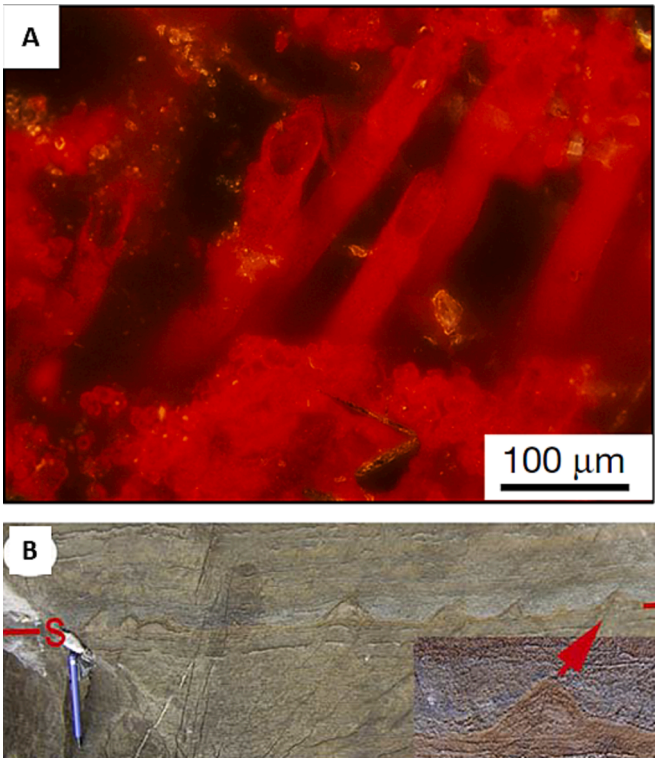

Fig. 3. Purported morphological biosignatures from the (Hadean?)-Eoarchaean or even younger rocks (cf. Lan et al., 2022). (A) Hematite tubes from the 4.3 or 3.7 Ga Nuvvuagittuq BIF (Dodd et al., 2017). (B) Purported stromatolites from the 3.7 Ga Isua Greenstone Belt (Nutman et al., 2019).

et al., 2022). Also, the parallel orientation of the filaments is at odds with the normally haphazard orientation of natural Fe-oxidising microbes (e.g., Hribovšek et al., 2023) and their large size, between 2 and 14 μm in diameter and up to 500 μm in length, contrasts with other Palaeoarchaean filaments that are ≤ 1 μm in diameter (e.g., Westall et al., 2006; Cavalazzi et al., 2021).

4. Eo-Palaeoarchaean (4.0–3.2 Ga)

4.1. Geological environment

Cratons of Eo-Palaeoarchaean age occur on most continents. The preservation of these cratons has been attributed to significant changes in the geodynamics of crustal formation between the Hadean and the Eoarchean, from stagnant lid to horizontal tectonics (Mulder et al., 2021) or a mixture of these regimes (Stern, 2018).

Solar luminosity would still have been much lower than today but would have slowly increased with time (Fig. 2C; Bahcall et al., 2001), while solar UV radiation would have been slowly decreasing but still very high compared to present values (Fig. 2B). Although diminishing in intensity (Marchi et al., 2021), impact delivery of extra-terrestrial material would have continued, as evidenced by layers of impact spherules occurring in Palaeoarchaean horizons of the Pilbara and Barberton Greenstone Belts (Lowe and Byerly, 2018), as well as the presence of extra-terrestrial carbonaceous matter in 3.33 Ga Barberton sediments (Gourier et al., 2019). Evidently, large impacts would have significantly affected environmental conditions in the surrounding area for any forms of life.

In a recent review of the Archaean atmosphere, Catling and Zahnle (2020, and references therein) note a variety of proxies that have been used to constrain Archean atmospheric composition, including chemical traces in seafloor or palaeosol minerals, atmospheric isotopic signatures in sediments, and fluid inclusions of seawater with dissolved air and microbial gases. Estimated ranges are large, depending upon individual proxies. Figure 1 gives a broad overview of variations in the composition of the atmosphere through geological time. Pertinent for the Eo-Palaeoarchaean eras are nitrogen levels (~0.3 bars) that were slightly lower than at present, relatively high CO_2 levels of about 0.1 bar, gradually decreasing methane levels (~ 10^{-3} bars), and perhaps trace levels of oxygen < 10^{-7} bars) (Stüeken and Buick, 2018; Catling and Zahnle, 2020). Considering the problem of the faint young sun, the main greenhouse gas during the Archaean would have been CO_2, with the addition of CH_4 of both volcanic and microbial origins (cf. Wolf and Fournier, 2018). Such high levels of methane have given rise to the hypothesis of an organic haze (e.g., Pavlov et al., 2001). Other trace gases the Eo-Palaeoarchaean atmosphere would have included water vapour and CO. The paucity of molecular oxygen in the Eo-Palaeoarchaean atmosphere would have been conducive to high UV radiation levels at the Earth's surface (Cockell and Raven, 2004).

The partial pressure of CO_2 in the atmosphere would have a greater or lesser effect on seawater pH, depending upon temperature with higher pCO_2 resulting in low pH and *vice versa* (Catling and Zahnle, 2020). Moderate temperatures of around 40 °C are suggested by Krissansen-Totton et al. (2018), which would result in a pH of between 6.4–7.4. On the other hand, rock/water temperatures, as measured by oxygen and silicon isotopes in chert layers associated with sediments, provide a range of temperature values, with higher temperatures up to 50–76 °C being suggested (van den Boorn et al., 2010; Tartèse et al., 2017; Lowe et al., 2020). While the possibility of glaciation at about 3.45 Ga was suggested by de Wit and Furnes (2016), sedimentological evidence strongly points in the other direction (Lowe and Byerly, 2020).

Geochemical proxies have been used to suggest the existence of "whiffs of oxygen", localised or short-term appearances of O_2 in the environment prior to the Great Oxidation Event at 2.4 Ga, for example, Mo, Re, U, and S isotope measurements for the Neoarchaean (Anbar et al., 2007). However, already by 3.7 Ga Rosing and Frei (2004) hypothesise on the presence of planktonic oxygenic photosynthesisers and locally oxic seawaters from carbon isotope signatures of –25 ‰ and the existence of U enrichment in the Isua deep sea shales using the rationale that uranium (IV) oxide is more soluble in oxidised waters. In fact, uranium (IV) oxide becomes more enriched in Proterozoic sediments as the ocean bottom waters gradually became oxidised.

We note that there are several abiotic ways of forming small amounts of oxygen on a local scale before the GOE. We have already mentioned the high flux of UV radiation to the surface of the Earth. Formation of reactive oxygen species would have occurred in the atmosphere and in aqueous microdroplets at the air–water interface (e.g., Rosing et al., 1996; Frei et al., 1999). UV radiolysis of H_20 would have been particularly relevant in shallow water, littoral environments and on land (see Cockell and Raven, 2004; Westall et al., 2006; Nutman et al., 2017), although Avilà-Alonso et al. (2017) hypothesise on the possibility of UV attenuation in shallow Palaeoarchaean seawater as a result of dissolved Fe ions. Another means of producing reactive oxygen in shallow environments would have been through dissociation of high-pressure water vapour escaping from shallow water hydrothermal vents (Westall et al., 2023b). There were, thus, many ways of producing micro-scale amounts of oxygen in the early Archaean that need to be appreciated in a discussion of potential microbial biomes.

While most of the preserved sedimentary environments from the Eo-Palaeoarchaean geological interval represent shallow water environments, some enclaves of deep-water sediments were preserved from this era. For example, the BIFs of Isua are described as representing deep water chemical deposits (Nutman et al., 2017), as are various fine grained, metamorphosed mudstones of the Pilbara and Barberton Greenstone Belts. For the record, we need to emphasise here that "deep water" simply means deposition below wave base. Wave base today is at a depth of about 20 m (Dietz and Fairbridge, 1968), but is obviously variable depending upon local geomorphology and can reach greater depths during storms. For example, the storm wave base for the Gulf coast of Florida and the Atlantic side is 50 and 100 m, respectively (Peters and Loss, 2012). Although episodic phenomena, storms can create more important and lasting effects on sedimentation in a basin (Morton, 1988). This is in contrast to Flemming (2024) who concludes that bedforms and associated sedimentary structures produced by the storm waves are most likely to be altered or obliterated by subsequent fair-weather swells. Given the evidence for storm deposits (shore face deposits) in the Palaeoarchaean, these considerations are of importance. Moreover, the closer position of the Moon during the Eo-Palaeoarchaean likely meant that wave base could have been deeper in specific locations. The preserved crustal fragments from this early period represent mostly flooded proto-continents (Arndt et al, 2012) on top of which were semi-circular, growth-fault-bounded basins several hundreds of kilometres in diameter and between 50–60 m in depth according to the sedimento-structural analysis of Nijman et al. (2017) for the Pilbara. Tidal action in these environments may have been amplified by the closer moon and tidal resonance amplification (*op. cit.*). Sub wave-base, turbiditic sediments are described for the Isua sediments (Rosing, 1999) and also for some of the Barberton lithologies (Byerly et al., 2019).

In contrast, Retallack and Schmitz (2023 and references therein) have identified a number of palaeosols beneath and within their newly dated 3.3 Ga Strelley Pool Chert Formation that formed under a temperate climate, an anoxic atmosphere with CO_2 levels 4–10 times present atmospheric levels, and in low relief coastal environments that included estuaries, rivers and floodplains. Palaeosol identifications were based on field observations, petrology, molar weathering ratios, the chemical index of weathering, and major element concentration ratios. Note that these identifications of Palaeoarchaean palaeosols in the Pilbara are contested (e.g., van Kranendonk and Pirajno, 2004; Brown et al., 2006). However, while coastal sediments are well represented in the Palaeoarchaean terrains (Lowe, 1999; de Vries et al., 2010), rare subaerial sediments attest to the presence of exposed landmasses. However, there is geochemical evidence for terrestrial fluvial input into

the early coastal waters in both Barberton and the Pilbara that is documented through elevated LREE signatures compared to HREE, as well as Pr/Nd versus Y/Ho ratios (Hickman-Lewis et al., 2020b; Clodoré et al., 2024).

The rocky and sedimentary substrates hosting microbial biomes were mostly volcanoclastic and hydrothermal, occurring at various water depths through to clastic tidal flats (Noffke et al., 2013; Howard et al., 2024). Evidence for hydrothermal activity comes from veining and fracturing, especially at the tops of lava flows and through the overlying sedimentary deposits (e.g., Hofmann and Harris, 2008), as well as elemental leaching of the upper crust and silica saturation of hydrothermal effluent and the seawater adjacent to the rocky or sedimentary interface that resulted in pervasive silicification (Hofmann and Harris, 2008). Chemically deposited layers of silica may have been related directly to hydrothermal effluent or simply due to pervasive oversaturation of the seawater with respect to silica (Trower et al., 2014; Ledevin, 2018). With respect to silica concentrations in seawater, we also note that *in situ* devitrification of the volcanic sediments will raise concentrations of silica in the pore waters.

The environmental conditions that we have briefly outlined above are necessarily generalised. Of importance for microbial biomes are the microbial-scale environmental parameters that would affect environments ranging from possibly as much as several kilometres, down to the sub-millimetric scale. At these small scales, there would be a wide range of potential habitats, each exhibiting different conditions and probably each hosting different life forms, as will be described below.

All the identified Eo-Palaeoarchaean sediments and biosignatures were preserved by rapid silicification owing to the supersaturation of silica in the sea water, particularly at the rock/water interface (Westall and Hickman-Lewis, 2018). Where they occur in shallow water facies, silicification was likely augmented by evaporative processes.

4.2. Eoarchaean evidence of life

We have already commented on the possible traces of life in the 4.3 Ga or 3.7 Ga Nuvvuagittuq jaspilite (Dodd et al., 2017; Papineau et al., 2022) (Fig. 3A). Apart from these rocks, the 3.8–3.65 Ga Isua Greenstone Belt contains purported traces of life in the form of carbon isotope signatures (Schidlowski, 2001), or ^{13}C-depleted graphite interpreted as a chemofossils of planktonic life forms (Rosing, 1999), organic molecules of possible biogenic origin trapped in inclusions on metastable garnets (Hassenkam et al., 2017), and putative stromatolites (Fig. 3B, Nutman et al., 2016, 2019). Stromatolites are laminated biosedimentary structures exhibiting vertical relief, whose formation is linked with microbial activity in phototrophic biofilms that mediates the precipitation of calcium carbonate in microbial extracellular polymeric substances (EPS), as well as the trapping of clastic material by the sticky EPS (cf. Reid et al., 2000; Allwood et al., 2006, 2007). However, a number of abiotic processes have been suggested to explain these purported biogenic signatures (cf. van Zuilen et al., 2002). The purported stromatolites occur in fine- to medium-grained dolomite in a low deformation area. The rocks are interpreted to have been deposited in a shallow marine setting, based on geochemical data and preservation of sedimentary structures. However, the interpretations of the Isua stromatolites (Nutman et al., 2016) have elicited much debate and they have been reinterpreted as tectonic folds by Allwood et al. (2018) and Zawaski et al. (2020). The amphibolite grade metamorphism to which the Isua rocks have been subjected clearly complicate the preservation and interpretation of potential biogenic remains.

We noted above the problem of syngenicity and the possibility of younger contamination of older rock samples, using an example of BIF from the Isua Greenstone Belt (Westall and Folk, 2003). This phenomenon extends also to the schists analysed in some of the above studies (Westall, personal observations), thus introducing contaminants to analyses made on bulk samples. This observation does not negate the results of the previous analyses made; certainly, there is strong evidence of life at Isua times and, therefore, depleted carbon isotopes are to be expected. The actual values may be slightly skewed as a result of more recent contamination. The recent contamination also accounts for the finding of yeast cells by Pflug and Jaeschke-Boyer (1979).

Hassenkam et al. (2017) investigated carbonaceous inclusions in a metastable garnet crystal in metapelites from Isua using *in situ* FTIR, demonstrating carbon bonded to nitrogen and oxygen, and probably also to phosphate. The compositional characteristics of the molecules are consistent with the degree of metamorphism of the host rock and, therefore, Hassenkam et al. concluded that the carbonaceous remains were those of 3.7 Ga biogenic organisms.

4.3. Palaeoarchaean evidence of life

The relatively low metamorphic grade (lower greenschist to greenschist, generally < 350 °C) of the Pilbara and Barberton cratons means that both rocks and potential fossilised traces of life are well-preserved. Other similarly aged cratons exist, e.g., the Dharwar and Singhbhum-Orissa cratons in India, but they are more metamorphosed. The Palaeoarchaean Pilbara and Barberton formations already document a rich variety of phototrophic and chemotrophic remains, emphasising the relatively high degree of evolution attained by life at this early stage. There have been a number of reviews of early life in recent years (Javaux, 2019; Lepot, 2020; Homann, 2019; van Kranendonk et al., 2018; Sugitani, 2018; Hickman-Lewis et al., 2018; Hickman-Lewis and Westall, 2021). Therefore, we will not attempt to address all the occurrences and descriptions, the interested reader is encouraged to look at the above-mentioned reviews and the articles referenced therein. Our aim here is to highlight a few examples that illustrate the early traces of life in terms of metabolism, habitat and biome.

4.3.1. Phototrophic microbial biofilms and mats

An interesting aspect of the Palaeoarchaean terrains is that there are frequent occurrences of littoral environments exposed to sunlight. Some of the oldest described biosignatures come from environments similar to what are today described as sabkha, *i.e.*, supratidal mud or sandflats formed in semi-arid to arid climates that are characterised by an accumulation of evaporite-saline minerals, as well as tidal-flood, and aeolian deposits. Microorganisms in these environments need to be able to cope with osmotic stress owing to the high salt concentrations (typically salt crusts form on top of the microbial mats), while they are also exposed to strong UV flux. It appears that the salt crusts can attenuate the penetration of UV radiation into a mat (Kminek et al., 2003; Cockell and Raven, 2004) (e.g., Fig. 4E, F). In fact, study of modern microbial mats dominated by photosynthetic microorganisms demonstrates the complexity of processes active at various levels within a mat. The top layer of such mats comprises EPS and pigments that protect the underlying cells (Visscher and Stolz, 2005; Braissant et al., 2009). This protective layer then sustains a suite of microorganisms using diverse metabolic strategies to degrade their organic remains (Oren, 2002). These metabolisms, today, include hydrolysis of organics, aerobic respiration, and sulphate reduction, the latter leading to sulphurisation during early diagenesis (Summons, 1993) and an active sulphur cycle (Jørgensen et al., 1979). The complexity of microbial communities and their metabolic interactions in mats is also discussed in Reid et al. (2000), Baumgartner et al. (2009) and Stal and Caumette (2013).

There is strong evidence for the presence of phototrophic microbial mats that produced sedimentological structures, such as microbially-induced sedimentary structures (MISS) and stromatolites from the very beginning of the Palaeoarchaean. Considering the importance of phototrophic mats as biosignatures during the Precambrian, we have illustrated their formation and fossil examples in Figs. 4 and 5. Noffke et al. (2013) describe MISS on bedding surfaces of volcanic sandstones in the 3.48 Ga Dresser Formation of the Pilbara (Fig. 5 panel 1) and used μCT and sulphur isotope investigations to document a taxonomically

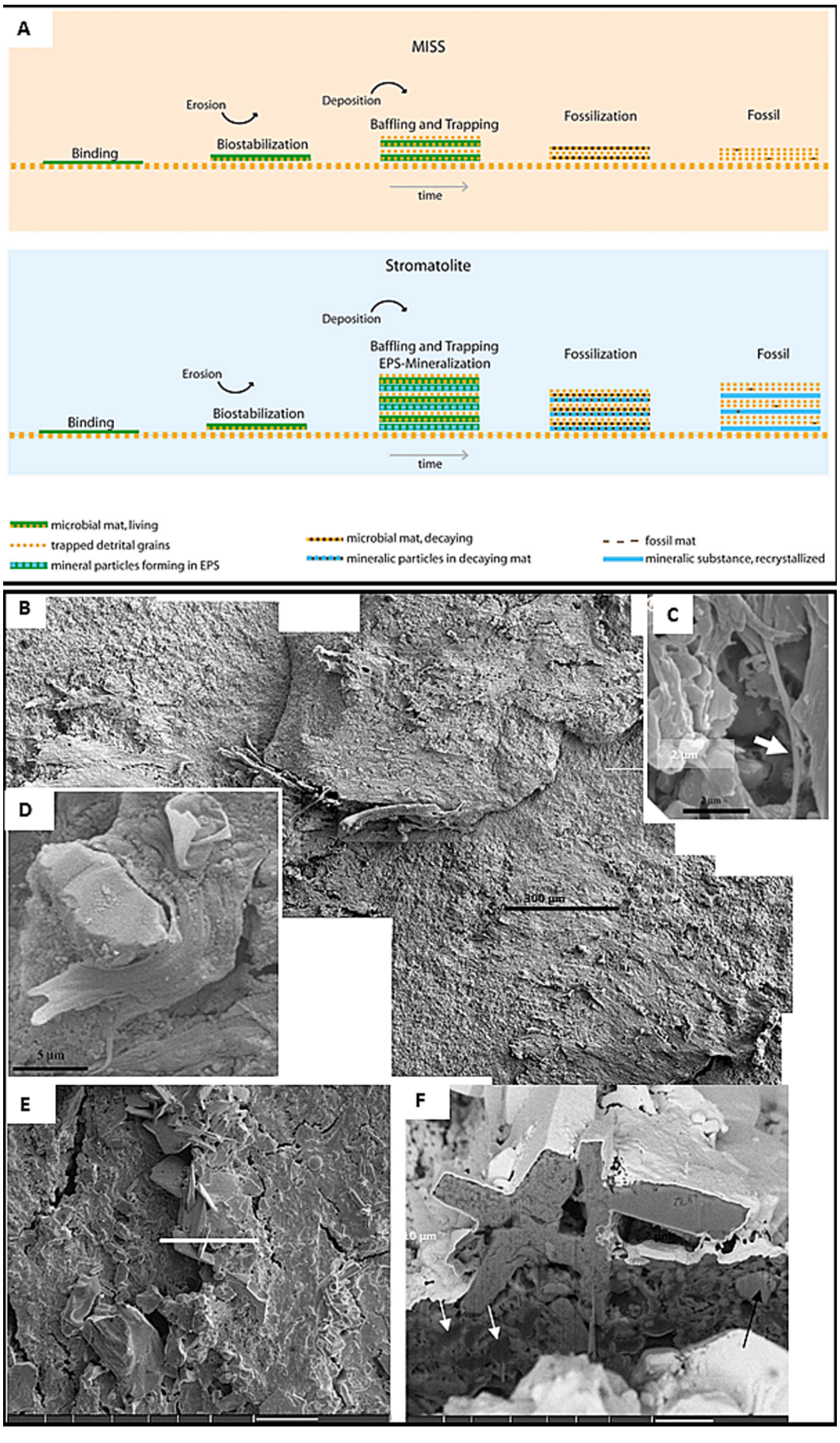

(caption on next page)

Fig. 4. Microbially induced sedimentary structures (MISS). (A) Schematic distinction between the preservation of MISS and stromatolites (Noffke and Awramik, 2013). (B-F) 3.33 Ga fossilised, epibenthic microbial biofilm, Barberton Greenstone Belt showing (B) an overview of the streamlined biofilm, (C) the tiny microbial filaments (arrow) and their EPS that formed the biofilms, (D) entrapped detrital particle, (E) evaporitic crystals (pseudomorphed gypsum) embedded in the exposed surface of the biofilm, (F) FIB section along white line in (E) showing incorporation of crystals into the surface of the biofilm (Westall et al., 2006).

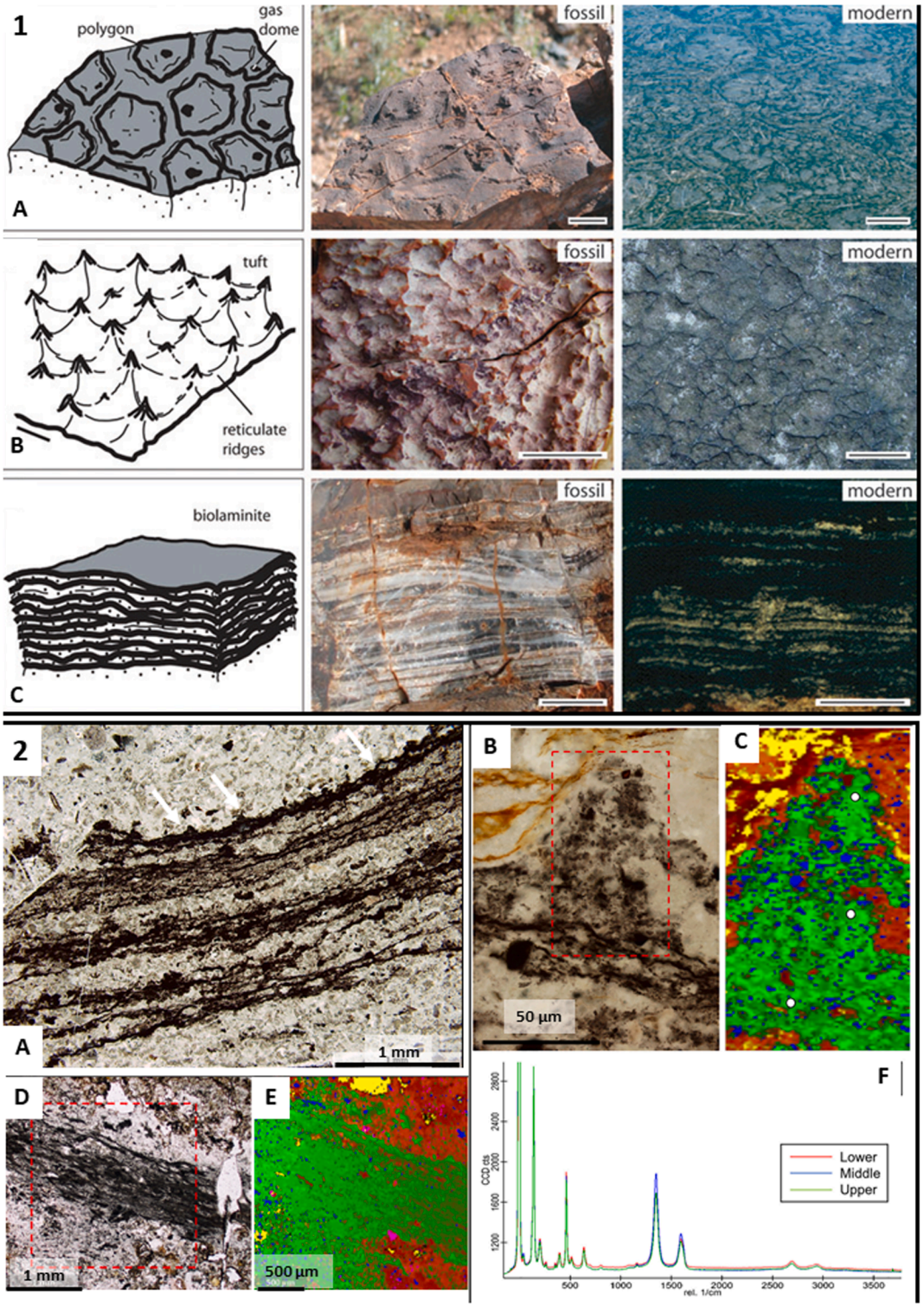

Fig. 5. Fossilised Archaean MISS. Panel 1. Variety of MISS textures found in the 3.48 Ga Dresser Formation tidal flat sediments (Pilbara) and their modern counterparts including (A) mud cracks, (B) tufted textures, (C) parallel mat laminations (Noffke et al., 2013). Panel 2. MISS textures from the 3.47 Ga Middle Marker Formation, Barberton. (A) Tufted mat texture with detail of tuft in optical microscopy, (B) and Raman spectral map (C) showing the carbonaceous nature of the tuft, (D) optical and (E) Raman spectral map of the fine, carbonaceous laminations of the microbial mats (Raman spectral maps: green = carbon; yellow/orange = quartz; blue = anatase), (F) Raman spectrum showing the mature nature of the carbonaceou matter with the D and G peaks centred around 1350 and 1580 cm^{-1} (Hickman-Lewis et al., 2018).

diverse community associated with the MISS (Howard et al., 2024). The environmental context is interpreted as being similar to a modern sabkha, where phototrophic, filamentous microorganisms associated with microbial polymer interact with sediments, forming an intricate, interweaving network that stabilises sediment surfaces (Noffke, 2009). Living in an exposed environment at the edge of the Dresser sea, MISS exhibit the effects of desiccation, such as polygonal oscillation cracks and gas domes, erosional remnants and pockets, and mat chips. In thin sections from the Dresser MISS, microscopic laminae comprising the MISS fabrics are carbonaceous and clearly demonstrate trapping and binding of sedimentary grains. The similarity between the textures and habitat of the Dresser Formation mat-like features, and those in modern and ancient sabkha environments suggests formation by photosynthesising microorganisms. The main difference between these MISS and stromatolites is that the former show early diagenetic mineralisation whereas the latter arise from syngenetic mineralisation (cf. Fig. 4A; Noffke and Awramik, 2013). The Dresser Formation, therefore, records a complex ecosystem of microbial mats formed by photosynthesising microorganisms. After discussing the possibility that the photosynthetic primary producers could have been oxygenic cyanobacteria, Noffke et al. (2013) conclude that they were more likely to have been anoxygenic phototrophs. We note that preserved cyanobacterial fossils are not recorded until the Mesoproterozoic (Demoulin et al., 2019; see also Arp et al. 2001 on the mineralisation of cyanobacteria).

More understanding of the Palaeoarchaean phototrophic communities comes from another example that has been extremely well-preserved owing to extremely rapid preservation by silica concerning a biofilm from the 3.33 Ga Josefsdal Chert, Barberton (Westall et al., 2006, 2011a). The exquisite preservation of a 10 μm thick biofilm permitted its investigation on a nanometer scale in the kind of detail normally used for modern microbial mats (Fig. 4B-G). Formed on top of volcanoclastic sands in a shallow water, littoral environment, the carbonaceous biofilm exhibits evidence of formation under flowing water (parallel orientation of the top layer of filaments, overturning of portions of the biofilm in the direction of flow). It was also subjected to subaerial exposure, as evidenced by desiccation cracks and the precipitation of a suite of pseudomorphed evaporite minerals, including aragonite, calcite, gypsum and halite, intercalated between different layers of the biofilm. The upper layer of the ~ 10 μm thick film comprises of fine filaments < 0.5 μm in diameter and up to tens of microns in length, all coated with a thick layer of polymer. Below the top layer of filaments, the biofilm comprises degraded organic matter intermixed with nanocrystallites of aragonite (incipient *in situ* calcification) and impregnated with silica, in an alveolar, partially granular texture. Trapped particles of quartz and volcanic particles occur in the biofilm. The biofilm and the surrounding sediment were rapidly coated and impregnated by silica, as indicated by the turgidity of the filaments. One of the interesting features of this biofilm is the documentation of metabolic stratification, as would be found in modern photosynthesising mats. Two features point to heterotrophic degradation of the organic matter and exudates (e.g., EPS) produced by the primary producers: (1) the presence of nanocrystals of aragonite, and (2) the presence of the sulphur molecule thiophene and an elevated concentration of sulphur (up to 1 %). These would have been the by-products of sulphate-reducing microorganisms. Given the high flux of UV radiation at that time, the biofilm probably survived because of a thick coating of polymer and dead cells, and partly because of the salt crusts. Interestingly, there is no evidence of oxidised conditions associated with the film. Hickman-Lewis et al. (2020b) analysed a number of phototrophic biofilms, some of them tufted, from the Barberton Greenstone Belt, including its oldest preserved sediments of the Middle Marker (Fig. 5, panel 2; Hickman-Lewis et al., 2018) to determine their local environmental conditions, *i.e.*, on a microbial scale, as opposed to the general, bulk environmental conditions. They found no evidence of oxygenic conditions associated with the phototrophic biofilms. They did, however, document increased riverine input when the biofilms and mats flourished, suggesting that terrestrial nutrients may have stimulated microbial growth.

As a result of their relatively large size, phototrophic microbial biofilms and mats lend themselves readily to ecological studies. Thus, Tice and Lowe (2004) and Tice (2009) documented a series of three different mat morphologies in the 3.42 Ga Buck Reef Chert, Barberton, formed in very shallow water conditions, whose distribution suggests control by either light intensity or small variations in the ambient current energy.

While most of the phototrophic microbial facies occur in volcanoclastic sediments, there is one significant exception. The 3.4 Ga Strelley Pool Chert in the Pilbara formed on a carbonate platform that developed away from terrestrial sedimentary input. Consequently, it hosts the oldest preserved stromatolites (Hofmann et al., 1999; Allwood et al., 2006) that reveal much information on their ecology (Fig. 7A). Different stromatolite facies associations occur in different microenvironments of the carbonate platform, although some stromatolite types occurred across different palaeoenvironments. The controlling factors were the interplay between biological and environmental processes, such as variations in water depth, sediment influx and hydrothermal activity. Sediment influx to the platform was low, as was the influence of hydrothermal activity, but evaporitic precipitation also contributed to the formation of the stromatolites. Thus, on a small scale, covariation of microbial mats with stromatolite development followed environmental changes, suggesting adaptation of the benthic microbial populations to these changes.

The Strelley Pool Chert is one of the rare known occurrences of Palaeoarchaean stromatolites. Since it formed on a sediment-starved carbonate platform, while the other Palaeoarchaean phototrophic mats and biofilms developed on volcaniclastic sands, one may hypothesise that absence of clastic sediment input was a controlling factor in stromatolite formation as opposed to MISS-forming microbial mats. However, tabular phototrophic mats in the 3.33 Josefsdal Chert in Barberton developed in a semi-restricted basin between episodes of volcanic activity-related clastic sedimentation over a relatively long period of time but there is no indication of stromatolite formation (Westall et al., 2015). This argues against the constraint of clastic sedimentation.

Stromatolitic structures were also identified in Palaeoarchaean deposits in Barberton, including the 3.4 Ga Kromberg Formation (de Wit et al., 1982 [later interpreted as liesegang structures by Nijman, Westall and de Wit in the field]), the 3.3 Ga Fig Tree Formation (Byerly et al., 1986) and the 3.3 Ga Witkop Formation, Nondweni Greenstone Belt (Wilson and Versfeld, 1994). Byerly et al. (1986) note that the stromatolites, identified in three locations in the Barberton Greenstone Belt, formed in shallow water on basement highs with sparse sediment influx and in relatively tranquil water conditions. Subaerial exposure and desiccation occurred under evaporitic conditions. These stromatolites were widespread, exhibited morphological variability, and were associated with a variety of sedimentary lithologies. Moreover, the common occurrence of tourmaline within the stromatolitic laminae suggests evaporation of seawater containing silica, magnesia, iron- and boron of hydrothermal exhalative origin. The Nondweni stromatolites were formed in a shallow-water environment on top of volcanics and strongly influenced by hydrothermal activity (Hofmann and Wilson, 2007). In contrast to the carbonate platform of the Strelley Pool Chert, the South African stromatolites are clearly associated with shallow water volcanic environments strongly affected by hydrothermal activity.

4.3.2. *Banded iron formations*

Banded iron formations (BIFs) have sometimes been used as proxies for microbial phototrophy, for example, through anoxygenic photosynthesis using iron as an electron donor (Kappler et al., 2005; Konhauser et al., 2007; Posth et al., 2014. Dreher et al., 2021). We note, however, that other microbial metabolisms have been suggested as contributing to BIF production, including chemolithotrophic iron

oxidisers in low oxygen conditions (Field et al., 2016; Chan et al., 2016). While abiotic mechanisms for contributing to the deposition of iron minerals in the BIFs are recognised (e.g., Rasmussen et al., 2017, 2019), Dreher et al. (2021) conclude that the greatest contribution is from microbes. Thus, based on Fe isotopic measurements, BIFs 3.8–3.6 Ga occurring in the Isua greenstone belt (Polat and Frei, 2005) are attributed to anoxygenic photosynthetic processes (Czaja et al., 2013). While major BIF deposits of Palaeoarchaean age have not been preserved, there are numerous occurrences of jaspilite deposits and their surficial oxidised expressions (pink and white banded chert). These, too, may have resulted from a combination of abiotic and biogenic processes, such as Fe^{2+} oxidising and Fe^{3+} reducing metabolisms. For Dreher at al. (2021), the combination of Fe^{2+} oxidising and Fe^{3+} reducing biological processes is critical to the formation of BIFs. We noted above the purported morphological and sulphur isotopic evidence for life in the 4.3 Ga or 3.7 Ga Nuvvuagittuq jaspilite. The degree of metamorphism makes interpretation of a biological morphology challenging (Fig. 3A) (Dodd et al., 2017) but the $\delta^{34}S$ data are suggestive of microbial S disproportionation (Papineau et al., 2022). Jaspilites in the 3.48 Ga Dresser Formation in the Pilbara are attributed to photoferroautotrophs, with variations in the iron isotopes reflecting different contributions of marine and freshwater influence (Johnson et al., 2022). There is also rare, morphological evidence of phototrophic microbial involvement in a jaspilite deposit from the 3.33 Ga Josefsdal Chert in Barberton in which the remains of the microbial mats have been preserved (Westall et al., 2015a). Jaspilites occur in the 3.33–3.26 Ga Mendon Formation deposited immediately above the Josefsdal Chert, but they are interpreted as deep-water sediments (Lowe, 1999; Trower and Lowe, 2016). Nevertheless, the published petrological images show that fine, anastomosing carbonaceous films are associated with the Fe-rich layers, similar to the shallow water biofilms and mats from the Josefsdal Chert (Westall et al., 2015a), as well as shallow water phototrophic mats and biofilms in the 3.42 Ga Buck Reef Chert (Tice and Lowe, 2004).

4.3.3. Hydrothermal environments

The 3.48 Ga Dresser Formation in the Pilbara is a volcano-sedimentary succession comprising replaced micritic carbonates and evaporites deposited under shallow-water, low-energy (sabkha-type) conditions, interbedded with sandstone and conglomerate, the latter formed during periods of growth faulting and tectonic activity (Buick and Dunlop, 1990; Noffke et al. 2013 and references therein). Growth fault-associated hydrothermal fluids pseudomorphed the original sedimentary mineralogy. Noffke et al. (2013) described a variety of MISS structures formed in an ancient coastal sabkha environment, identical to those formed in similar environments throughout geological time. Recently, a novel interpretation of the Dresser Formation as a submerged, low eruptive caldera very strongly affected by hydrothermal fluids has been proposed (see review, van Kranendonk et al., 2018), but is not unanimously accepted. In the newly proposed interpretation, metre-sized barite pods exhibiting streamer phenomena highly suggestive of hot spring, geyserite deposits were identified as hot spring pools (Djokic et al., 2017, 2021; van Kranendonk et al., 2018). Small scale stromatolitic textures are associated with the geyserite deposits (Djokic et al., 2017, 2021; van Kranendonk et al., 2018). Note that the sabka coastal environment and caldera hypotheses may not be mutually exclusive: calderas in shield volcanoes can form at shallow water depths, for example adjacent to the Figi Fracture Zone (Fouquet et al., 2018). The Campi Flegrei volcanic area on the southern Italian coast next to Naples, where part of the caldera margin is submerged, is another example (Steinmann et al., 2018). In an evaporitic setting, the Afar depression can be cited (e.g., Yirgu et al., 2014).

Nevertheless, the Dresser Formation documents widespread evidence for a variety of life forms based on a diversity of metabolic processes and electron donors/acceptors (van Kranendonk et al., 2018) and colonising not only shallow water environments, but also subaerial hydrothermal environments, as well as the underlying feeder veins (Ueno et al., 2006; Morag et al., 2016). Carbonaceous filaments from Dresser Formation cross-cutting chert veins have very light carbon isotopic signatures (−56 ‰) suggestive of microbial methanogenesis (Ueno et al., 2006). Moreover, studies of the sulphur isotope fractionation signatures of barite/pyrite pairs in Dresser Formation hydrothermal deposits also point to microbial sulphate reduction (Ueno et al., 2008). More recently, Mißbach et al. (2021) documented that organic compounds in fluid inclusions in hydrothermal barite from the Dresser Formation, including H_2S, COS (carbonyl sulphide), CS_2 (carbon disulphide), CH_4, acetic acid, organic (poly-)sulfanes, and thiols, may have contributed to the feedstock of sulphur and methanogenic metabolisms.

Similarly, carbonaceous filaments occur in other feeder veins, for example in the 3.42 Ga Buck Reef Chert in Barberton. In this case, Cavalazzi et al. (2021) described possible methanogenic filaments (Fig. 6C) colonising the walls of the feeder veins through which fluids with different compositional and pH gradients flowed, providing energy and nutrients to lithoautotrophic organisms. The evidence of life in hydrothermal fractures in the Palaeoarchaean crust is testimony to the widespread distribution of life already flourishing 3.5 billion years ago. Today, it is widely recognised that the crust is host to a biome that developed in autonomy over hundreds of millions of years (Onstott et al., 1999, 2019) and certainly by Palaeoarchaean times life had spread to the subsurface.

Interestingly, Glickson et al. (2008) compared carbonaceous remains from high temperature, hydrothermal environments in the Dresser Formation (and the Hoeggenoeg Formation in Barberton) with the hydrothermal chemolithotroph *Methanocaldococcus jannaschii*. The latter organism, together with *Pyrococcus abyssi*, was used in an experiment to silicify chemolithotrophic Archaea under anoxic and relatively hot (60 °C) conditions as analogues of Palaeoarchaean life (Orange et all., 2009). While the cells of *M. jannaschii* lysed immediately and only the abundant EPS of the organisms were fossilised, those of *P. abyssi* did not lyse and were perfectly preserved. The conclusion was that *M. jannaschii* was unlikely to be preserved as fossilised cells, although their degraded remains and organic signatures could be preserved in a silica matrix. This study underlines the fact that what is preserved on the rock record is only a fraction of what was once there.

Hydrothermal environments were important for life inhabiting different types of microenvironments in the Dresser Formation, as well as elsewhere on the Palaeoarchaean Earth. Westall et al. (2015) and Hickman-Lewis et al. (2020a) documented carbonaceous clots (Fig. 6D, E) concentrated in volcanoclastic sediments of the 3.33 Ga Josefsdal Chert that were very strongly influenced by hydrothermal activity. In all cases, the clots had formed around a volcaniclastic kernel. These authors concluded that the volcanic particles had been initially colonised by chemolithotrophs and subsequently by chemoorganotrophs that oxidised the dead organic matter of the lithotrophs.

4.3.4. Subsurface environments

It is now widely recognised that life in the continental crust today is abundant (Onstott et al., 1999, 2019). However, there is less information about life in the sedimentary subsurface of the Palaeoarchaean although there is evidence that it was present chert feeder veins (Ueno et al., 2008; Cavalazzi et al., 2021). We know today that microbial life occurs in deep-sea sediments (Jørgensen and Boetius, 2007) and has been documented down to depths of 2 km (Parkes et al., 2014). Deep-sea sediments from the Palaeoarchaean, as such, are not preserved. As noted above, subwave base deposits are described from certain sedimentary formations, such as the 3.42 Ga Buck Reef Chert of Barberton, but deeper water facies are generally only preserved in the younger, Mesoarchaean units (Lowe, 1999). Nevertheless, even in shallow waters, subsurface volcanoclastic sediments hosted subsurface life.

Westall et al. (2006, 2011b, 2015b) described monolayers of very small, carbonaceous coccoidal structures (<1μm in size) occurring on the surfaces of volcanic clasts and in the dusty volcanic matrix of tidal sediments from the 3.45 Ga Kitty's Gap Chert in the Pilbara (Fig. 6A, B).

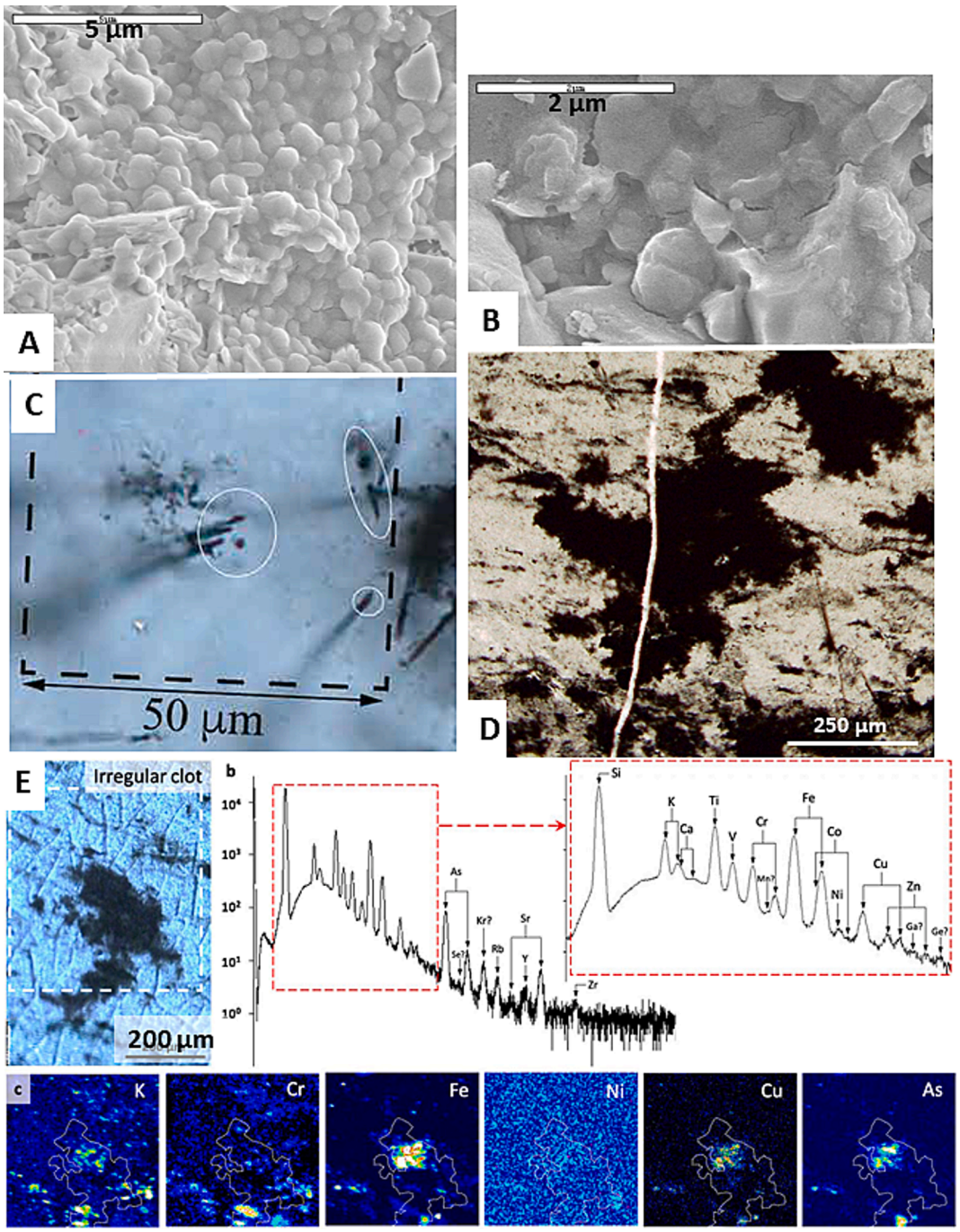

Fig. 6. Various microbial signatures from the Palaeoarchaean. (A) Colony of chemotrophic microfossils with detail of individual cells (B) from the 3.45 Ga Kitty's Gap Formation, Pilbara (Westall et al., 2006). (C) Filaments in a 3.42 Ga hydrothermal chert vein, Kromberg Fm. (Cavalazzi et al., 2021); (D, E) Stellate carbonaceous clots (D) interpreted as chemotrophic colonies from hydrothermal sediments, 3.33 Ga Josefsdal Chert (Westall et al., 2015; Hickman-Lewis et al, 2020a), with PIXE elemental spectrum (b) and elemental maps (c) from the dotted area in the optical micrograph in (E), illustrating that the clots grew around a small volcanic particle (now altered to phyllosilicate and highlighted by K, Fe, Cu, As) (op.cit.).

The combined biosignatures, morphological, carbon isotopes, nanostructure of the carbonaceous matter, and trace element compositions are indicative of a biological origin. The close association of these structures with volcanic substrates would suggest a lithotrophic metabolism. Indeed, concentrations of transition elements associated with the organic matter in these sediments (Clodoré et al., 2024) demonstrate that the volcanic particles were important sources of nutrients for the lithotrophs that colonised them. However, Wacey (2018) noted that volcanic glass bubbles could be coated with organic matter and suggested that this could be an abiotic explanation for some of the structures, including larger spherules and ellipsoids, observed in Palaeoarchaean cherts. Indeed, most volcanic particles in the Palaeoarchaean sediments are coated with carbonaceous matter (e.g., Clodoré, 2024). Such coatings today are caused by the rapid formation of an organic conditioning film sourced from dissolved organic matter in seawater (Bhagwat et al., 2021). This film then becomes the substrate for the attachment of benthic microorganisms that, in environments rich in nutrients, such as hydrothermal environments, then become substrates form chemoorganotrophs, as documented by the Kitty's Gap Chert and also, as described below in cherts from Barberton.

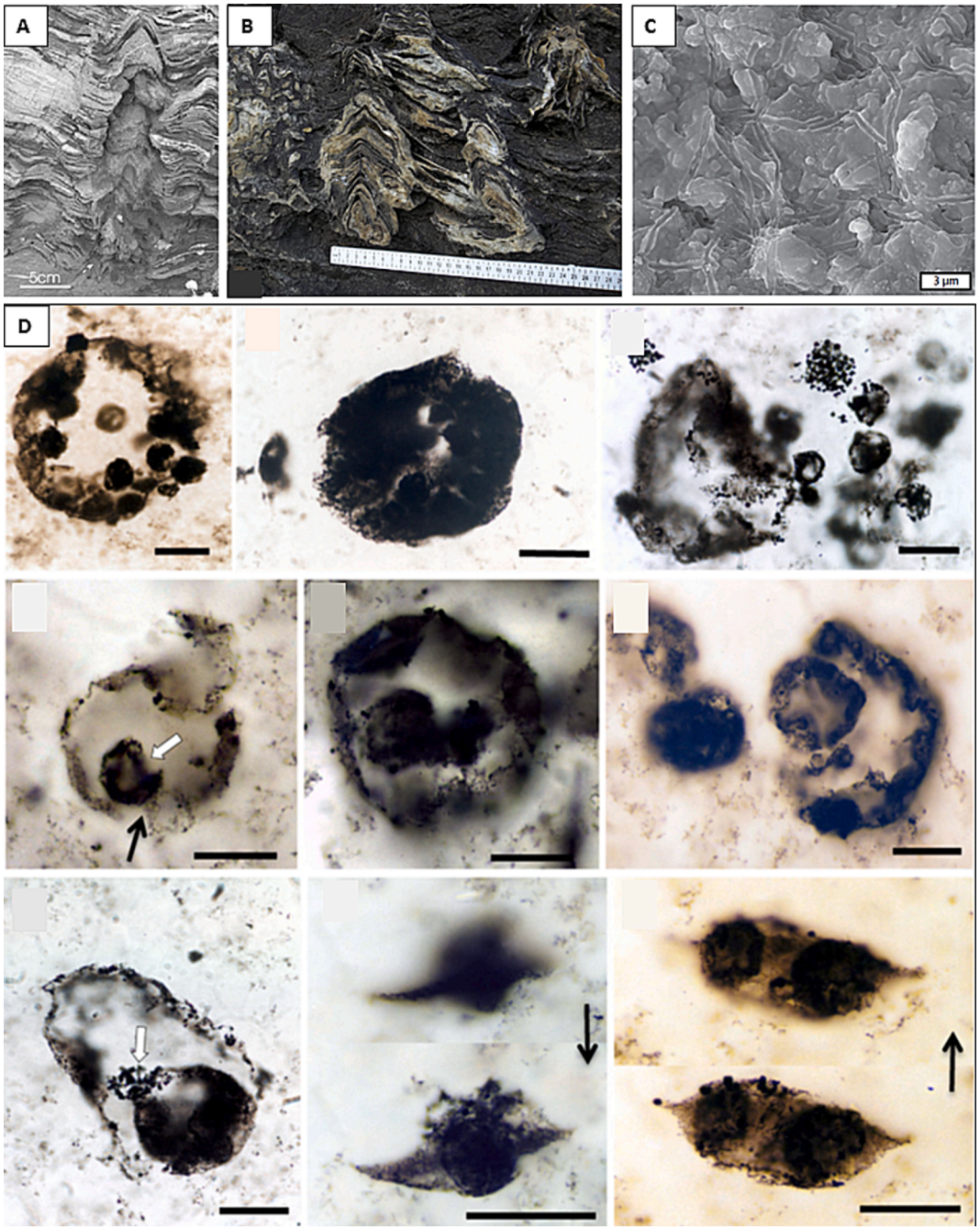

Fig. 7. Palaeo-Mesoarchaean microfossils. (A) Conical stromatolite from the 3.4 Ga Strelley Pool Formation, Pilbara (Allwood et al., 2007). (B) Conical stromatolites from the Chobeni Formation, Pongol (Siahi et al., 2016). (C) Rod-shaped chains of microbial casts in silica from vadose cracks in siliciclastic sediments of the 3.30 Ga Moodies Group (Homann et al., 2016). (D) Morphological variations in the acritarchs from the 3.0 Ga Farrel Quartzite (Sugitani et al., 2009).

Effluent in the nutrient-rich environment of hydrothermal systems would have been enriched in small carbon molecules, such as ketones and H_2. The environment of the volcanic facies of the 3.33 Ga Josefsdal Chert in Barberton was metal-rich, warm-hot, anoxic, and strongly influenced by hydrothermal activity with its associated chemical disequilibria (Westall et al., 2018). Layers of clotted, carbonaceous sediments represent variable mixtures of volcanic clasts very heavily coated with organic matter, and stellar, carbonaceous aggregates that grew *in situ* in a mixture of chemically-precipitated silica gel and volcanic dust (Fig. 6D, E) (Westall et al., 2015a; Hickman-Lewis et al., 2020a). As opposed to the mono-layer colonies of lithotrophs in the Kitty's Gap Chert (Westall et al., 2006, 2011b, 2024 in review), this biomass development is attributed to thermophilic chemoorganotrophs possibly using methanogenic and/or diazotrophic metabolisms, as well as potentially other metabolisms, such as sulphate reduction (Hickman-Lewis et al., 2020a).

4.3.5. *Acritarchs and other structures*

The Strelley Pool locality has also revealed a wide range of enigmatic, large coccoidal and lenticular structures of potential biological origin that have been reviewed by Wacey et al. (2011, 2018) and Sugitani (2018). These carbonaceous features exhibit characteristics compliant with biogenicity, including morphology, size distribution, taphonomic features, evidence of cellular reproduction, light carbon isotopes, and associated pyrite with sulphur isotopic signatures suggestive of sulphur metabolising microorganisms. The structures are

large, of the order of several tens of microns in diameter, and many comprise acid-resistant carbonaceous matter. Wacey et al (2018) later modified their interpretation to suggest that some of these features could be carbon-coated volcanic vesicles. Of interest is the fact that these large structures occur in sediments of the same age distributed over different formations, in the Panorama, Warralong, and Goldsworthy greenstone belts (Sugitani, 2018 and references therein). Similar structures of similar age are described from the Barberton Greenstone Belt (Walsh, 1992; Oehler et al., 2017; Hickman-Lewis et al., 2018). Sugitani (2018) explains the diversity of morphologies as reflecting a diversity of types of microorganisms and life strategies. Assemblages of smaller spheroids are interpreted as the remains of planktonic colonies, while some of the larger structures and their associated features are considered to have represented different stages of complex life cycles, including the production of daughter cells by larger cells, and planktonic or resting stages. If some of the structures were planktonic, they may have been photosynthetic. Sugitani (2018) notes that the large size and complexities exhibited by these structures are more akin to those found in algae, rather than prokaryotes. He reflects on the possibility that they may represent early cyanobacteria, or possibly sulphur bacteria. We note that molecular biological clocks suggest that cyanobacteria may have appeared in the Palaeoarchaean (Sánchez-Baracaldo et al., 2022).

Retallack and Schmitz (2023) report microfossils in their interpreted palaeosols from the 3.3 Ga Strelley Pool Formation, similar to other large, coccoidal or lenticular structures in that formation described by Sugitani (2018) and Sugitani et al. (2018) and references therein, and in the 3.42 Kromberg Formation, Barberton (Walsh, 1992; Oehler et al., 2017), as well as younger formations. These acritarchs, were interpreted as sporangia of actinobacteria, sulfur-oxidizing photosynthetic bacteria, and methanogens (Rettallack et al., 2016).

A very recent experiment suggests an alternative explanation for many of the larger, enigmatic structures and acritarchs in the Eo-Palaeoarchaean sediments. Hypothesising that wall-less cells must have evolved before cells with walls, Kanaparthi et al. (2024) devised an experiment to study the structural changes and behaviour of cells whose walls had been eliminated. They found that the wall-less cells exhibited many of the morphological features documented by interpreted cells in the Pilbara and Barberton sediments. The wall-less cells were often larger and some divided by producing internal daughter cells, similar to those identified by Sugitani (2019). The implications of these new findings for the interpretation of Eo-Palaeoarchaean biosignatures need to be digested (cf. Zhu and Szostak, 2009; Budin and Szostak, 2011).

4.4. Summary and discussion of traces of life in the Eo-Palaeoarchaean

The Eo-Palaeoarchaean heralds the earliest preservation of sedimentary deposits, their preservation related changes in crustal heat flow, geodynamics, crustal rheology, and probably to significant silicification. Many have noted the importance of silicification of terranes from this period (Lowe, 1999; Hofmann and Harris, 2008; Pirajno and Huston, 2019; Byerly et al., 2019; Ledevin, 2019). It has been proposed that early seawater was saturated with respect to silica as a result of a global, widespread input of hydrothermal silica, documented by a ubiquitous Eu anomaly in the sediments (Hofmann and Harris, 2008). Contributing to this would be input related to weathering of exposed land surfaces, and, where there was interaction between seawater and volcanic rocks (sediments and lavas), to devitrification. Indeed, Westall et al. (2015a, 2018) note stronger, more rapid silicification of rock/sediment/water interfaces during periods of volcanic activity, rather than during intervening episodes of quiet, non-eruptive deposition.

The preserved Eo-Palaeoarchaean sedimentary environment is represented primarily by shallow water environments comprising semi-circular basins up to a couple of hundred kilometres in diameter and drowned calderas probably not deeper than 50–100 m in depth (Nijman et al., 2017; van Kranendonk et al., 2018), although some sediments appear to have been deposited below wave-base (Lowe, 1999; Rosing, 1999; Fedo et al., 2001). While many of the shallow water environments may have been restricted basins, the Strelley Pool carbonate platform stands out as probably being open to the ocean (Allwood et al., 2006). Note that sabkha-type environments have also been identified in the Dresser Formation (Noffke et al., 2013).

One of the characteristic features of the Palaeoarchaean sediments is their rhythmicity as exemplified by alternating black and white cherts and jaspillites. Cyclicity in the production of global volcanic activity and hydrothermal fluids (e.g., Steinhoefel et al., 2009) has been suggested, as well as cyclicity based on climate forcing (Posth et al., 2008; Ledevin, 2019).

The Eo-Palaeoarchaean environment was anoxic, although abiotic processes would have locally produced very minor amounts of oxygen, notably in shallow water, UV-bathed environments and shallow water high pressure hydrothermal systems. Overall pH was probably slightly acidic, although pH would have varied locally, depending upon alkaline hydrothermal activity and alteration of ultramafic rocks and sediments. Rock/water temperatures would have been high (up to 75 °C, van den Boorn et al., 2010; Tartèse et al., 2017; Lowe et al., 2014) during volcanic activity. UV flux to the surface would have been also high (Cockell and Raven, 2004). Throughout the Eo-Palaeoarchaean, there would have been spatially and temporally limited local variations in environmental conditions that could have been exploited by different kinds of microorganisms. In the abundant shallow water environments identified, salinity would have likely have been high, owing to evaporation. Fluvial runoff from exposed landmasses also affected the adjacent coastal environments (cf. Hickman-Lewis et al., 2020b).

The wide distribution of microbial biosignatures underlines the fact that life flourished in all possible environments: in the photic zone on shallow water surfaces and possibly in the planktonic realm,as well as in coastal sabkha-like environments, in and around hydrothermal systems, within subsurface sediments, and in hydrothermal crustal fractures. These environments hosted organisms using anoxygenic phototrophic, chemoorganotrophic and chemolithotrophic metabolisms. Note that, in the case of the Dresser Formation, Noffke et al. (2013) raised the possibility that the phototrophic mats were formed by cyanobacteria but ultimately concluded that they could also have been formed by anoxygenic phototrophs. While traces of O_2 were likely to have been produced by abiotic processes, as noted above, the Palaeoarchaean environment was anoxygenic and there is no direct evidence for the presence of oxygenic cyanobacteria or eukaryotes (cf. Sugitani, 2018). One explanation for such structures could be that early cellular life may not have had cell walls, which may explain why some of the cellular features are uncharacteristically large for primitive, anoxic prokaryotes (Kanaparthi et al., 2024). In some cases, the biosignatures suggest methanogenesis or methanotrophy, sulphate reduction and iron cycling.

Of significance is the similarity in the kinds of biosignatures found in the Pilbara and Barberton cratons. This suggests that, at least by the Palaeoarchaean (and possibly already during the Eoarchaean) life was widespread, inhabiting all available biomes. The ubiquity of life at this early period in Earth's history, particularly the evidence for phototrophy, leads to the conclusion that the shallow water habitats that hosted phototrophic microbial mats and biofilms occurred frequently and that, perhaps protocontinents were common, although few have survived. Most of the preserved biosignatures are of benthic organisms, few are hypothesised to be planktonic. How could the benthic organisms be so widely distributed world-wide? While the distribution of planktonic phototrophs by ocean currents would be normal, it may also have been the case for some of the benthic phototrophic mats. Storm activity affecting the shallow water environments and ripping up benthic mats was common. Carbonaceous clots also show evidence of transport (Walsh, 1992; Walsh and Lowe, 1999). Stellar-shaped carbonaceous clots identified as chemotrophic microbial communities formed *in situ* in the Josefsdal Chert benthic sediments but rolled clots also occur in these sediments and may represent transported chemotrophic colonies. Thus, it may have been possible that both benthic phototrophic mat fragments

and chemotrophic clots could have been transported on ocean currents and thus distributed. Such a distribution would have been facilitated if there were numerous protocontinental environments on small plates around the globe (e.g., van Kranendonk, 2010).

The microfossils and other chemical biosignatures were preserved largely by rapid silicification that impregnated and embedded cellular structures, microbial colonies and biofilms and their organochemical compounds (Westall and Hickman-Lewis, 2018). Silicification combined with *in situ* calcification produced stromatolites (Allwood et al, 2009). Much of the degraded organic matter from dead organisms and colonies was disseminated within the volcanic (and sometimes silica gel) matrix of the sediments (Westall et al., 2015a; Clodoré et al., 2024). Preservation of organic matter in metastable minerals, such as carbonate or garnet, also occurred, the latter in the case of the Isua metapellite (Hassenkam et al., 2017).

An impressively wide range of biosignature types is preserved. They include morphological features, as described above, and various characteristics of the organic matter including its molecular composition, elemental composition, isotopic composition, and microstructure. Associated microbially-induced mineral precipitation (also early diagenesis) includes carbonates (aragonite, dolomite, siderite, ankerite), and pyrite and the associated sulphur isotopes of the latter.

We have not attempted to detail arguments for or against the biogenicity of all of the occurrences mentioned: there are a number of publications that deal with this aspect (e.g., Wacey, 2009, 2018; Lepot, 2020). We recognise the strong likelihood that the Eo-Palaeoarchaean sediments would contain organic matter from a mixture of sources – biogenic, as well as hydrothermal, extra-terrestrial and reworked. At times, it may not be possible to distinguish the mixtures (e.g., Gourier et al., 2019). Nevertheless, the large variety of biosignature types is testimony to widespread, flourishing of life, especially in the Palaeoarchaean and, by extension, probably in the Eoarchaean, although the high metamorphic grade of those rocks complicates identification. The many lines of evidence for Eo-Palaeoarchaean biosignatures contradict the implication that virtually all spherical, ovoid and filamentous structures found in Archaean cherts were formed by abiotic processs (Lepot, 2020).

One caveat concerns the interpreted Strelley Pool palaeosols and the acritarchs they host (Retallack and Schmitz, 2023). If these are really palaeosols, there is the question of how the acritarchs could have found their way into the soils. The interpretation of Retallack and Schmitz presupposes the existence of complex life forms living in soils on exposed land masses.

We noted above the problem of syngenicity of biosignatures in ancient rocks. Over the last couple of decades, there is more awareness of the problem and analytical techniques using *in situ* methods have been able to overcome this challenge.

In conclusion, the Palaeoarchaean sediments are the best preserved, oldest sediments in Earth history. For this reason, we have provided as much detail as possible to cover the variety of life forms and biosignatures, without being exhaustive. Life in the Palaeoarchaean, and probably in the Eoarchaean, was already highly diversified, had colonised all possible habitats, except perhaps land surfaces exposed to the atmosphere, and used a diversity of metabolisms. It lived and flourished in an polyextreme environment of high UV, salinity, temperature, concentrations of trace and transition elements, and salinity, but these were the conditions in which life first emerged and developed. Preservation, at times, exquisite preservation of the microbial remains, as well as preservation of their sedimentary habitats was due primarily to high silica saturation in the seawater (and pore waters of the volcanic sediments) that permeated all lithologies and biological matter.

5. Meso-Neoarchaean

5.1. Geological and environmental evolution

The Meso-Neoarchaean eras were marked by the amalgamation of increasingly stable crustal cratons and an increase in volcanism, especially komatiitic volcanism, although there was a gradual decrease in mantle heat flow (Arndt and Nisbet, 2012; Hawkesworth et al., 2020). This resulted in the appearance of larger passive margin continental shelf areas and epicontinental seas that exerted a positive influence as a sink of CO_2 through weathering, on the availability of nutrients, such as phosphorus, and thus, on the flourishing of microbial life, especially phototrophs.

Continental crust may be formed by a number of different processes (O'Neill et al., 2013; Roberts et al., 2015, 2024). Archaean continental crust consolidated around primitive, K-poor granites (TTGs) obtained from melting and fractionation of basaltic crust. Later K-rich granites formed in a variety of settings (*op. cit.*) that necessitated horizontal tectonics. Crustal formation throughout geological time has been episodic: while most of the Mesoarchaean is characterised by a slowdown in crustal and TTG formation compared to the Palaeoarchaean, the Neoarchaean saw a strong renewal of activity that produced possibly the greatest amount of newt crust (and TTGs) (O'Neill et al., 2013).

There is clear evidence that some form of horizontal plate tectonics and crustal cratonic amalgamation occurred in the Mesoarchaean (Roberts et al., 2015, 2024; Dhuime et al., 2012; Hawkesworth et al., 2020), with consequent erosion of core TTG granites and deposition of more quartzose sediments, e.g., the 3.2 Ga Moodies Group in Barberton (Heubeck, 2018) and the 3.0 Ga Farrel Quartzite, Pilbara (Sugitani et al., 2009), both interpreted as coastal to fluvial deposits. The increasing availability of sediment supply owing to the growth of continents, controlled changes in the clastic sediment record through geological time (Spencer, 2020). Epicontinental and continental basins formed on top of more stable crust during the Meso-Neoarchaean (Wilson et al., 2013). While volcano-sedimentary greenstone successions still formed during the Palaeoproterozoic, they gradually gave way with time to more cratonic sediment sequences. Sediments were deposited in a variety of tectonic environments, ranging from rift to passive margin settings, controlled by isostatic movement contiguous with crustal flexure related to sediment loading, to compressional and strike-slip basins (Grotzinger and Ingersoll, 1992).

The existence of more emergent landmass had a corresponding effect on climate and the supply of nutrients to the oceans (cf. the influence of fluvial supply on phototrophic microbial mat development in the 3.472 Ga Middle Marker horizon, the 3.33 Ga Josefsdal Chert, and other sedimentary formations, Hickman-Lewis et al., 2020b). The Pongola Supergroup, for example, preserves unambiguous evidence for both epicontinental and continental basin development atop stable crust (Wilson et. al., 2013). The stabilised continents may have hosted subaerial habitats, such as the acid volcanic lakes preserved in the 3.0 Ga Dominion Group of the Kaapvaal Craton (Agangi et al., 2021). Despite the increased volcanic activity, silicification of the sedimentary facies was not as prevalent as during the Eo/Palaeoarchaean, occurring rather in late-stage diagenetic/alteration scenarios. This suggests that, possibly, the heavy silicification characteristic of the Eo/Palaeoarchaean may have been stimulated by rapid devitrification of the mafic volcanic sediments, as well as hydrothermal input. As of the Mesoarchaean, sediments became increasingly quartzitic, with the erosion of exposed continental masses, as well as more carbonate-enriched in the shallow water environments. This continues into the Neoarchaean. Govind et al. (2021), for example, note relatively high $^{87}Sr/^{86}Sr_i$ values for the Neoarchean carbonate rocks of the Vanivilas Formation, Dharwar Craton (2.7 Ga), suggestive of chemical weathering of Palaeoarchaean crust.

In the Pilbara craton, quartzitic sediments occur in the ca. 3.2–3.0 Ga Farrel Quartzite in northeast Pilbara, exhibiting evidence of shallow-

water deposition in fluvial, coastal plain, beach, deltaic and shallow-water submarine fan environments, with some evidence for palaeosols and evaporite deposits of coastal salinas (Hickman, 2012). The younger ca. 2.7–2.63 Ga Jeerinah Formation of the Fortescue Group comprises mainly clastic sedimentary rocks deposited in a passive margin basin following continental breakup of the Pilbara Craton at ca. 2.71 Ga (Hickman, 2023). In the 2.7 Ga Neoarchaean Superior craton in Canada, poorly sorted, immature fluvial polymict conglomerate and sandy sediments of felsic origin were deposited in a high-relief and active tectonic (Haugaard et al., 2023). Other Meso-Neoarchaean cratons exhibiting felsic-derived clastic sediments include the 2.9 Ga Singhbhum craton, eastern India (Charkrabarty et al., 2021), and the ca. 2.8 Ga Pitangui and Rio das Velhas greenstone belts in Brazil (Brando Soares et al., 2017).

One interesting observation is that, based on analysis of finely laminated sediments from the Neoarchaean Joffre Member of the Brockman Iron Formation, NW Australia, the distance between the Earth and Moon was 321,800 ± 6,500 km and the day length 16.9 ± 0.2 hours (Lantink et al., 2022).

Atmospheric compositions were probably similar to those of the Eo/Palaeoarchaean, with most of the CO_2 and CH_4 coming from volcanic outgassing. Methane will also have been sourced from microbial methanogenetic activity. As we will see below, proxies suggest continuing minimal to almost non-existent oxygen levels (Fig. 1; Roberge et al., 2019; Catling and Zahnle, 2020; Zahnle, 2006; Lyons et al., 2014). However, there is increasing evidence for the appearance across the globe of localised free oxygen associated with large, carbonate stromatolitic platforms. This is documented geochemically in a number of localities using various chemical proxies. For example, the 3.0–2.9 Ga Pongola Supergroup hosts carbonate and shaley/BIF sediments that exhibit a small negative Ce anomaly in the case of a stromatolitic carbonate platform (Siahi et al., 2018), or negative $\delta^{56}Fe$ values in pyrites that record the oxidation of Fe in oxygenic shallow oceans, coupled with biogenic Fe reduction during diagenesis (Eickmann et al., 2018). The Mozaan Group of the Pongola Supergroup contains manganese enriched shales and BIFs that are interpreted to be evidence of local photosynthetic oxygenation (Ossa et al., 2016). In Canada, the 2.93 Ga Red Lake of Ontario carbonate deposits are characterised by high Mn concentrations and positive Ce anomalies, suggestive of local oxidation (Afroz et al., 2023). In India, Mukhopadhyay (2020) reports BIFs in association with manganiferous formations and microbial carbonates from the Neoarchaean (as well as back through to the Palaeoarchaean) that are interpreted to reflect the redox stratification of oceanic hydrosphere related to oxygenation of early atmosphere.

Brüske et al. (2020) used U isotopes as a proxy for determining the redox state of ocean waters since U is redox sensitive and there are generally isotopic offsets between the oxidized and reduced reservoirs. Analyses pf Palaeoarchaean to Palaeoproterozoic samples (shales carbonates and BIFS) from the Barberton Greenstone belt, Zimbabwe Craton and Pilbara Craton showed, however, that there was only minor U isotope enrichment in Palaeo-Neoarchaean samples, *i.e.*, little oxidative weathering.

Bosco-Santos et al. (2020, 2022) documented evidence for localised oxygenation in early Neoarchean sediments in the ca. 2.7 Ga Rio das Velhas and the Pitangui Greenstone Belts. In the latter case, Bosco-Santos et al. (2020) used the sulphur isotopic composition of sedimentary sulphides to document an early input of sulphate from oxidative weathering. Other geochemical signatures (attenuation of sulphur mass independent fractionation, Fe_{HR}/Fe_T, Ce anomalies, and rare earth element fractionation) are consistent with the presence of free oxygen.

Yet another proxy for oxygenation is iodine. Fang et al. (2024) analysed iodine concentrations in carbonates from across the North American craton ranging in age from Mesoarchaean to Palaeoproterozoic, demonstrating non-zero carbonate I/(Ca + Mg) ratios that are suggested to indicate localized oxygen of biogenic origin in Archean and Paleoproterozoic shallow marine environments.

Finally, another approach is to model the increase in marine and atmospheric oxygen levels, with a consideration of the recycling and build-up of carbonate, as well as the emerging continents and degassing of the mantle (Peng et al., 2022), all underlining the importance of the interplay between long-term cycles of oxygen, phosphorus and carbon.

In summary, there is abundant geochemical evidence for the presence of oxygen oases in Meso-Neoarchaean cratons across the globe. We will see below that the main "culprit" for the appearance of oxygen is the emergence of oxygenic phototrophs but recycling and build-up of carbonate, emerging continents and degassing of the mantle are also implicated (e.g., Sánchez-Baracaldo et al., 2022; Peng et al., 2022).

5.2. Meso-Neoarchaean life

The major particularity of the Meso-Neoarchaean was the appearance of significant formations of carbonate platform stromatolites created principally by phototrophic microorganisms, many associated with proxy signatures for oxygen as noted above. The occurrences are many and spread globally (the Southern African craton, the Pilbara/NW Australian cratons, the Brazilian cratons, and the North American craton). A review of Archaean stromatolite/microbial mat occurrences by Schopf et al. (2007) documents principally domical and stratiform structures occurring in Palaeo-Mesoarchaean cratons in Australia, South Africa, Zimbabwe, Canada, and India, with columnar stromatolites appearing principally in the Mesoarchaean and dominating the Neoarchaean, particularly present in Canada and Australia, as well as in India, Zimbabwe and South Africa. Schopf et al.'s (2007) review does not consider the later described 2.7 Ga tabular stromatolites of the Carajás Basin in the Brazilian craton (e.g., da Luz and Crowley, 2012; da Costa et al., 2023). Apart from that of Schopf et al. (2007), a number of reviews document the fossiliferous evidence for life in the Meso-Neoarchaean and even into the Palaeoarchaen, e.g., Lepot (2020), Hickman-Lewis and Westall (2021) covering Southern Africa, Fairchild et al. (2012) covering Brazil, and Grey and Awramik (2020) who provided an overview of stromatolites through time.

In the following, we do not intend to make a compendium of all known occurrences of traces of life in this period but, instead, consider only a few examples from each craton to illustrate variability in environment of formation and type of structure.

5.2.1. Southern African cratons

The 32.2—32.09 Ga Moodies Group sediments record the first significant (ca. 3.6 km thick) immature to mature quartzose sedimentary deposits in the Kaapvaal craton (Heubeck, 2019). They formed in alluvial, fluvial, deltaic, tidal to shallow-marine environments and comprise conglomerates, siltstones and minor volcanic rocks and ferruginous sediments. Importantly, the quartzitic clastic sediments record the erosion of granitoid rocks representing continental core material and indicating the presence of long-lasting, stabilised continents (*op. cit.*). Indeed, the tectonic setting for the formation of these thick sedimentary deposits is interpreted to be in subsiding troughs formed between rising granitic plutons, *i.e.*, in a vertical tectonic setting rather than a horizontal one. Rising and falling sea levels would have created a variety of environments for hosting life, from fluvial environments, through to deltaic, tidal and shallow marine ones. The unprecedented extent of preserved environments permits evaluation of the microbial record that spans terrestrial environments to shallow water ones.

Noffke et al. (2006), together with Heubeck (2009) were the first to recognise the presence of MISS in the tidal sedimentary facies. Indeed, one of the key findings is that phototrophic microbial mats dominated these environments, in both relatively quiet dynamic situations and high-energy settings (Homann et al., 2015, 2016). Homann et al. (2015) described the earliest known examples of cavity-dwelling microbiota (coelobionts) (Fig. 7C) that created mini-stromatolitic structures within bedding parallel cracks in peritidal clastic sediments. Unusually, biomorphological casts of chain-forming rod-shaped are preserved in a siliceous matrix. Analysis of C and N isotopes of the associated

kerogenous remains suggest possible chemotrophic or photosynthetic metabolisms with indications of adaptations of the biosphere to terrestrial settings (Homann, 2019). Homann (2019) concludes that the "Moodies microbial mats show some striking morphological similarities to modern cyanobacterial mats".

The ca. 3.0 Ga stromatolites (Fig. 7B) of the Chobeni Formation, Nsuze Group (Pongola Supergroup, South Africa) formed in a siliciclastic, volcanoclastic carbonate and tide dominated shallow marine environment with a shoreline that was open to ocean. While microbially-induced sedimentary structures (MISS, cf. Noffke, 2009) occur in siliciclastic sediments, there is a wide variety of other microbial biosignatures that are found in the carbonate facies, including stromatolites, ooids, and oncoids (Mason and von Brunn, 1977; Beukes and Lowe, 1989; Siahi et al., 2016, 2018). The environment was strongly influenced by shallowing up sedimentary cycles from subtidal to inter/supratidal that reflect fluctuating sea levels. Following the different cycles, digitate, stratiform, and small-scale domal stromatolites formed in the supratidal to upper-intertidal settings, while larger domes, conical/columnar stromatolites and possibly biogenic oncoids were restricted to higher energy, lower intertidal and shallow subtidal settings. As noted above, various proxies suggest local oxygenic conditions (Ossa et al., 2016; Siahi et al., 2018; Eickmann et al., 2018), suggesting that water was oxidised during photosynthesis, thus releasing oxygen as a by-produce and,thus, supporting the presence of oxygenic photosynthesis.

Noffke et al. (2008) described MISS from the siliciclastic facies of the 2.9 Ga Nhlazatse Section of the Pongola Supergroup, documenting four different microbial mat facies including endobenthic and epibenthic microbial mats comprising planar, tufted, and spongy subtypes, each related to a specific tidal zone, as in similar modern setting. While Noffke et al. (2008) tentatively identified the remains of cyanobacterial filaments associated with the MISS, they acknowledged that MISS may also be formed by anoxygenic phototrophs that leave similar morphological signatures.

An epicontinental setting is suggested for the 2.8 Ga Mushandike Limestone of the Masvingo Greenstone Belt, Zimbabwe craton that hosts low relief stromatolitic domes (Orpen and Wilson, 1981; Abell et.al., 1985). REE analyses of the carbonates (Kamber et al., 2004) indicate that the stromatolites formed in a highly restricted basin setting strongly influenced by fluvial input from the exposed, granitoid landmasses. Analysis of the carbon isotope signatures (averaging ca. – 27 ‰, Nisbet et al., 2007) suggest that the microorganisms were oxygenic photosynthesisers using form I Rubisco, similar to cyanobacteria.

5.2.2. The Pilbara craton

The 3.0 Ga Farrel Quartzite in the Pilbara host a remarkable collection of carbonaceous acritarchs whose morphological diversity and complexity (Fig. 7D) suggest further evolution of microbial life in the Mesoarchaean (Sugitani et al., 2007, 2009, 2011). Geo-organochemical studies of the acritarchs confirms the biogenicity of the organic matter (Oehler et al., 2010; Delarue et al., 2018). The morphological diversity of the structures led Sugitani et al., (2007) to attempt a taxonomic classification (thread-like, film-like, small (<15 μm) and large (>15 μm) spheroidal, and spindle-like). Concentrating only on the spheroids, Sugitani et al. (2009) identified four subdivisions ((1) simple single-walled spheroids, (2) thin-walled spheroids having a diffuse envelope, (3) thick-walled spheroids, and (4) spheroids having an extensively folded wall) that, together, are suggestive of various reproductive phases. If correct, these observations emphasise the degree of evolution of life in the Mesoarchaean but we recall the experiments of Kanaparthy et al. (2024) suggesting that early cells had not yet developed cell walls and, thus, could have produced a wide variety of morphologies.

Retallack et al. (2016) took examination of the Farrel Quartzite further and suggested that it represents a pedogenic environment characterised by a sulphate rich sediment, unusual for the Mesoarchaean anoxic environment, with the high ferrous/ferricmolecular weathering ratios and iron depletion similar to those in swamp soils today. Evaporite crystals indicate that the soils were not waterlogged (Sugitani et al., 2003). Retallack et al. (2016) suggest that the described microbiota (e.g., Sugitani et al. 2007, 2009, 2011) include actinobacteria, purple sulphur bacteria, and methanogenic Archaea, comparing the individual morphotypes to specific species, with purple sulphur bacteria being responsible for the precipitation of minerals, such as barite. Furthermore, they note that opaque grains in the soils may have protected the biota from harmful ultraviolet radiation (c.f. Sagan and Pollack, 1974).

The ca 2.7 Ga Tumbiana Formation of the Fortescue Group, NW Australia formed in shallow ephemeral evaporative lakes (Buick, 1992; Awramik and Buchheim, 2009; Coffey et al., 2013). It hosts stromatolites (Fig. 8C) associated with carbonaceous matter having carbon isotope signatures indicative of phototrophic microorganisms, as well as methanogens and methylotrophs. Although there is no geochemical indication of oxygenic photosynthesis, Buick (1992) concluded that the intercontinental stromatolites were formed by oxygenic phototrophs because the lack of sulphate (sedimentary iron and sulphur mineralisation) indicates a paucity in the volcanic and hydrothermal discharges into the basin, and therefore a lack of basic nutrients for anaerobic phototrophy. He concluded: "Thus, the late Archaean biota had perhaps reached the maximum level of metabolic complexity and diversity possible in a suboxic world inhabited exclusively by prokaryotes". However, sulphate was not common in the Palaeoarchaean where there is abundant evidence for anoxygenic photosynthesisers, as described above.

Flannery (2010) also concludes that the microorganisms producing the stromatolites of the Tumbiana Formation were most likely to be oxygenic phototrophs, *i.e.*, cyanobacteria, because of the amount of biomass produced, the presence of tufted mats, today only produced by oxygenic photosynthesisers, as well as the geochemical evidence for oxygen. Although he claims that these tufted mats are the oldest known, they have been described from Palaeoarchaean sediments (e.g., Hickman-Lewis et al., 2018), where they are associated with anoxic environmental parameters. Evidently, in the absence of oxygenic photosynthesisers, anoxygenic species exhibited the same, light-seeking behaviour.

5.2.3. The North American craton

Mesoarchaean carbonate platforms are preserved also in North America. McIntyre and Fralick (2017) describe laterally-linked and isolated domal stromatolites, as well as low relief domes from the (2.93 Ga) Red Lake carbonate platform, northwest Ontario, Canada. As with the Pongola stromatolites, morphological differentiation was controlled by physical parameters, such as water depth, with *Stratifera* and *Colleniella* type stromatolites occurring in the peritidal zone, while only *Stratifera* occurred in the more deeper water regions of the platform. Here, proxies suggest oxygenic phototrophy with the oxygen reacting with Fe-rich ocean waters to precipitate Fe oxides, thus contributing to the formation of BIFs in the deeper regions of the platform (Afoz et al., 2023). Close in age to the Red Lake carbonate platform is that of ca. 2.8 Ga Mosher Carbonate at Steeprock in south central Canada (Fig. 8A, B), the oldest large exposure of a Mesoarchaean carbonate platform, up to 500 m in thickness (Fralick and Riding, 2015). The stromatolites here formed on a shallow water platform at the edge of open water that, with time, became increasing restricted. Together, negative Ce anomalies, positive Gd anomalies and reduced positive Eu, as well as very large, metre-sized stromatolitic domes, indicate significant phototrophic biomass development. The authors conclude that the stromatolites (comprising domal, pseudocolumnar, columnar and fenestral stratiform morphologies) were produced by oxygenic photosynthesisers, such as cyanobacteria (Riding et al., 2014). Contributing environmental factors were the extent of oxygen production, initial terrestrial run-off, and interplay withthe open ocean waters that was sub- or anoxic and rich in

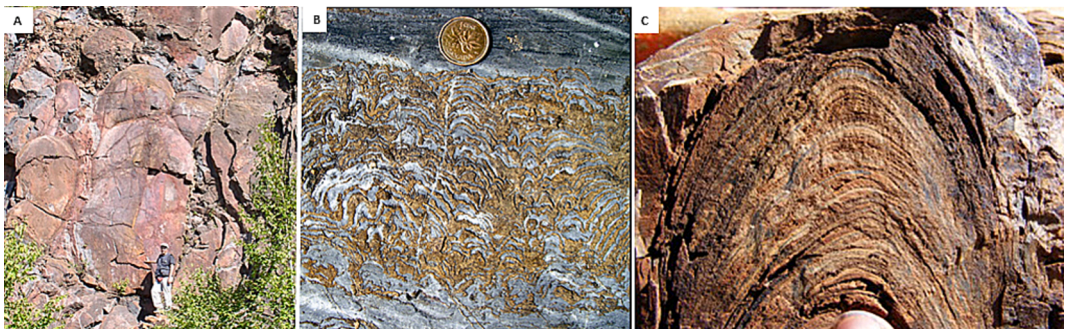

Fig. 8. Stromatolites from the Mesoarchaean. (A) Large, domical stromatolites from the 2.8 Ga Steeprock Formation, Canada (photo F.W.). (B) Field photograph of the crinkly dolomitic laminae in the Steeprock stromatolites (Fralick and Riding, 2015). (C) Conical stromatolite from the 2.7 Ga Tumbiana Formation, Western Australia (Coffey et al., 2013).

bicarbonate and dissolved iron, as well as with water depth and platform size (Fralick and Riding, 2015; Riding et al., 2022). The oxygen production on the platform resulted in a seaward chemocline, a decrease in the Mn/Fe ratio, and accumulation of Fe, Mn and Ce cerium oxides (Fralick et al., 2024).

5.3. Neoarchaean life

Carbonate deposition, carbonate platforms and stromatolites continue to dominate the Neoarchaean palaeontological record, although geochemical biosignatures (carbon, sulphur isotopes) indicate the presence of non-photosynthetic life forms as to be expected in any phototrophic microbial mat community where the organic matter produced by the primary phototrophs is consumed by heterotrophs (Stal, 2012). Of interest in the Neoarchaean of Southern Africa is the emergence of large domical stromatolites, up to several metres to tens of metres in height and length, that contrast with the smaller, more discrete stromatolitic morphotypes in Palaeo-Mesoarchaean formations.

5.3.1. Southern African craton

Neoarchaean biosignatures and their respective environmental conditions of the Neoarchaean in Southern Africa are reviewed in detail in Hickman-Lewis and Westall (2021). Here, we summarise the pertinent points. The Neoarchaean sedimentary formations of Zimbabwe comprise the 2.7 Ga Manjeri Formation and the slightly younger, 2.65 Ga Cheshire Formation. Columnar stromatolites are well developed in shallow water sediments in the Manjeri Formation, where REE + Y analyses indicate both anoxic marine (*i.e.*, shallow water environments with access to the open ocean) and hydrothermal fluids influences (Grassineau et al., 2002). Long-duration environmental cyclicity in the Cheshire Formation attests to stable lagoonal conditions (with open access to the ocean), as well as minimal continental detrital influence, with the cyclic chemical variability possibly influenced by seasonal changes (Martin et al., 1980). Shallow water stromatolites in the Cheshire Formation comprise domical macrostructures of decimetre- to metre-scales, as well as tabular stromatolites, and form larger reefs. They also exhibit conical *Conophyton*-like structures and branching columnar forms (Martin et al., 1980), thus attesting to the diversity of Neoarchaean stromatolite types existing in Southern Africa. This is underlined by sulphur and carbon isotope evidence for metabolisms using the complete sulphur cycle, methanogenesis and methylotrophy, as well as rubisco activity indicative of anoxygenic and oxygenic photosynthesis (Grassineau et al., 2001, 2006), all typical of phototrophic microbial mat communities (cf. Stal, 2012). In contrast to the previous, mostly marine environments, the giant domical stromatolite mounds and conical and cuspate microbialites of the 2.7 Ga Huntsman Quarry in the Bulawayo greenstone belt formed in hydrothermally influenced marine conditions, however, with considerable inputs from proximal continents (*i.e.*, a light REE-enriched riverine contribution (Sumner, 2000; Kamber et al., 2014).

In South Africa, the slightly older, 2.78 Ga Ventersdorp Supergroup hosts small lobate, domical, columnar and linked pseudo-columnar stromatolites formed during periods of clastic input quiescence in a high-energy environment (Wilmeth et al., 2019). Other localities in the Hartbeesfontein Basin exhibit low relief, domical to conical stromatolites (Pope et. al., 2000), whose changing morphology may be related to either changes in hydraulic energy or chemical stress (Hickman-Lewis et al., 2019). Cambell Rand Subgroup and the Malmani Subgroup of the Transvaal Supergroup, together, represent a major 2.3–2.6 Ga old carbonate buildup (Beukes 1987; Schröder et al., 2008). Again, microbialite (including stromatolites) and carbonate deposits reflect environmental conditions ranging from high energy platform margins to quieter lagoons, intertidal flats and supratidal regions. Similarly, stromatolites in the 2.64 to 2.52 Ga Griqualand West Basin of the Transvaal Supergroup flourished in semi-restricted marine and epicontinental environments (Eriksson and Altermann, 1998). The dominance of shallow water phototrophs may have resulted in an increase of oxygen in the biosphere, as suggested by increasingly heavy carbon isotope fractionations, from approximately −40 ‰ to −25 ‰, upward through the Campbellrand-Malmani stratigraphy (Eroglu et al., 2017). Thus, it appears that oxic environments gradually became more important from the Meso- to Neoarchaean in Southern Africa.

Despite the concentration of interest on Meso-Neoarchaean stromatolites and carbonate microbialites, geochemical evidence of chemotrophic microorganisms consists of carbon isotope fractionations in 2.59 to 2.50 Ga sediments of the Campbellrand platform indicative of a range of autotrophic carbon fixation mechanisms and heterotrophic processes including fermentation and methanotrophy (Fischer et al., 2009). Large coccoidal microfossils buried in finely laminated deep-water chert in the Gamohaan Formation have been compared to sulphur-oxidising bacteria, such as Thiomargarita (Czaja et al., 2016), evidence of a sulphuretum supported by analysis of sulphur isotopes (Kamber and Whitehouse, 2007; Kaufman et al., 2007). Moreover, nitrogen isotope increases of > 2 ‰ in the ca. 2.53 Ga Gamohaan Formation relative to values from the Palaeoarchaean suggest coupled nitrification and denitrification (chemolithotrophic pathways) or anaerobic ammonium oxidation reactions (Godfrey and Falkowski, 2009). The necessity of access to free oxygen for these metabolic pathways supports the emergence of widespread oxygenic ecosystems around this time.

5.4. Summary Meso-Neoarchaean

The Meso-Neoproterozoic saw the appearance of consolidated, stable continents with the development of adjacent continental platforms on their passive margins. A gradual decrease in internal mantle heat flow (with episodic increases related to large increases in volcanic activity) and an increase in horizontal plate tectonics contributed to the

phenomenon of the building of stable continents. Concomitant with the establishment of continents and their tectonic mountain ranges came erosion down to the granitic cores of the continents (still K-poor TTG granites), a marked change in the composition of terrigenous sediments that became more quartzitic, and the release of nutrients essential for life, in particular phosphorus. Intracratonic basins and fluvial systems added to environments that could be colonised by life. Microbial life colonised terrestrial fluvial environments as of about 3.22–3.209 Ga (Moodies Group, Barberton, Homann, 2019) and evidence for phototrophic stromatolites in ephemeral intercontinental basin lakes occurs in the 2.7 Ga Tumbiana Formation, Pilbara (Buick, 1992; Lepot et al., 2008) confirms the gradual extension of life inland, away from continental margins. It is possible that life transitioned towards terrestrial environments at an earlier stage, but these were not preserved in the rock record (although Retallack and Schmitz (2023) identified potential coastal plain sediments and associated spindle-shaped structures, possibly microfossils, in the Palaeoarchaean Strelley Pool Chert). With respect to the Southern African craton, Hickman-Lewis and Westall (2021) noted the gradual migration of life into terrestrial biomes concomitant with the growth and stabilisation of continents, a situation that Cawood et al. (2018) compares with the "Matworld" scenario of Lenton and Daines (2016).

Perhaps the most striking change in microbial evolution is the development of extensive carbonate platforms and large, at times giant, stromatolites across the globe. As with the Palaeoarchaean stromatolites at 3.4 Ga Strelley Pool Chert, environmental conditions and stresses in terms of water depth, dynamics and nutrient availability affect the morphology of the stromatolites. The relative abundance of phosphate and other transition metals brought in by rivers from erosion of the newly available continental cores would have contributed to biomass development. The abundance of biomass documented by the development of the large carbonate platforms and stromatolites attests to the availability of nutrients and, perhaps even without the geochemical evidence for increasingly oxygenic conditions through the Meso-Neoarchaean period, to the evolution of a more efficient metabolism, that of oxygenic photosynthesis. The evolution of oxygenic photosynthesis from anoxygenic photosynthesis was key to the further evolution of life on Earth through the revolution of the energetic and enzymatic fundamentals of life (Homann-Marriott and Blankenship, 2011). The latter authors state that "The repercussions of this revolution are manifested in novel biosynthetic pathways of photosynthetic cofactors and the modification of electron carriers, pigments, and existing and alternative modes of photosynthetic carbon fixation. Furthermore, the presence of large, acritarch-like microfossils occurring in shallow water sediments, such as those of the Palaeoarchaean Strelley Pool Chert (Sugitani et al., 2015), the Mesoarchaean Moodies Group (Javaux et al., 2010), or the Farrell Quartzite (Grey and Sugitani, 2009) beg the question as to whether they represent phototrophic organisms (benthic or planktonic) or even primitive eukaryotes (although, as noted above, such structures could be explained as wall-less cells (Kanaparthi et al., 2024).

Energy for maintaining metabolic processes in all life forms is processed by the flow of electrons from an electron donor to electron acceptor, controlled by protein complexes that always contain metallo-organic cofactors. There are different ways of storing energy, either by dissipating the energy gradient (generating or breaking chemical bonds) or by the presence of membrane-bound complexes that couple the transfer of electrons across the membrane to the generation of an ion gradient and transmembrane electrical potential. Energy thus produced is stored in ATP (adensoine triphoqphate), a chemiosmotic mechanism was likely present in the last common ancestor and has been carried forward to the three presently persisting domains of life, Bacteria, Archaea, and Eukarya (Lane et al., 2010). While oxygen can be produced by nitrite-driven anaerobic methane oxidation by oxygenic bacteria (Ettwig et al., 2010), it is only through oxygenic photosynthesis that large quantities of the gas can be generated (Homann-Marriott and Blankenship, 2011). Oxygenic photosynthesis is a process by which the decomposition of water is carried out by a water-splitting complex in oxygenic photosynthesisers containing a manganese (Mn) cluster in Photosystem II. The energy provided by the photon enables the photolysis of water through an electron transport chain, facilitating the production of O_2, protons, and electrons needed for the rest of the photosynthetic process. Table 1 illustrates the amount of energy obtained from various reductants, highlighting the huge difference between reduction of H_2O and other common reductants. It was the evolution of this particular process that provided Meso-Neoarchaean phototrophs with the potential for significant biomass development, limited only by nutrient availability Sánchez-Baracaldo et al., 2022). Nisbet and Fowler (2014) consider the change in phototrophic mat communities and architecture as an evolution through the "age of Rubisco" from the CO_2-specific form I Rubisco to a more specialised and efficient enzymatic machinery that resulted in ecological advantages. The evolution of photosynthetic bacteria was complex and involved lateral gene transfer of photosynthetic components and one or more endosymbiotic events (Homann-Marriott and Blankenship, 2011).

Anoxygenic photosynthesisers may already have appeared by 3.7 Ga (Czaja et al., 2013) and were definitely widespread by 3.5 Ga (Noffke et al., 2013). The question then is, when and how did oxygenic phototrophs emerge? Sánchez-Baracaldo et al. (2022) reviewed evidence based on comparative structural biology, phylogenetic analyses and molecular clocks, experimentation and ecological studies, which suggests that some form of water oxidation coupled with phototrophy existed already in the Palaeoarchaean (Fig. 9). The limiting factors would have been the availability of other reductants for electron transfer, such as Fe^{2+}, H_2S, and H_2 since, when present, even today cyanobacteria can switch to anoxygenic photosynthesis using these reductants. Thus, only when the availability of these reductants started to become reduced through geochemical changes in seawater related to geological evolution, could microorganisms with the capacity for oxidising the most commonly available reductant, water, take over from anoxygenic phototrophs. Limited availability of phosphorus as a nutrient would also have contributed to a delay in the appearance of oxygenic phototrophs. The early oxygenic phototrophs were primarily benthic and, therefore, limited to shallow water coastal and terrestrial environments. Major diversification of cyanobacteria occurred in the Neoarchaean although lack of preservation of cyanobacterial fossils hinders more precise estimations. This diversification included multicellularity, an increase in cell size and differentiation of cells used for specific metabolic tasks. Sánchez-Baracaldo et al. (2022) note that, although Neoarchaean and Proterozoic benthic microbial mats and stromatolites were widespread in these environments, their biomass was nowhere near as high as that of the later appearing planktonic algae that accompanied a major increase in atmospheric oxygen.

Although phototrophic ecosystems have specific environmental

Table 1
Redox midpoint potentials of electron donor and electron carrier redox couples (after Homann-Marriott and Blankinship (2011)).

Reductant	Redox couple	Redox midpoint potential at Ph7 (V)
Hydrogen	$H_2/2H^+$	-0,42
Sulphide	$H_2S/^0$	-0,24
Ferrous iron	$FE^{2+}/Fe(OH)_3$	0,15
Hydrogen peroxide	H_2O_2/O_2	0,27
Water	**$H_2O/1/2O_2$**	**0,815**
ferroxidoxin (red)	Fd(red)/Fd(ox)	-0,43
NADPH	NADPH/NADP	-0,32
menaquinol	MQ(red)/MQ(ox)	-0,07
Ubiquinol	UQ(red)/UQ(ox)	0,1
Plastquinol	PQ(red)/PQ(ox)	0,01
Rieske FeS cluster	RFeS(red)/RFeS (ox)	0,100-0,270

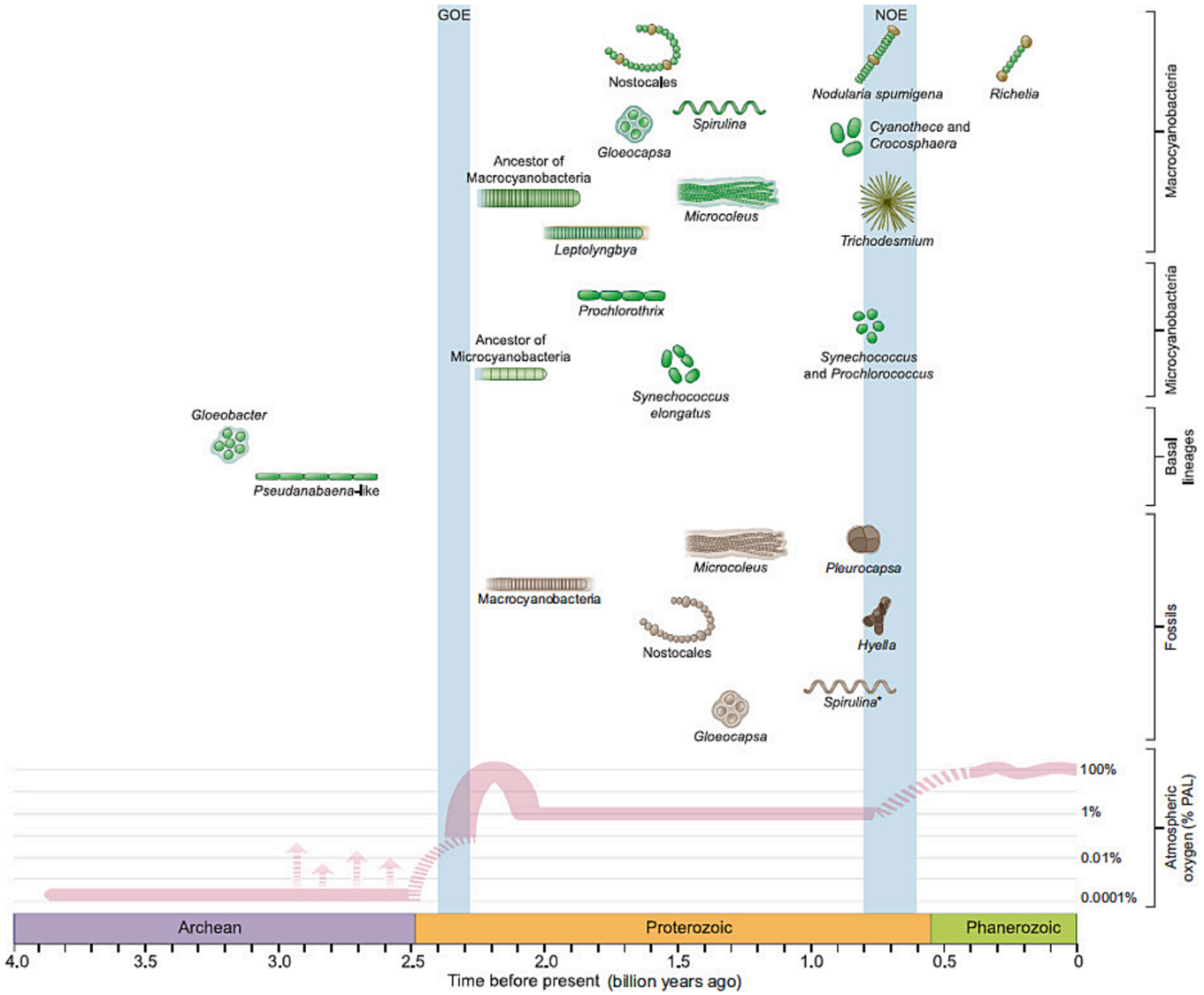

Fig. 9. Evolution of oxygenic phototrophs through geological time (Sánchez-Baracaldo et al., 2022).

requirements, *i.e.*, access to sunlight, this is not the case for chemosynthetic microbial communities. Nevertheless, chemosynthesisers form an integral part of a phototrophic mat community (Stal, 2012) with which their geochemical signatures are frequently associated.

While stromatolites flourished in the Meso-Neoarchaean period, nevertheless, there was a delay in a concomitant rise in atmospheric oxygen. This was influenced largely the presence of chemical buffers, such as ferrous iron, which, when oxidised, forms magnetite, hematite, and siderite, typical components of BIFs. Deposition of BIFs may be attributed to the evolution of oxygenic phototrophs, particularly from the Mesoarchaean onwards, although ferric mineral production by anoxygenic phototrophs using ferrous oxide as an electron donor were probably the main agent prior to the Mesoarchaean (Olson and Blankenship, 2004). However, as noted above, there is clear geochemical evidence for a rise in oxygen through the nitrogen cycle (Godfrey and Falkowski, 2009), from chromium signatures (Frei et al., 2009), and the evidence from sulphur isotopes (Farquhar et al., 2007). However, the Neoarchaean rise in atmospheric oxygen was not monotonic, rather it was characterised by oscillations up to ca 2.5 Ga (Gumsley et al., 2017).

A noticeable evolution between the Palaeoarchaean and the Neoarchaean is the decrease in the preservation of carbonaceous microfossils. Certainly, the coarse-grained clastic sediments that started to appear in the Mesoarchaean are less conducive to microfossil preservation as such (an exception being the fine-grained chert matrix of rod-shaped casts occurring in vadose deposits of the Moodies Group (Homann et al., 2016). Mantle heat flow started to decrease towards the end of Mesoarchaean and into the Neoarchaean, thus there would have been a gradual decrease in the amount of ocean silica produced by hydrothermal venting. Nevertheless, as we noted above the apparent importance of silica as a fossilising agent with respect to Palaeoarchaean carbonaceous microfossils, with an important contribution of dissolved silica coming from devitrification of the predominant volcanic sediments. With the introduction of quartzitic sediments, more difficult to dissolve than volcaniclastics in the early oceans, organic microbial components were degraded and oxidised before silicification could occur.

Carbonate is less favourable as a fossilising agent than silica. Summons et al. (2011) note the following mineral matrices in order of ascending preservation: ice, halite, sulphates, carbonates, phyllosilicates, silica, hematite, and phosphates. Microfossil preservation in the Meso-Neoarchaean formations is rare. Kazmierczak et al (2009), however, describe coccoidal casts in microbial mats whose mucilaginous matrix was fossilised by calcium carbonate with an admixture of Al–K–Mg–Fe silicates, similar to modern benthic colonial cyanobacterial mats.

6. Proterozoic

6.1. Geological and environmental evolution

Episodic geological evolution linking mantle to atmospheric processes during the Proterozoic continued with cycles of continent building and massive volcanism associated with the breakup of supercontinents, particularly centred around 2.1, 1.9, and 1.1 Ga (O'Neill et al., 2013; Hawkesworth et al., 2020). These are summarised by the latter authors as being indicated by upper mantle depletion events in ε_{Nd}, Nb/Th, osmium isotope and $^4He/_3He$, in the palaeomagnetic, palaeomagnetic intensity and sulphur isotope mass-independent fractionation data. Modelling of the various causes of mantle overturn from episodic subduction, mantle avalanches, basalt–eclogite transition episodicity to the dynamics of the 'basalt barrier' at the 670 km discontinuity, all produce the same end effect (O'Neill et al., 2013).

6.1.1. The Great oxidation event

The Palaeoproterozoic is dominated by the so-called Great Oxidation Event (GOE, Holland, 2002; Lyons et al., 2014) that coincided with the first global glaciation event (between ca. 2.46 and 2.426 Ga, Gumsley et al., 2017). The GOE was a "tipping point" for the rise of oxygen in the atmosphere and upper ocean after neutralisation of the various buffers (such as reduced mantle H_2, C, S, Fe^{2+}) that consumed free oxygen as it was produced by oxygenic phototrophs. As noted above, the gradual decline in the availability of reductants other than water (Fe^{2+}, H_2S and H_2) stimulated the flourishing of oxygenic phototrophs. The increased oxidation of the oceans and production of molecular oxygen stimulated the productivity of oxygenic phototrophs even further, which resulted in the production of more oxygen and therefore biomass. As a consequence, organic carbon was removed from the environment by deposition and burial, as indicated by the carbon isotope signatures (e.g., Bekker et al., 2001). At the same time, mantle events led to the production of significant effusions of volcanic rocks to form the first Large Igneous Provinces (LIPs) that formed on an amalgamated super continent comprising the Transvaal, Pilbara, and Superior-Korelia provinces (Fig. 10, Gumsley at al., 2017; Chen et al., 2022). Erosion of these low-latitude terrains provided nutrients (including phosphorus) for the development of phototrophic mats in the shallow water environments of the extensive continental platforms.

The preplacement of prviously reducing (and "greenhouse") gases in the atmosphere, such as methane and hydrogen, by oxygen led to decreasing global temperaturesand global glaciation. The change from a reducing atmosphere to an oxidising one is strongly marked in the mass dependent/mass independent sulphur isotope record (Farquhar et al., 2007), characterised by the importance of mass independent sulphur isotope fraction ation before the GOE compared with variations in carbon isotope fractionations before and after the GOE (with a similar carbon isotope scenario following the Sturtian glaciations of the Neoproterozoic). The massive rise in atmospheric oxygen and the consequent massive increase in biomass development led to the strongest known carbon isotope excursion in the geological record, the Lomagundi Excursion event that lasted from 2.3 to 2.1 Ga (Karhu and Holland, 1996). The anomalous behaviour of the carbon isotope record during the Lomagundi Excursion probably represents intense burial of reduced, biological carbon and indicates an increase of more than an order of magnitude of oxygen in the atmosphere. The following drop in atmospheric oxygen levels may have been controlled by intense continental weathering, drawing down the still limited amount of atmospheric oxygen (Bekker and Holland, 2012).

The Mesoproterozoic from about 1.8–0.8 Ga is often referred to as the "boring billion" in which carbon isotope compositions are remarkably stable (e.g., Lyons et al., 2014). It was characterised primarily by deep ocean anoxia as opposed to the moderately oxidising conditions of the upper ocean and terrestrial surfaces (Canfield, 1998). Geochemical evidence from redox sensitive elements (Mn, Cr, for example) suggest that, locally, ocean shelves exhibited signs of euxinic conditions, which would have affected biome conditions through feedback mechanisms related to biomass production, H_2S generation and metal availability. However, for much of the Palaeo-Mesoproterozoic, while surface waters were oxygenated, the deep oceans were anoxic and Fe^{2+} rich, although there is increasing geochemical evidence for seafloor oxygenation during this period. For example, Xu et al. (2023) conclude that more than half the global seafloor was oxygenated in the period between 1.60–1.54 Ga on the basis of molybdenum isotopes coupled with sulfur and carbon isotope compositions and trace element contents from the carbonates and mudstones of the Gaoyuzhuang Formation in the North China Craton. This changed in the Neoproterozoic when a combination tectonic processes led to the pileup of LIPs on the equatorially centred supercontinent Rodinia that subsequently broke up (Li et al., 2008). Increased chemical weathering of the igneous material resulted in a large increase in the flux of biolimiting nutrients to depositional basins and, thus, to increased biomass development and higher organic carbon burial (Gumsley et al., 2013). Concomitant to increased biomass development and oxygenation of the environment was the formation of giant iron and manganese deposits.

For all the apparent monotony of the Mesoproterozoic, important evolutionary advances were made with the appearance of eukaryotes, organisms comprising membrane-bound organelles that were, for the majority, aerobic. However, limitations in the availability of oxygen likely inhibited the evolution of animals until the second significant oxidation event associated with the Sturtian glaciation that was provoked by a concatenation of geological and biological processes including the assembly of large landmasses at low latitudes, LIPs, incipient rifting, enhanced erosion and the production of nutrients, enhanced biomass development and high rates of organic carbon burial leading to surface oxygenation, and Snowball Earth glaciations (Fig. 10; Gumsley et al., 2017).

6.2. Proterozoic biosphere

The Proterozoic is dominated by the widespread development on all cratons of stromatolites (prokaryotes) and carbonate platforms. This was the "golden age" of stromatolites, created by communities of microorganisms, primarily with phototrophs as the primary producers (Figs. 9, 11, 12). In shallow water environments, whether platform or intracratonic, oxygenic phototrophic communities that had already displaced anoxygenic ones in the Meso-Neoarchaean dominated, while in the non-phototrophic biosphere, oceans or otherwise, chemotrophs continued their discrete existence. However, a major change in the evolution of life during the Proterozoic was the development of the Eukarya. Whenever they may first have first appeared (some believe during the Meso-Neoarchaean, others later in the Proterozoic), their gradual rise in the Proterozoic was predicated on the availability of oxygen and the diversification of cyanobacteria (see review in Sánchez-Baracaldo et al., 2022).

6.2.1. Prokaryotes

6.2.1.1. Stromatolites. Fig. 11 illustrates a variety of Proterozoic stromatolites while Fig. 12 shows the distribution of stromatolites (anoxygenic then oxygenic) throughout geological time (Awramik, 1991), illustrating the gradually increasing abundance of these phototrophic microbialites during the Proterozoic, culminating in the Neoproterozoic before a seemingly catastrophic fall off at the Proterozoic/Cambrian boundary. Not only did these phototrophic consortia increase in abundance but their diversity also increased during the Proterozoic (Awramik, 1991). Despite the increase in abundance and diversity throughout the Proterozoic, it was the Palaeoproterozoic that saw the evolution of all the major morphological groups of stromatolites,

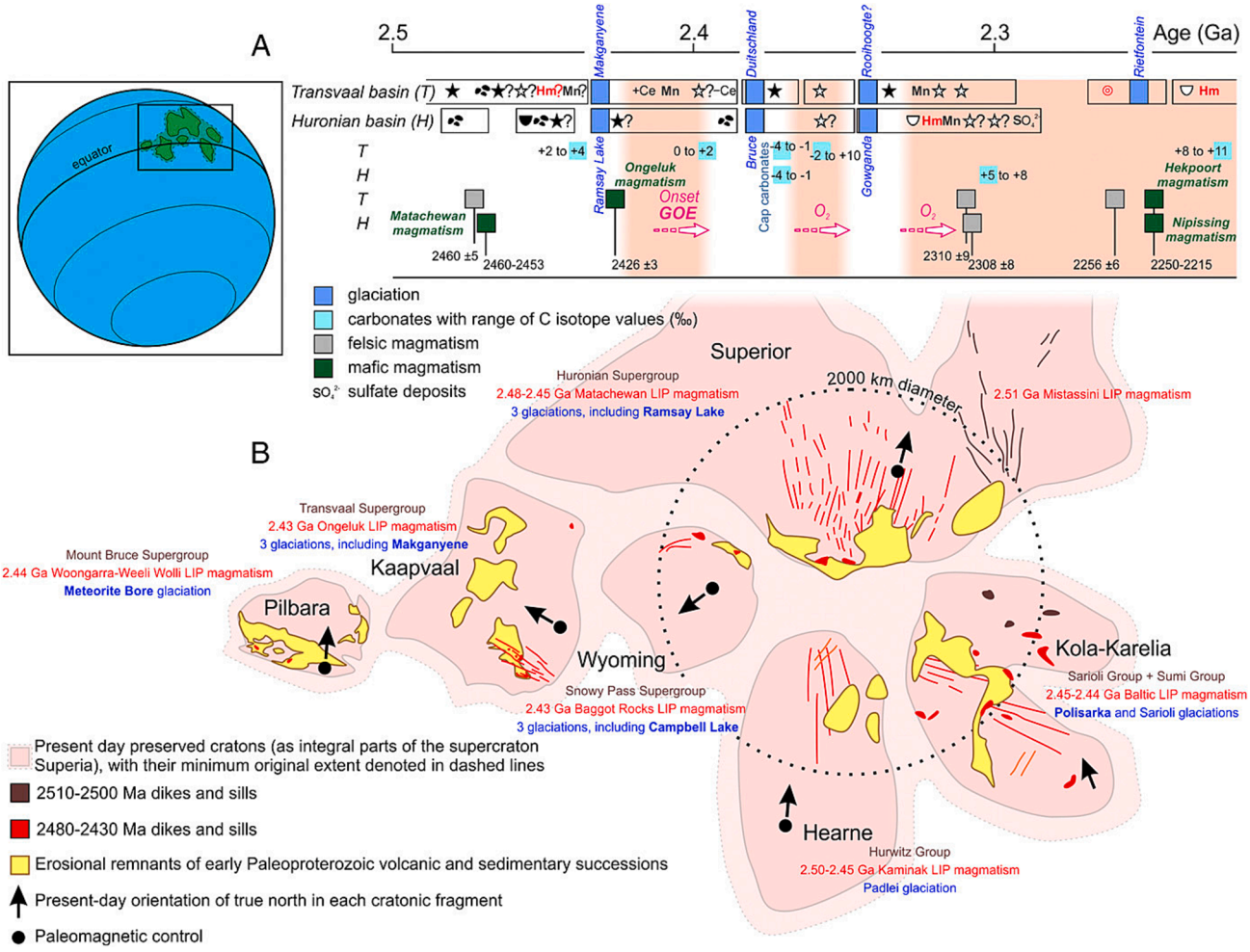

Fig. 10. The supercraton Superior. (A) Graph illustrating the approximate chronology of the glaciations and atmospheric oxygen oscillations according to the related redox indicators in the Huronian and Transvaal basins. (B) Reconstruction of the Neoarchaean-Palaeoproterozoic cratonic fragments of the supercraton Superior that were positioned near the palaeoequator. (Inset) The hypothesized palaeolatitude of these Archean cratons in the early Paleoproterozoic (Gumsley et al., 2017).

including columns, branching columns, cones, cylindrical cones, branching cones, domes, planar-laminated structures, and encapsulated laminar structures (oncoids) (Awramik and Sprinkle, 1999). The Mesozoic is commonly known as the "boring billion" but was actually the period of maximum stromatolite development as they diversified from the early Riphean (1650 to 1350 Ma) and into the middle Riphean (1350 to 1000 Ma) *(op. cit.)*. As the above authors note, "Biospheric, hydrospheric, atmospheric, and lithospheric conditions favored a major expansion of microbial life in shallow marine environments. No disruptive events or changes of significant magnitude and duration are recorded, at the resolution available, that might adversely have affected stromatolite communities". With the development of suitable basins and photic environments, cyanobacteria probably underwent a major adaptive radiation that included the appearance of new species of cyanobacteria that were better able to accrete sediment, thus forming new vertical stacking arrangements of laminae (Awramik, 1991). Awramik (*op. cit.*) hypothesised that the Riphean increase in stromatolite diversity may have been stimulated by the appearance of eukaryotes.

In an early but still highly relevant review of stromatolites, Monty (1974) examined the factors contributing to the growth, diversity and demise of stromatolites during the Proterozoic and, in particular the "gigantism" of the constructs in this time period. He noted that "the extension and gigantism of Precambrian stromatolites are a direct response of exponentially growing procaryotes to optimal realized hyperspaces which, generalized at this time, will be met again but very sporadically and locally afterwards …. Among the most important parameters of this success stand the possibility of optimal use of energetic sources, the unrestricted availability of nutrients, and the absence of encrusting competitive groups". Both diversity and abundance of Proterozoic stromatolites are documented across the globe, as is their rapid decline as attested by the disappearance of many types of stromatolites, loss of morphological and microstructural growth features and concomitant appearance of new ones, and the rapid decline in stromatolite size (*op. cit.*). Monty noted that developments in the morphology of the stromatolites could have been driven by ecological and physiological evolutions in the biomes of the phototrophic communities, as well as changes in the overall environment, such as the partial pressure of CO_2 in the atmosphere and other local environmental parameters (e.g., water turbulence, depth and alkalinity).

Considering the gigantism in the Proterozoic stromatolites, Monty (1974) discounted the effects of environmental parameters, such as tides, platform subsidence rates and specific temperatures, and suggest that other factors, including energy sources and nutrient availability, would have been more important. These oxygenic phototrophs actually develop best under high CO_2 levels, as well as ready access to nitrogen (in the form of nitrates) and phosphorus from continental weathering. These conditions were abundantly fulfilled during the Proterozoic (Catling and Zahnle, 2020; Stüeken et al., 2016, 2020). Finally, there were no other competitive or predatory organisms to inhibit phototrophic microbial community formation. However, as Monty (*op. cit.*) pointed out, despite the overall perfect conditions for stromatolite development during the Proterozoic, there were limitations.

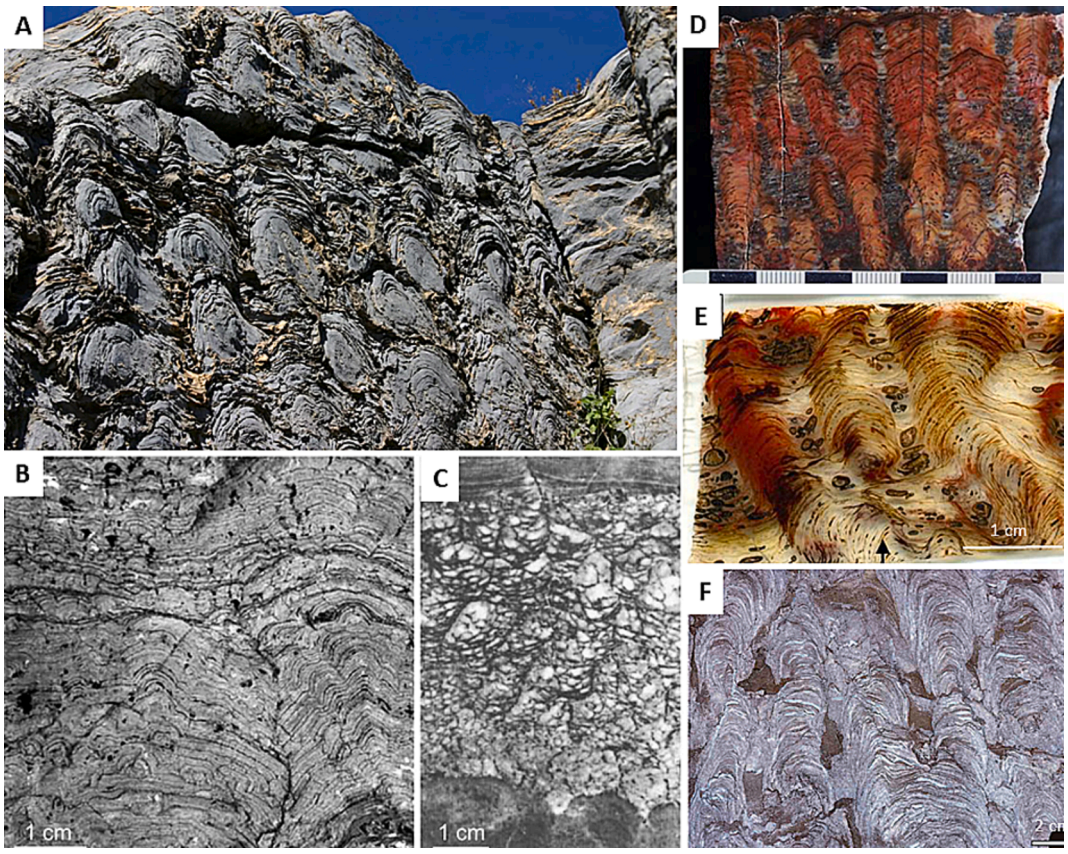

Fig. 11. Stromatolites from the Proterozoic. (A) Mesoproterozoic stromatolites from the Glacier National Park, Montana, USA (NPS). (B, C) Domical stromatolites from the 2.5 Ga Campbellrand-Malmani carbonate platform on the Kaapvaal craton (B) with micrographic detail of the fenestral texture (C) (Sumner, 2000). (D, E) Sectioned slab of stromatolites from the 1.9 Ga Gunflint Formation at Mink Mountain (D) (Arts, 2015) and optical micrograph of the columnar stromatolites (E) (Hubert, 2015). (F) Baicalia cf. rara from the Shisanlitai Formation, Neoproterozoic, Liaoning Province, China (Noffke and Awramik, 2013).

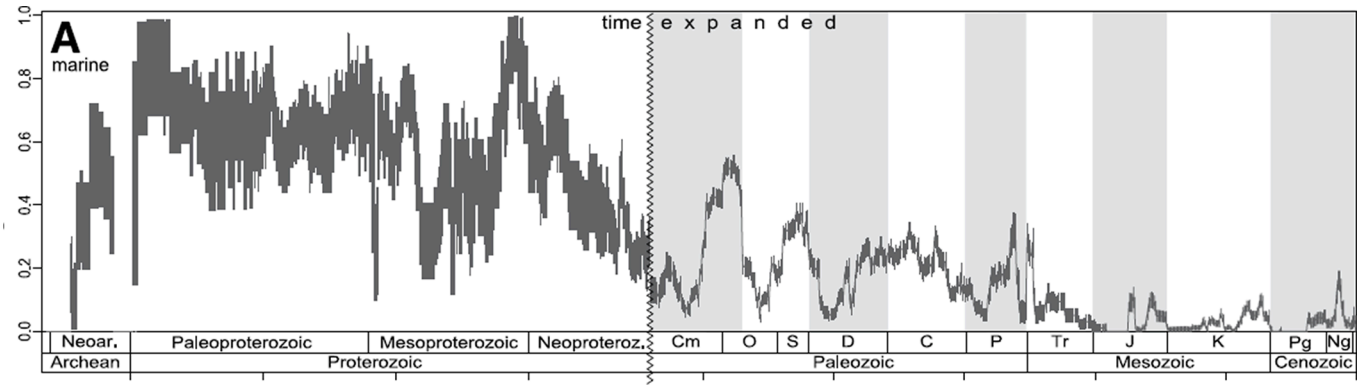

Fig. 12. Abundance of stromatolites throughout geological time based on North American data (Peters et al., 2017).

What were the limitations that led to the demise of the long-lived and flourishing stromatolites? It is commonly thought that, with the rise of animals and soft-bodied grazing organisms, stromatolites finally found an adversary (e.g., Awramik, 1991) and declined as the dominant prokaryotic phototrophic association to be replaced by other protistans, and metazoans that diversified to form more complex, multilevel ecosystems (Awramik and Sprinkle, 1999). However, Monty (1974, cf. also Riding, 2005) proposed an alternative explanation for their rapid disappearance, *i.e.*, that they were too successful. In a comprehensive review of stromatolite abundance in North America, Peters et al (2017) also noted that their decline started before the rise of metazoans (Fig. 13). As noted above, stromatolites and their cyanobacterial-dominated communities were responsible for the production of large amounts of oxygen, but these oxygenic phototrophic microorganisms develop best under conditions where there is a significant amount of CO_2. A decrease in atmospheric CO_2 would have inhibited their development and contributed to the flourishing of eukaryotic animals, such as green and red algae. Moreover, as Monty (1974) noted, blooms of algae produce toxins that have negative effects on potential eukaryotic grazers. This may have had an inhibiting effect on their rise in the Neoproterozoic. Reviews of stromatolites throughout geological time are covered by Riding (1999, 2000, 2008).

In a review of life during the Palaeoproterozoic, Javaux and Lepot (2018) highlighted the interplay of geochemical conditions at various

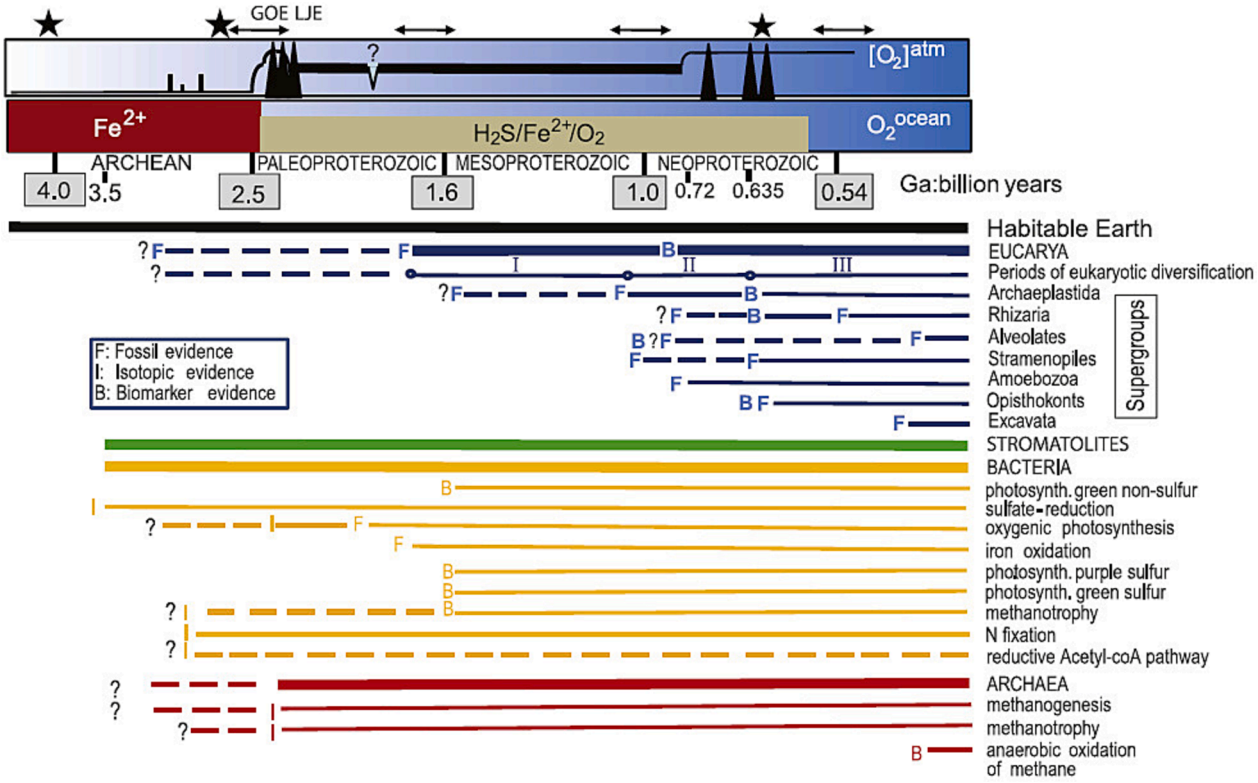

Fig. 13. Temporal evolution of microbial metabolisms with the global evolution of atmospheric and oceanic composition throughout geological time (Javaux and Lepot, 2018).

water depths and at various times in the oceans on the relationships between different types of microbial groups (prokaryotes and eukaryotes). Variations in anoxia, dysoxia or euxinic bottom water conditions indicate temporal and spatial changes in the redox state and composition of the bottom waters (Johnston et al., 2009). Significant differences in redox conditions characterised the period colloquially known as the "boring billion" (~1.9–1.8 to ~ 0.8 Ga), when sulfidic (H_2S-rich) anoxic conditions (euxinia) characterised continental shelves and epicontinental seas owing to prolific phototrophic development in the planktonic domains that produced organic matter to support sulphate reducer reduction (Poulton et al., 2010). Fig. 13 illustrates the covariation of microbial metabolisms with global atmospheric and oceanic compositions through geological time (Javaux and Lepot, 2018).

6.2.1.2. Other prokaryotic microbial traces. Javaux and Lepot (2018) underlined the difficulties in interpretation of biogenicity and the assignment of individual microfossils to specific domains and species. For example, the enigmatic cylindrical microfossil *Navifusa majensis* from the McDermott Formation, Tawallah Group, Australia (1.78–1.73 Ga) was interpreted as a fossil cyanobacterium. Moreover, on the basis of thylakoids preserved in *N. majensis* fossils from Tawallah Group and the Shaler Supergroup, Canada (1.01–0.9 Ga), Demoulin et al. (2019) conclude that there is direct evidence for oxygenic photosynthesis and for the existence of a metabolically active vegetative cell rather than a cyst (akinete) stage. Javaux and Lepot (2018) summarised the geochemical and morphological evidence indicating the existence of eukaryotes, cyanobacteria, green and purple sulphur bacteria, methanogenic archaea and/or bacteria, sulphate-reducing bacteria, methanotrophic bacteria and/or archaea, iron-oxidizing bacteria, anoxygenic photosynthetic bacteria, and denitrifying bacteria. This diversity is linked to changes in ocean chemistry with respect to the availability of specific transition metals necessary for metabolisms necessary for assimilating nitrogen, such as Fe, Mo, Ni, Cu and V (Anbar and Knoll, 2002; Buick, 2007; Glass et al., 2009; Johnston et al., 2009; Konhauser et al., 2009). For example, the 1.64 Ga Barney Creek Formation contains biomarkers for green and purple sulfur bacteria (anoxygenic photosynthesisers) (Brocks et al., 2005).

The presence of a stratified ocean during the Palaeoproterozoic would have had significant effects on the metabolisms of phototrophic organisms. Above the euxinic levels, cyanobacteria may have used anoxygenic strategies based on H_2S and/or they may have been supplanted by anoxygenic photosynthetic bacteria metabolizing H_2S or Fe^{2+} (Johnston et al., 2009). Note that toxicity from Fe^{2+} may have affected planktonic cyanobacteria (Swanner et al., 2015).

Stüeken et al. (2016) used the nitrogen isotope record, combined with additional information on redox availability and sulphur and iron cycling on the early Earth, to investigate important changes in the nitrogen cycle during the Precambrian. They concluded that there had to have been an early origin of biological N_2 fixation since a large biosphere could not have been supported by the available abiotic nitrogen sources. Moreover, the increase in evidence for nitrate through the Neoarchaean and Palaeoproterozoic corresponds with other evidence for an increase in oxygen at the same time. They also noted that nitrate availability alone was not a major driver of eukaryotic evolution. Finally, speciation and size of Proterozoic organisms may be related to the abundance of ferrous iron and sulphide (*op.cit.*).

6.2.2. Eukaryotes

The Proterozoic and Phanerozoic eons can be called the age of the Eukarya. Traditionally, the Eukarya is considered as one of the three domains of life, the other two being the Bacteria and the Archaea (Woese et al., 1990). More recent phylogenetic analyses provide support for a "two-domain" scenario, with the Eukarya nested within the Archaea (Eme et al., 2017; Hug et al., 2017). Indeed, the Eukarya seems to have emerged within an archaeal group called Heimdallarchaeia or the more inclusive archaeal group of Asgard or Asgardarchaeota (Eme et al., 2023). If true, then the universal tree of life consists of two domains, the Bacteria and the Archaea, which are separated from each other by the

deepest phylogenetic divide, with the Eukarya being a clade within the Archaea.

The prospect that the Eukarya may lose its domain status does not relegate its evolutionary importance because it embodies a number of key innovations. Indeed, the origin of eukaryotic cells is considered as a transformative event and a major transition in evolution (Maynard Smith and Szathmary, 1997). Typical eukaryotic cells contain membrane-bound intracellular structures, including nuclei, mitochondria, and, for photosynthetic eukaryotes (such as algae and plants), chloroplasts. They are also distinguished from prokaryotic cells by DNA-associated histone, eukaryotic gene regulation, and tubulin- and actin-based cytoskeletons, which enable endocytosis and exocytosis. Unfortunately, with few exceptions, most of these cellular and intracellular features are not easily fossilisable, making it difficult to differentiate simple, smooth-walled, unicellular eukaryotes from prokaryotic cells in the fossil record. As a result, unambiguous identification of eukaryotic fossils is often dependent upon more readily fossilisable and recognisable morphological features that may be derived, guided by comparison with living eukaryotic organisms. Excluding convergent evolution of such derived morphological features, these approaches necessarily limit our vision to the crown-group Eukarya, which represents the minimal clade that includes all living eukaryotes and their last common ancestor. In other words, these approaches do not specifically address the identification of stem-group eukaryotes (extinct lineages that lie outside a crown group but are more closely related to the crown group than to any other living group), particularly considering that a number of stem-group eukaryotes are likely prokaryotic (Xiao, 2022).

Our view of living eukaryotes is often biased towards familiar life forms that are multicellular and macroscopic, such as animals, fungi, plants, and seaweeds. However, many eukaryotes are unicellular and microscopic. These microscopic eukaryotes occupy the basal branches of the eukaryote tree (Keeling and Burki, 2019), with complex multicellularity (*i.e.*, multicellularity with cell differentiation) evolving a number of times within the eukaryotes (Knoll, 2011). Major clades of living eukaryotes include the Opisthokonta (e.g., animals, fungi, and their relatives), Amoebozoa, Archaeplastida (e.g., red algae, green algae, and glaucophytes), Stramenopila + Alveolata + Rhizaria (collectively known as SAR and examples of which are brown algae, dinoflagellates,

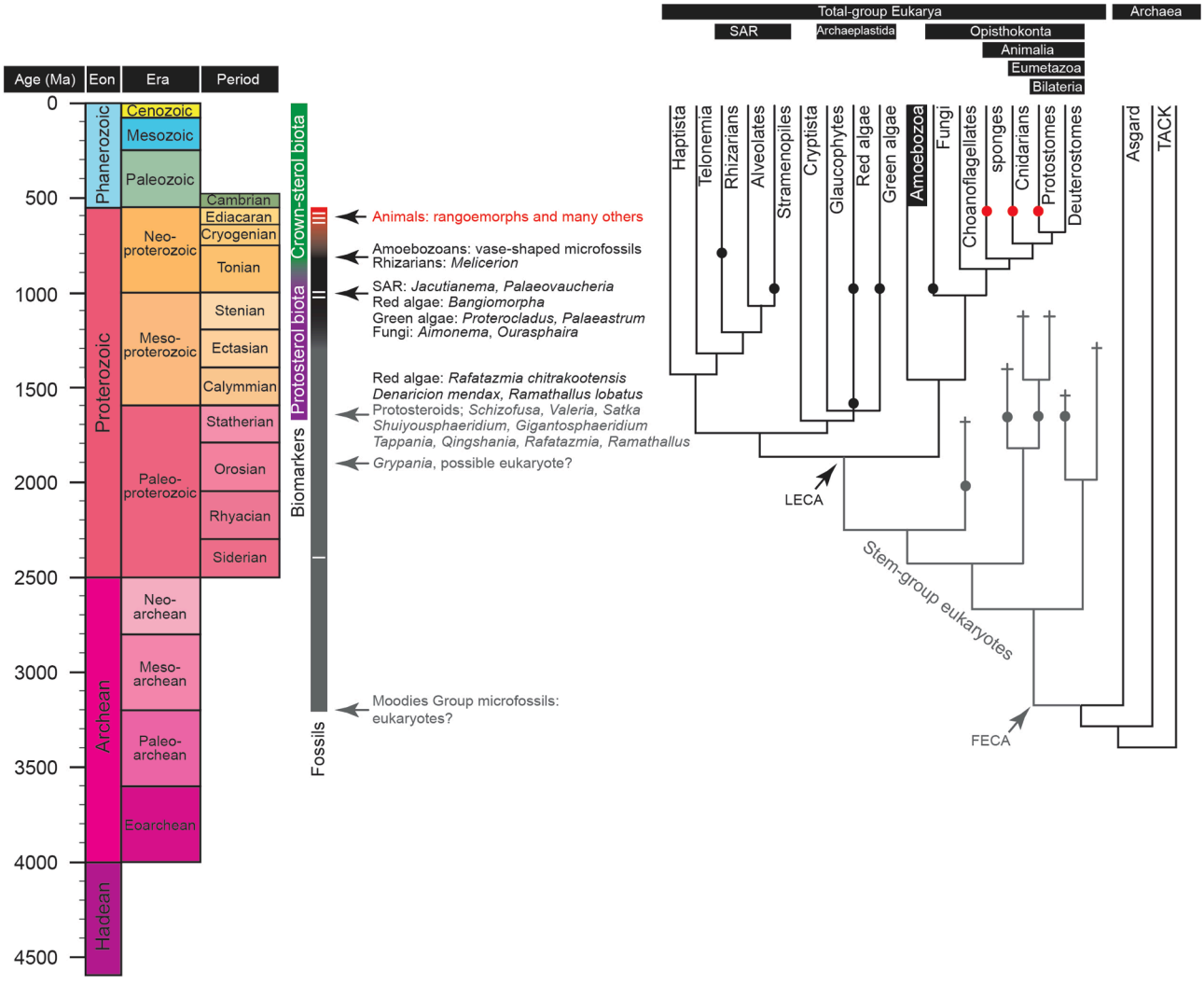

Fig. 14. Summary of Proterozoic eukaryote fossils. From left to right are: (1) geological time scale in million years before the present (Ma), eons, eras, and periods; (2) biomarkers exhibiting an age of protosterols (produced by stem-group eukaryotes and/or prokaryotes) and an age of sterols (produced by crown-group eukaryotes), after Brocks et al. (2023); (3) the three stage of eukaryote evolution (I: origin to stem-group diversification; II: crown-group diversification; III: radiation of multicellular eukaryotes including animals); (4) representative eukaryotic fossils discussed in the text; (5) phylogenetic tree of eukaryotes, showing major groups discussed in the text (Archaeplastida, SAR, Opisthokonta, and Amoebozoa). Phylogenetic divergence points are based on molecular clock estimates (e.g., Chernikova et al., 2011; Parfrey et al., 2011; Eme et al., 2014; Porter, 2020; Strassert et al., 2021). Major eukaryotic groups are labelled. Grey branches mark stem-group eukaryotes. Circular dots, colour-coded to match the three stage of eukaryote evolution, show schematically phylogenetic interpretations of some Proterozoic eukaryotic fossils. See text for details. LECA: last eukaryotic common ancestor. FECA: first eukaryotic common ancestor.

and foraminifers, respectively), Cryptista, Haptista (e.g., coccolithophores), and several other minor groups, with the rooting of the eukaryote tree unresolved (Keeling and Burki, 2019; Burki et al., 2020) (Fig. 14).

The timeline of eukaryote evolution is of geological importance because eukaryotic groups play important roles in geological and environmental processes. For example, coccolithophores are major primary producers in marine ecosystems in modern oceans and likely since the Triassic (Falkowski et al., 2004). In some marine environments, a single coccolithophore species, *Emiliania huxleyi*, accounts for 75 % or more of the total number of photosynthetic plankton (Holligan et al., 1993). As additional examples, the diversification of animals at the Proterozoic-Phanerozoic transition had a profound impact on the marine ecosystem and geochemical cycles (e.g., Canfield and Farquhar, 2009), and the ecological rise of eukaryotic primary producers in the Neoproterozoic likely played an important role in the evolution of the global carbon cycle and marine redox structures (Brocks et al., 2017; Brocks et al., 2023).

Molecular clocks provide a means to estimate the timeline of eukaryote evolution, although these estimates come with large ranges and uncertainties. For example, molecular clock estimates of the divergence of crown-group eukaryotes (*i.e.*, the age of the last eukaryotic common ancestor, or LECA; Fig. 14) range from > 2,300 Ma to ~ 1,000 Ma (Chernikova et al., 2011; Parfrey et al., 2011; Eme et al., 2014; Porter, 2020; Strassert et al., 2021), almost spanning the entire Paleo-Mesoproterozoic. Within the crown-group eukaryotes, the divergence of the crown-group Archaeplastida (which marks the origin of the primary plastid) is also a matter of debate, with estimated divergence time ranging from ~ 2,000 Ma to ~ 1,200 Ma (Strassert et al., 2021; Bowles et al., 2023). Likewise, molecular clock estimates of crown-group animal divergence time range from ~ 800 Ma to ~ 600 Ma (Dos Reis et al., 2015; Dohrmann and Wörheide, 2017).

Given the large uncertainty in molecular clock estimates, the fossil record – including body, trace, and molecular fossils (the latter also known as biomarkers) – provides an indispensable archive of eukaryote evolution. There have been numerous reviews on the fossil record of Precambrian eukaryotes focusing on taxonomic diversity (Knoll et al., 2006; Cohen and Macdonald, 2015), morphological disparity (Huntley et al., 2006; Xiao and Dong, 2006; Bykova et al., 2020), phylogenetic framework (Porter, 2020; Porter and Riedman, 2023), and evolutionary innovations (Javaux, 2007; Javaux, 2011; Xiao, 2013; Knoll, 2014; Butterfield, 2015). Below, we provide a brief review of Proterozoic eukaryote fossils (Fig. 14), updated from Xiao (2013) in the context of a phylogenetic framework to differentiate stem- vs. crown-group eukaryotes (Knoll, 2014; Butterfield, 2015; Porter, 2020; Xiao, 2022; Porter and Riedman, 2023).

Xiao (2013) proposed three stages of Precambrian eukaryote evolution: Stage I when stem group eukaryotes evolved (Neoarchaean–Mesoproterozoic); Stage II characterised by deep divergence of major eukaryote clades (late Mesoproterozoic–early Neoproterozoic); and Stage III represented by the radiation of multicellular eukaryotes (Ediacaran). Other reviews of Precambrian eukaryotes also recognise similar stages (Javaux, 2011; Knoll, 2014), although there are some minor differences in time of transition from one to the next stage. These stages are based mainly on body fossils, but they are broadly consistent with the geological distribution of eukaryote biomarkers (Brocks et al., 2023), lending some confidence that there are true signals in the Precambrian eukaryotic fossil record, no matter how sketchy it is.

6.2.2.1. Stage i (Neoarchaean? – Mesoproterozoic): Origin of eukaryotes and diversification of stem-group representatives. What is the oldest eukaryotic fossil? Are there Archean eukaryotic fossils? These are challenging questions, not the least because the oldest eukaryotes must have been morphologically simple – indeed, some early stem-group eukaryotes were likely prokaryotic (Xiao, 2022), but also because Archaean sedimentary rocks are limited and metamorphosed to various degrees. To date, no convincing eukaryotic fossils have been reported from the Archaean. Previous reports of eukaryotic biomarkers from Archaean rocks (e.g., Brocks et al., 1999; Brocks et al., 2003) have later been shown to be contaminants (Rasmussen et al., 2008). Relatively large (~120 μm in diameter) leiospheric organic-walled microfossils from the 3200 Ma Moodies Group in South Africa (Javaux et al., 2010) could be eukaryote microfossils, but as rightfully pointed out by the original authors, a bacterial interpretation cannot be excluded.

Since the proposed coupling between the diversification of aerobic eukaryotes and the rise of atmospheric O_2 levels (Knoll, 1992), it is widely speculated that eukaryotes evolved in the Palaeoproterozoic, concurrently with or shortly after the ~ 2.4—2.3 Ga Great Oxidation Event (Holland, 1994; Luo et al., 2016). Bengtson et al. (2017b) reported the discovery of fungus-like filaments from 2,400 Ma vesicular basalt in the early Palaeoproterozoic Ongeluk Formation of South Africa. If confirmed, this represents one of the oldest eukaryotic fossils. More research, however, is needed since the age of these fossils, between 2,400 Ma and 2,060 Ma (Bengtson et al., 2017b) is not tightly constrained, and the fungal affinity and biogenicity needs further substantiation (Berbee et al., 2020; McMahon et al., 2021).

Several late Palaeoproterozoic successions – including the Ruyang Group in the southwestern margin of the North China Craton, dated between 1711 ± 37 Ma and 1647.8 ± 3.4 Ma (Lyu et al., 2022), the Changcheng Group in the northern margin of the North China Craton, dated between 1,673 ± 10 Ma and 1,626 ± 9 Ma (age constraints summarised in Miao et al., 2024a), and the 1,700–1,600 Ma Semri Group of the lower Vindhyan Supergroup in central India (age constraints summarised in Bengtson et al., 2017a) – are particularly important in the study of Paleoproterozoic eukaryotes. Earlier investigations of Palaeoproterozoic eukaryotic fossils were focused on compressed carbonaceous macrofossils, such as *Grypania* (Fig. 15A–B), *Chuaria*, and *Tawuia*, which are present in the Palaeoproterozoic Changcheng Group and Negaunee Formation (Hofmann and Chen, 1981; Han and Runnegar, 1992; Zhu et al., 2000; but see Lamb et al., 2007), although these taxa are better known from younger rocks of Mesoproterozoic and Neoproterozoic ages. These fossils have been interpreted as eukaryotes (Walter et al., 1990; Sharma et al., 2009; Li et al., 2020; Tang et al., 2021), or alternatively as large bacteria cells or colonies (Steiner, 1994; Sharma and Shukla, 2009). In addition, irregularly shaped carbonaceous compression macrofossils from the Tuanshanzi Formation of the Changcheng Group have been interpreted as multicellular eukaryotes akin to living seaweeds (Yan, 1995b; Zhu and Chen, 1995; Yan and Liu, 1997; Qu et al., 2018), but they could alternatively represent ruptured fragments of microbial mats. These uncertainties have not been resolved because the taxa are morphologically simple, lack phylogenetically diagnostic morphological features, and could be polyphyletic in origin. Thus, Palaeoproterozoic carbonaceous compression macrofossils offer suggestive but inconclusive evidence for early eukaryote evolution.

Similarly, organic-walled microfossils (or acritarchs) with a smooth-walled spherical vesicle over 100 μm in diameter, often described as various species of *Leiosphaeridia* or related genera, provide suggestive but ambiguous evidence for Palaeoproterozoic (or even Archaean) eukaryotes. As mentioned above, leiospheres over 100 μm in diameter are present in the Archaean Moodies Group (3200 Ma) in South Africa (Javaux et al., 2010). Poorly preserved leiospheres have also been reported from the 2,150–1,950 Ma Hutuo Group in North China (Yin et al., 2020), and abundant well-preserved leiospheres are known from late Palaeoproterozoic Changcheng and Ruyang groups in North China (Yan and Liu, 1993; Agić et al., 2017; Miao et al., 2019; Miao et al., 2024a). Some leiospheres from the Ruyang Group contain a tantalizingly nucleus-like intracellular inclusion within the vesicle, although this structure more likely represents condensed protoplasts or reproductive spores rather than membrane-bound nuclei (Pang et al., 2013). Some leiospheres from the Changcheng Group – variously described under the

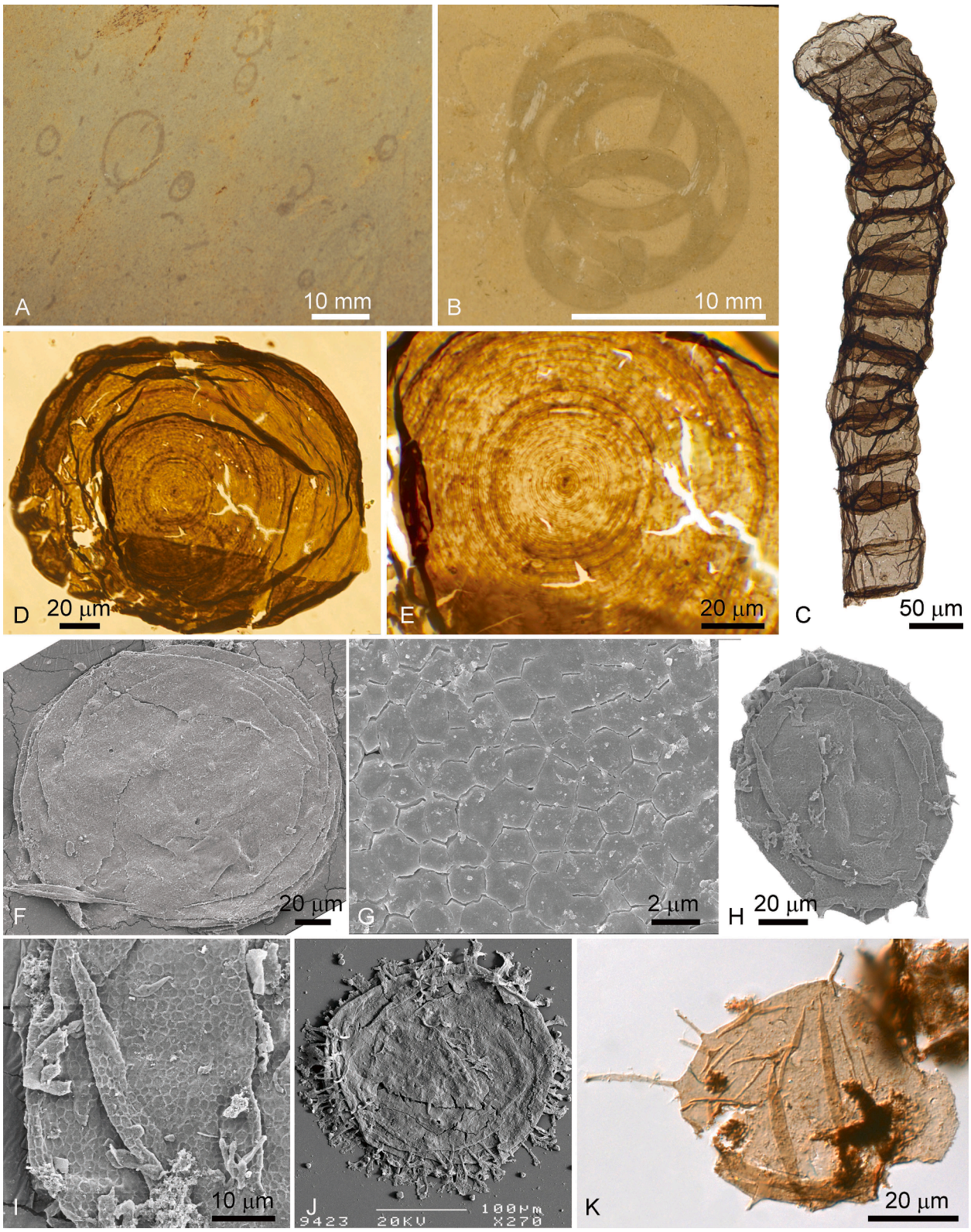

Fig. 15. Representative Stage I fossils. A–B: Grypania spiralis specimens from the Palaeoproterozoic Negaunee Formation (~1,900 Ma) in Michigan (Han and Runnegar, 1992; Schneider et al., 2002) and the Mesoproterozoic Gaoyuzhuang Formation (~1560 Ma) in North China (Walter et al., 1990), respectively. C: Qingshania magnifica from the Palaeoproterozoic Chuanlinggou Formation of the Changcheng Group in North China (Miao et al., 2024b). Courtesy of M. Zhu. D–J: Valeria lophostriata (D–E), Dictyosphaera macroreticulata (F–G), and Shuiyousphaeridium macroreticulatum (H–J) from the Palaeoproterozoic Ruyang Group in North China (Pang et al., 2015; Agić et al., 2017). E and I are magnifications of D and H, respectively. (D, E, J) Courtesy of K. Pang. K: Tappania plana from the Mesoproterozoic Kamo Group in Siberia. Courtesy of K. Nagovitsin. (A–B) are reflected light photographs; (C–E, K) are transmitted light photomicrographs; (F–J) are scanning electron photomicrographs.

genera *Schizofua* (Yan, 1982), *Schizovalvia* (Yan, 1985), and *Diplomembrana* (Yan, 1985) – show evidence of medial splits (Peng et al., 2009; Miao et al., 2019; Miao et al., 2024a), which have been interpreted as excystment structures (Moczydłowska and Willman, 2009). A eukaryotic affinity for these leiospheres was inferred on the basis of the large vesicle size, medial excystment structures, and vesicle wall ultrastructures (Lamb et al., 2009; Moczydłowska and Willman, 2009). A potential caveat is that vesicle size, medial excystment, and vesicle wall ultrastructures may not be diagnostic of eukaryotic affinities (Knoll et al., 2006). Hence, these leiospheres offer only tentative evidence for Palaeoproterozoic eukaryotes.

More convincing Palaeoproterozoic eukaryotic fossils are represented by acritarchs with vesicle-wall sculptures, which present greater morphological complexity than simple leiospheres. For example, *Valeria lophostriata* is characterised by concentric striations (Fig. 15D–E), indicative of the presence of a eukaryotic cytoskeleton system. This species has been reported from numerous Palaeoproterozoic (and Meso-Neoproterozoic) successions, including the Ruyang Group (Xiao et al., 1997; Pang et al., 2015; Agić et al., 2017), the Changcheng Group (Miao et al., 2019), the Limbunya Group (>1642 ± 3.9 Ma) in northern Australia (Riedman et al., 2023), and the ~ 1,650 Ma Mallapunyah Formation of the McArthur Group in Australia (Javaux, 2007). *Thecatovalvia annulata* (see also Yan and Liu, 1993; Yan, 1995a) and *Valvimorpha annulata* (Yan and Liu, 1993; nomen nudum) from the Chuanlinggou Formation of the Changcheng Group are morphologically similar to and perhaps taxonomically synonymous to *Valeria lophostriata*. Another example is *Satka colonialica* from the Chuanlinggou Formation (Miao et al., 2019), whose vesicle wall either bears plate-like structures (Miao et al., 2019) or broadly domical processes (Tang et al., 2015; Porter and Riedman, 2016), both of which are indicative of a eukaryotic affinity. A third example is *Dictyosphaera macroreticulata* (Fig. 15F–G), which is similar to the acanthomorphic acritarch *Shuiyousphaeridium macroreticulatum* (Fig. 15H–J) in having a vesicle wall constructed from interlocking polygonal plates but lack processes. *Dictyosphaera macroreticulata* and its synonyms (e.g., *Dictyosphaera delicata*) have been reported from the Palaeoproterozoic Ruyang Group (Xiao et al., 1997; Yin et al., 2005; Agić et al., 2015) and Changcheng Group (Miao et al., 2019), numerous Mesoproterozoic successions [e.g., the Roper Group in northern Australia (Javaux and Knoll, 2017), Dismal Lakes Group in Arctic Canada (Loron et al., 2021; where *Dictyosphaera smaugi* is also present), and the Greyson Formation of the Belt Supergroup in the USA (Adam et al., 2017), and the Xiamaling Formation in North China (Miao et al., 2021)], and the Meso-Neoproterozoic Shaler Supergroup (Loron et al., 2019a; where *Dictyosphaera tacita* is also present). The wide geographic distribution and continual geological record of *Dictyosphaera macroreticulata* add confidence to the notion that Palaeoproterozoic eukaryotes may have been widespread.

The confidence is boosted by the reports of multiple acanthomorphic (process-bearing) acritarchs from Palaeoproterozoic successions. Acanthomorphs can be conclusively interpreted as eukaryotes because only eukaryotes are known to have the cytological apparatuses necessary to produce processes (Knoll et al., 2006). In this respect, several Palaeoproterozoic acanthomorphs stand out as the most important taxa. Examples include *Tappania plana* (Fig. 15K) (and its junior synonyms *Tappania tubata* and *Tappania gangaei*; Agić et al., 2017; Javaux and Knoll, 2017), *Shuiyousphaeridium macroreticulatum* (Fig. 15H–J), *Shuiyousphaeridium pilatum*, *Gigantosphaeridium fibratum*, and *Gigantosphaeridium floccosum*; these genera were first reported from the Ruyang Group (Xiao et al., 1997; Yin, 1997; Li et al., 2012; Agić et al., 2015; Agić et al., 2017). *Tappania plana* has a worldwide distribution in Palaeo-Mesoproterozoic strata, with occurrences in the Chuanlinggou Formation of the Changcheng Group in North China (Miao et al., 2024a), the Semri Group (~1630–1600 Ma) of the lower Vindhyan Supergroup in central India (Prasad et al., 2005), the Limbunya Group (>1642 ± 3.9 Ma) in northern Australia (Riedman et al., 2023), the Palaeo-Mesoproterozoic Bahraich Group in the Ganga Basin of northern India (Prasad and Asher, 2001; Xiao et al., 2016), the early Mesoproterozoic Singhora Group of the Chhattisgarh Supergroup in southeastern India (Singh et al., 2019), the Mesoproterozoic Roper Group (~1400–1500 Ma) in Australia (Javaux and Knoll, 2017), the Mesoproterozoic Greyson Formation (~1454–1576 Ma) of the Belt Supergroup in Montana of the USA (Adam et al., 2017), and the late Mesoproterozoic Kamo Group in Siberia (Nagovitsin, 2009). *Gigantosphaeridium fibratum* has also been reported from the Palaeoproterozoic Limbunya Group in northern Australia (Riedman et al., 2023), the Meso-Neoproterozoic Nelson Head Formation of the Rae Group, and the lower Shaler Supergroup in Arctic Canada (Loron et al., 2019a). *Shuiyousphaeridium macroreticulatum* is thus far only known from the Ruyang Group, although *Shuiyousphaeridium echinulatum* has been described from the late Palaeoproterozoic Chitrakut Formation of the Semri Group in central India (Singh and Sharma, 2014). However, further study is needed to investigate whether the Chitrakut specimens could by synonymous with *Gigantosphaeridium floccosum*; if a synonymy is established, then a new combination of *Gigantosphaeridium echinulatum* would be warranted. Regardless, these acanthomorphs firmly establish that the Asgard-Eukarya divergence must have occurred in the Palaeoproterozoic or earlier.

Not only eukaryotes, but also multicellular eukaryotes may have evolved in the Palaeoproterozoic. Bengtson et al. (2017a) reported septate filaments (*Rafatazmia chitrakootensis*) and multicellular thalli (*Ramathallus lobatus*) from the Tirohan Dolomite of the Semri Group in central India. *Ramathallus lobatus* is remarkably similar to *Thallophyca* thalli from the Ediacaran Doushantuo Formation in South China (Xiao et al., 2004). Both *Ramathallus* and *Rafatazmia* are interpreted as possible crown-group red algae (Bengtson et al., 2017a). If confirmed, the morphological complexity of the Tirohan fossils represent paleontological evidence for multicellular eukaryotes in the late Paleoproterozoic.

The Tirohan multicellular eukaryotes are joined by the septate filamentous microfossil *Qingshania magnifica* (Fig. 15C) from the Palaeoproterozoic Chuanlinggou Formation of the Changcheng Group in North China (Yan, 1989; Yan and Liu, 1993; Miao et al., 2024b). The multicellular filament of *Qingshania magnifica* even shows tantalizing evidence of cellular differentiation, with its expanded clavate terminal cell possibly representing a specialised reproductive cell akin to spores.

As mentioned above, a number of Palaeoproterozoic eukaryote taxa also extend into the Mesoproterozoic. These include *Tappania plana* (e.g., Adam et al., 2017), *Dictyosphaera macroreticulata* (e.g., Adam et al., 2017), and *Valeria lophostriata* (e.g., Javaux and Knoll, 2017), the last taxon also extending into the Neoproterozoic (Hofmann, 1999; Baludikay et al., 2016; Beghin et al., 2017). It is not until the Meso-Neoproterozoic transition, when a renewed burst of eukaryote diversification occurred, that a wide range of crown-group eukaryotes appeared.

To summarise, the fossil record indicates that the Asgard-Eukarya divergence occurred in the Palaeoproterozoic or earlier and that some Paleoproterozoic eukaryotes likely evolved multicellularity (Fig. 14). However, with the exception of the Tirohan red algae (Bengtson et al., 2017a), most Palaeoproterozoic eukaryotic fossils cannot be phylogenetically placed, with confidence, in any major groups of living eukaryotes (e.g., Opisthokonta, Amoebozoa, Archaeplastida, SAR, Cryptista, or Haptista). The current consensus is that these fossils likely represent stem-group eukaryotes (Javaux, 2011; Xiao, 2013; Porter, 2020; Cohen and Kodner, 2022; Porter and Riedman, 2023).

6.2.2.2. Stage II (Meso–Neoproterozoic transition): Diversification of crown-group eukaryotes. The Mesoproterozoic is often characterised as the "boring billion" (Buick et al., 1995) or the "balanced billion" (Mitchell and Evans, 2023). This may be true from the perspective of supercontinent cycles, global carbon cycle, atmospheric redox history, or even taxonomic diversity. However, from the perspective of

evolutionary divergence and innovation, the Mesoproterozoic does not seem to have been quiescent. Instead, the fossil record shows that, at the Meso-Neoproterozoic transition, or in the Stenian and Tonian periods, a renewed diversification of eukaryotes occurred, with the appearance of a number of new forms that can be phylogenetically placed in living eukaryote subclades with varying degrees of confidence. In other words, they represent the diversification of crown-group eukaryotes.

Archaeplastida: A number of Stenian and Tonian taxa have been interpreted as members of the Archaeplastida. The carbonaceous compressions *Sinosabellidites huainanensis*, *Pararenicola huaiyuanensis*, and *Protoarenicola baiguashanensis* from the Tonian Jiuliqiao Formation in North China (Li et al., 2023) are tubular fossils a few millimeters in diameter and centimeters in length, characterised by closely spaced transverse annulations (Dong et al., 2008). These fossils, as well as the morphologically similar form *Parmia anastassiae* from Tonian rocks in the Timan region of Russia (Gnilovskaya et al., 2000), may have been tubular archaeplastidans with a coenocytic construction (*i.e.*, multinucleate cells) akin to living siphonous green algae (Dong et al., 2008). Similarly, *Tawuia* specimens from the Stenian-Tonian Shiwangzhuang and Liulaobei formations in North China have been interpreted as possible coenocytic archaeplastidans (Tang et al., 2021). Another example of possible archaeplastidans from the Tonian Period is *Longfengshania stipitata* from the Little Dal Group in Canada (Hofmann, 1985) and the Changlongshan (= Luotuoling) Formation in North China (Du and Tian, 1986; Jing et al., 2022), which was likely a millimeter-centimeter-sized benthic archaeplastidan with a simple holdfast connected with an ellipsoidal thallus via a stipe. The presence of archaeplastidans at the Stenian-Tonian transition is also consistent with the discovery of nickel geoporphyrin moieties in *Arctacellularia tetragonala* from the ~ 1,000 Ma Mbuji-Mayi Supergroup in the Congo Basin (Sforna et al., 2022).

Several Stenian-Tonian taxa stand out because they have been

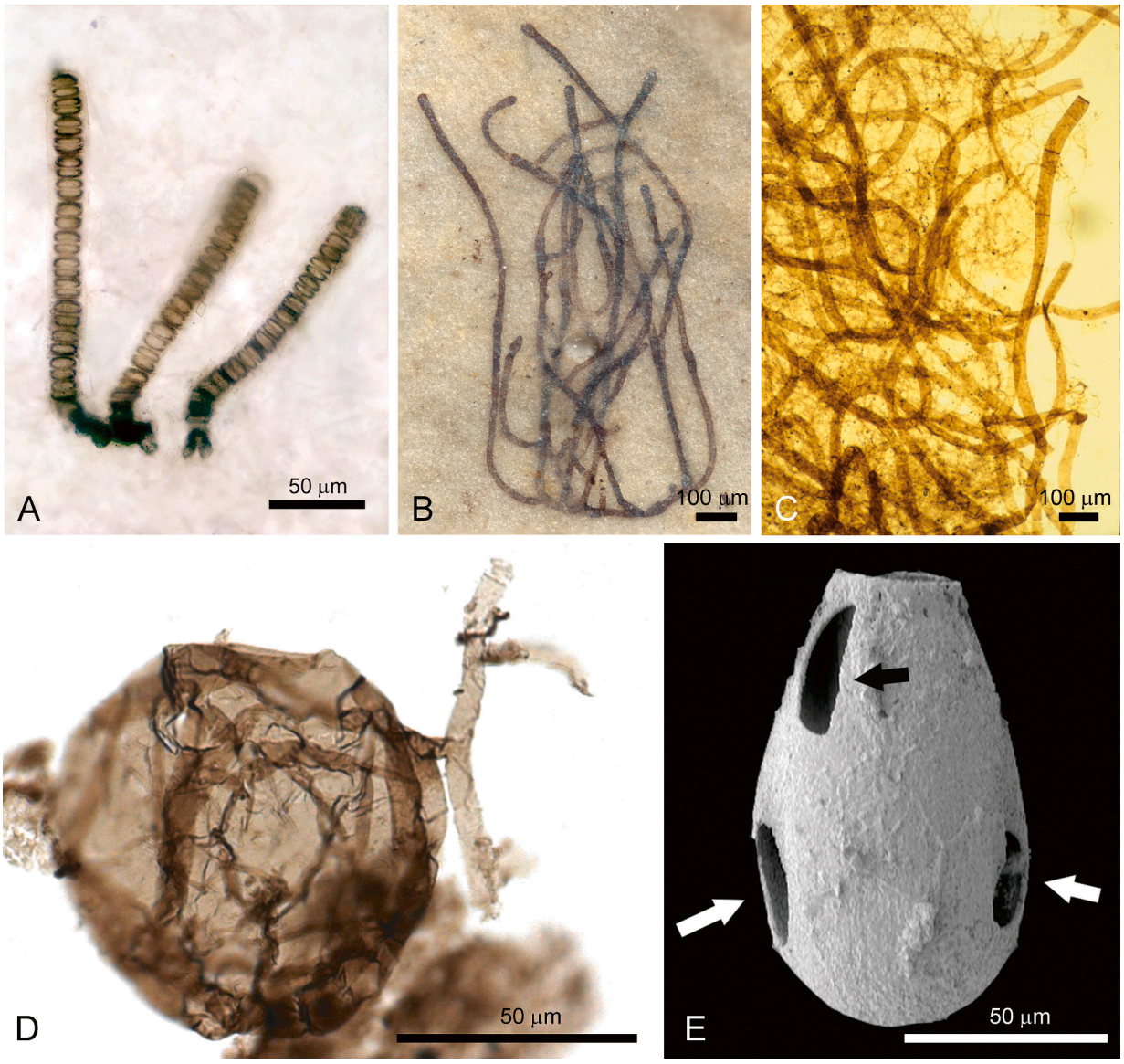

Fig. 16. Representative Stage II fossils. A: Bangiomorpha pubescens, a bangiophyte red alga, from the ~ 1,000 Ma Hunting Formation in Arctic Canada (Butterfield, 2000). Courtesy of N. J. Butterfield. B: Proterocladus antiquus, a siphonocladous green alga, from the ~ 1,000 Ma Nanfen Formation in North China (Tang et al., 2020). C: Palaeovaucheria clavata, a possible xanthophyte alga, from the ~ 1,000 Ma Lakhanda Group in southeastern Siberia. Courtesy of A. H. Knoll. D: Ourasphaira giraldae, a possible fungus, from the Grassy Bay Formation of the Shaler Supergroup in Arctic Canada (Loron et al., 2019b). Courtesy of C. C. Loron and E. J. Javauxa. E: Cycliocyrillium torquata, a vase-shaped microfossil interpreted as a lobose testate amoeba (amoebozoan), from the ~ 750 Ma Kwagunt Formation of the Chuar Group in Arizona, showing circular and semicircular drill holes (arrows) produced by predators (Porter, 2016). (A, C–D) are transmitted light photomicrographs; (B) is a reflected light photomicrograph; (E) is a scanning electron photomicrograph.

classified with specific archaeplastidan groups (*i.e.*, red and green algae), thus representing the crown-group Archaeplastida. *Bangiomorpha pubescens* (Fig. 16A) from the 1,047 Ma Angmaat and Hunting formations has been interpreted as a bangiophyte red alga (Butterfield, 2000; Gibson et al., 2018). This interpretation is based on a close morphological comparison with living bangiophytes, including the common feature of multicellular filaments with differentiated holdfasts and wedge-shaped reproductive cells (Butterfield, 2000).

At least two Stenian-Tonian microfossil genera, *Proterocladus* (Fig. 16B) and *Palaeastrum*, have been interpreted as green algae (Butterfield et al., 1994). Species of *Proterocladus* are known from the Svanbergfjellet Formation (ca. 811.5–752.7 Ma) in Svalbard (Butterfield et al., 1994), the Diaoyutai and Nanfen formations (ca. 1056–948 Ma) in North China (Tang et al., 2020; Li et al., 2023), the Khastakh Formation (ca. 820–720 Ma) of Siberia (Nagovitsin et al., 2015), and the Nonesuch Formation (ca. 1078 ± 24 Ma) in North America (Strother and Wellman, 2021). They are characterised by uniseriate and occasionally branching filaments with sparse septa, and compare very closely with living siphonocladous green algae such as Cladophora and Rhizoclonium (Tang et al., 2020). *Palaeastrum dyptocranum* (Butterfield et al., 1994), along with its possible synonyms *Palaeastrum hexangularis* and *Palaeastrum amplus* (Nagovitsin, 2001), may be another example of Stenian-Tonian green algae. *Palaeastrum* is known from the Svanbergfjellet Formation (ca. 811.5–752.7 Ma) in Svalbard (Butterfield et al., 1994), the Seryi Klyuch Formation (ca. 950–900 Ma) of the Tungusik Group in Siberia (Nagovitsin, 2001), lower Shaler Group (ca. 1,150–900 Ma) in Arctic Canada (Loron et al., 2019a), the Lakhanda Group (ca. 1015–1025 Ma) in southeastern Siberia (Hermann and Podkovyrov, 2010), the Chuar Group (ca. 780–740 Ma) in Arizona (Porter and Riedman, 2016), as well as the ~1500-Ma-old Kotuikan Formation in northern Siberia (Vorob'eva et al., 2015). It is characterised by colonies of spherical cells that are held together via attachment discs, similar to the living chlorophycean green alga *Coelastrum*.

SAR: The fossil record of SAR has also been reported from the Stenian and Tonian periods. The vase-shaped microfossil *Melicerion poikilon* from the Chuar Group has been interpreted as a euglyphid testate amoeba, thus representing a member of the rhizarian clade (Porter et al., 2003). *Palaeovaucheria clavata* (Fig. 16C) and *Jacutianema solubila* from the Lakhanda Group (Hermann, 1990), the latter also from the Svanbergfjellet Formation (Butterfield, 2004), are multicellular organisms characterised by a suite of reproductive features reminiscent of living xanthophyte algae, which belong to the stramenopiles, whose plastids were derived from a red alga through a tertiary endosymbiosis event via the cryptophytes (Stiller et al., 2014; Strassert et al., 2021). Butterfield (2015) later cast doubt on the xanthophyte interpretation of *Palaeovaucheria clavata*, arguing that a morphologically similar taxon, *Aimonema ramosa* from the Lakhanda Group in Siberia (Hermann and Podkovyrov, 2010), shows evidence of cell fusion, a feature not present in living xanthophytes. If *Palaeovaucheria clavata* and *Aimonema ramosa* are indeed synonymous or closely related, then a fungal interpretation would be more appropriate, as advocated by Hermann and Podkovyrov (2010), who implied that these two taxa are distinct and belong to xanthophytes and fungi, respectively.

Opisthokonta: There have been numerous reports of Stenian-Tonian opisthokonts, including both fungal and holozoan fossils. As mentioned above, *Aimonema ramosa* was compared with modern nematode-trapping ascomycetes on the basis of its reticulate mycelium with closed loops, indicative of secondary cell fusion (Hermann and Podkovyrov, 2010). In addition, various fossils from the Shaler Supergroup in Arctic Canada show evidence of cell fusion and have been compared with modern fungi. These include Tappania sp., *Cheilofilum hysteriopsis*, *Plicatosphaeridium impostor*, '*Clavitrichoides*', and '*Osculosphaera*' from the Wynniatt Formation (ca. 750–850 Ma) of the Shaler Supergroup (Butterfield, 2005a; Butterfield, 2005b). In addition, *Ourasphaira giraldae* (Fig. 16D) from the Grassy Bay Formation of the Shaler Supergroup has been interpreted as a fungus based on ultrastructures and FTIR microspectroscopic data (Loron et al., 2019b). It should be pointed out that *Tappania* sp. from the Wynniatt Formation may not be congeneric with *Tappania plana* from the Paleoproterozoic Ruyang Group (Yin, 1997), casting doubt on the proposition of Paleoproterozoic fungi based on *Tappania plana* (Butterfield, 2005a). Nonetheless, the presence of Stenian-Tonian fungal fossils implies that the Holozoa-Holomycota divergence must have occurred by the Stenian-Tonian periods. Indeed, Strother et al. (2021) proposed that *Bicellum brasieri* from the ~ 1,000 Ma Diabaig Formation of the Torridon Group in Scotland, which features a stereoblastula-like packet of cells differentiated into an outer cell layer surrounding an inner mass of isodiametric cells, may be a holozoan fossil.

Amoebozoa: Tonian amoebozoans are represented by numerous species of vase-shaped microfossils (Fig. 16E), excluding *Melicerion poikilon* from the Chuar Group, which is regarded as a euglyphid rhizarian (Porter et al., 2003). These microfossils are distributed globally in Tonian rocks between 789 Ma and 729 Ma (Riedman et al., 2017). Their vase-shaped tests compare very closely with the Arcellinida (Lahr et al., 2019; Porter and Riedman, 2019), which is a subclade of the Amoebozoa and may have begun to diversify in the Tonian Period according to a recent molecular clock study (Porfirio-Sousa et al., 2023). It is uncertain whether these vase-shaped microfossils had organic (Tingle et al., 2023) or biomineralised tests (Morais et al., 2017), although the presence of drill holes in some vase-shaped microfossils provide strong evidence for predation on these early eukaryotic organisms (Porter, 2016). Regardless, apatitic scale microfossils from the Fifteenmile Group (~811–720 Ma) in Alaska and northwestern Canada provide solid evidence for biomineralisation in Tonian eukaryotes (Cohen and Knoll, 2012; Cohen et al., 2017), although their phylogenetic affinity within the eukaryotes remains unresolved.

There are many other Stenian-Tonian microfossils that are likely eukaryotes but their phylogenetic affinities within the eukaryotes are not resolved (see Loron et al., 2019a for a review). One important taxon with a global distribution is the genus *Trachyhystrichosphaera*, which is an easily identifiable acanthomorph and has been reported nearly 20 Stenian-Tonian successions around the world (Beghin et al., 2017; Loron et al., 2019a; Pang et al., 2020). Further research is needed to constrain the phylogenetic affinities of these eukaryotes in order to explore their implications for crown-group eukaryote diversification.

To summarise, the fossil record shows that major extant eukaryote clades, including the Archaeplastida, SAR, Opisthokonta, and Amoebozoa must have diverged and diversified by the Stenian-Tonian periods. By inference based on the topology of the eukaryote tree (Fig. 14), all major extant eukaryote groups may have diverged by the Stenian-Tonian periods. Thus, the Stenian-Tonian periods represent the diversification of crown-group eukaryotes, and by the late Tonian Period, crown-group eukaryotes may have become ecologically important, as evidenced by the increase in the abundance of cholesteroids in the biomarker record (Brocks et al., 2023).

6.2.2.3. Stage III (Ediacaran): Radiation of multicellular eukaryotes and the initial animal diversification. Although multicellular organisms, notably red algae and green algae, appeared earlier in the Proterozoic, it is not until after the Cryogenian (~720–635 Ma) that multicellular eukaryotes radiated in diversity and abundance. The Cryogenian represents the greatest disruption of the Earth system and the biggest divide in the Earth system history. Two global glaciations or "snowball Earth events" occurred at the beginning and end of the Cryogenian Period (Hoffman et al., 2017). Cryogenian glacial diamictites are inherently unfavourable in terms of fossil preservation because of their coarse grain size. It is also possible that Cryogenian eukaryotes were restricted in ecological distribution and depauperate in taxonomic diversity. Nonetheless, there are reports of micro- and macrofossils from fine-grained sediments of Cryogenian age (e.g., Riedman et al., 2014; Ye et al., 2015), but their diversity is relatively low.

Eukaryote diversity rose sharply in the Ediacaran Period (~635–538 Ma). Although the stratigraphic subdivision and global correlation of the Ediacaran System remain a matter of debate (Xiao and Narbonne, 2020), there is an emerging picture of the first-order evolutionary patterns of Ediacaran eukaryotes (see Anderson et al., 2024 for a recent review). The early Ediacaran Period (~635–580 Ma) experienced a rapid diversification of relatively large (some reaching nearly 1 mm in diameter) acanthomorphic acritarchs or Doushantuo-Pertatataka acritarchs (DPAs; Fig. 17A) (Ouyang et al., 2021), benthic macroalgae (Yuan et al., 2011), and possibly animals (Xiao et al., 1998; Yuan et al., 2011). The late Ediacaran Period (~580–538 Ma) began with a brief ice age – the 580 Ma Gaskiers glaciation (Pu et al., 2016), followed by the most negative carbon isotope excursion in Earth history – the Shuram excursion (Grotzinger et al., 2011), perhaps additional glaciations (Wang et al., 2023), the rise and fall of the Ediacara biota (Fig. 17C–F) (Xiao and Laflamme, 2009; Darroch et al., 2023), the rise of crown-group animals (Schiffbauer et al., 2020; Darroch et al., 2023), and the advent of animal biomineralisation (Fig. 17H–I) (Hua et al., 2007), although the exact timing of these events remains to be clarified (Wood et al., 2019).

It is abundantly clear that early Ediacara acritarchs and macroalgae reached unprecedented morphological complexity and taxonomic diversity (Huntley et al., 2006; Knoll et al., 2006; Cohen and Macdonald, 2015; Bykova et al., 2020). The lower Doushantuo Formation in South China serves as an excellent example to illustrate this diversification event. In the Yangtze Gorges area of South China, the lower Doushantuo Formation (*i.e.*, Member II and equivalents) has yielded a number of multicellular algal fossils (Ouyang et al., 2021) and over 50 species of acanthomorphic acritarchs (Liu and Moczydłowska, 2019) – some of which are multicellular and may represent animals (Yin et al., 2007; Cohen et al., 2009). The Weng'an biota, which occurs in phosphorites of the lower Ediacaran Doushantuo Formation in Guizhou Province of South China, also preserves over 50 species of acanthomorphs (Fig. 17A) (Xiao et al., 2014a), along with numerous multicellular algae possibly belong to red algae (Fig. 17B) (Xiao et al., 2004) and possible animal fossils (Xiao et al., 2014b). The Lantian biota, which occurs in black shales of the lower Ediacaran Lantian Formation in Anhui Province of South China, contains two dozen of carbonaceous compression

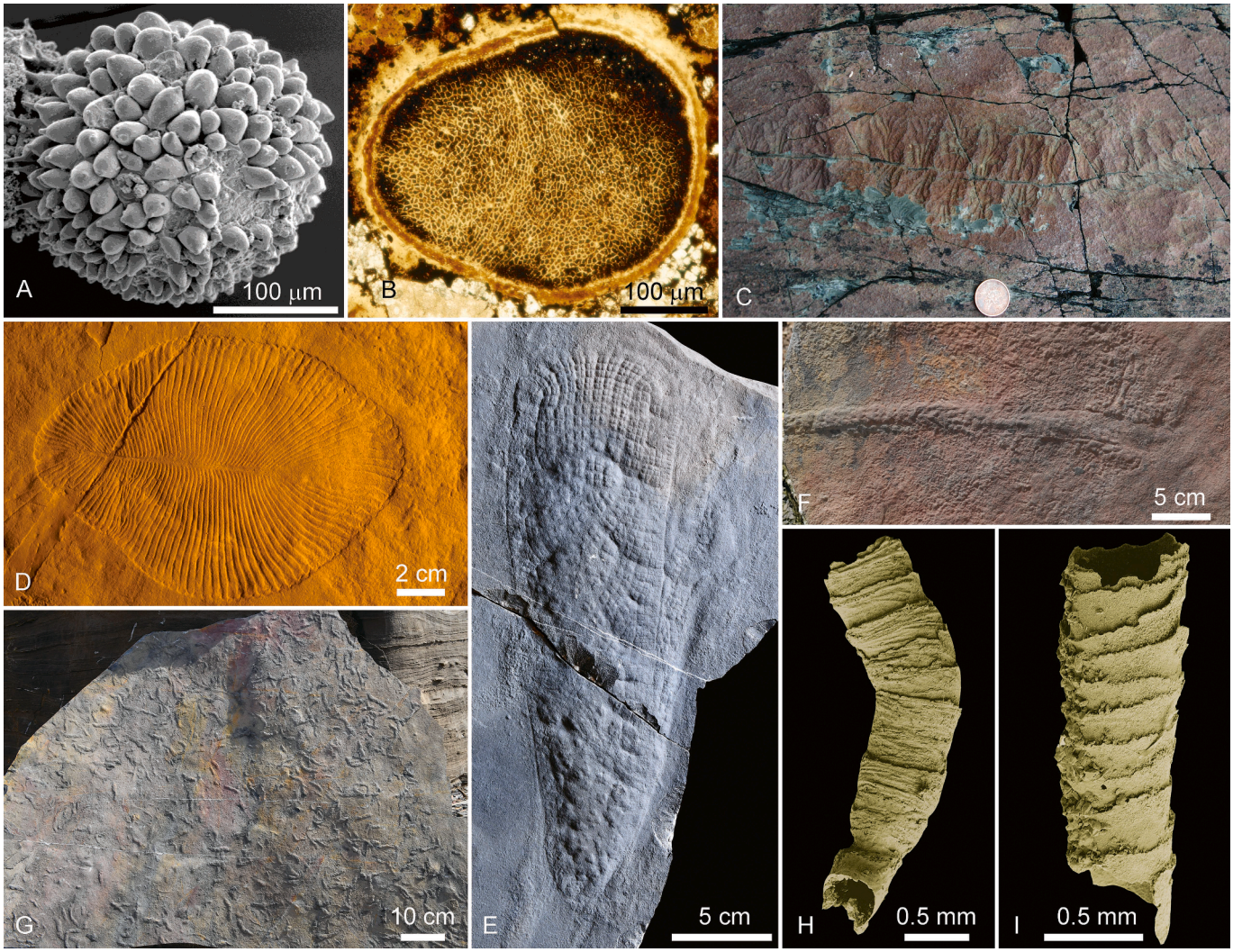

Fig. 17. Representative Stage III fossils. A–B: Mengeosphaera eccentrica, an Ediacaran acanthomorph (A) and a multicellular algal thallus (B) from the Doushantuo Formation (~600 Ma) at Weng'an, South China (Xiao et al., 2014b; Xiao et al., 2014a). C: Fractofusus misrai, a rangeomorph from the ~ 565 Ma Mistaken Point Formation in Newfoundland, Canada (Gehling and Narbonne, 2007). D: Dickinsonia costata from the ~ 560–550 Ma Ediacara Member in South Australia (Sprigg, 1947). E–G: Helicolocellus cantori (E), Yilingia spiciformis (F), and trace fossils (G; possibly Streptichnus ichnosp.) from the Shibantan Member of the Dengying Formation (~551–539 Ma) in South China (Chen et al., 2019; Xiao et al., 2021; Wang et al., 2024). H–I: Cloudina riemkeae, a biomineralised tubular fossil from the Dengying Formation (~551–539 Ma) in southern Shaanxi Province, South China (Hua et al., 2005). (A, H, I) are scanning electron photomicrographs; (B) is a transmitted light photomicrograph; (C–G) are reflected light photomicrographs.

macrofossils (Yuan et al., 2016), most representing macroalgae although some may be animals (Wan et al., 2016). Beyond South China, early Ediacaran fossil assemblages are known from the Krol A Formation in northern India (Xiao et al., 2022) and possibly the Ura Formation in Siberia (Moczydłowska and Nagovitsin, 2012), although the age constraint on the latter is tenuous.

Ediacaran acanthomorphs remain abundant and diverse in the upper Doushantuo Formation (Member III) in South China (Liu et al., 2014b) and possibly equivalent strata in Australia (Grey, 2005). However, their diversity declined subsequently, with only a few occurring in the late Ediacaran and possibly extending to the Cambrian (Golubkova et al., 2015; Ouyang et al., 2017; Anderson et al., 2019; Grazhdankin et al., 2020). It is uncertain exactly when this decline occurred, but it may have coincided with the ~ 580 Ma Gaskiers glaciation (Zhou et al., 2007) and concluded by the Shuram excursion, which has been constrained between 574.0 ± 4.7 Ma and 567.3 ± 3.0 Ma (Rooney et al., 2020), as very few Ediacaran acanthomorph taxa postdate the Shuram excursion.

As Ediacaran acanthomorphs fell in diversity, the Ediacara biota and macroscopic animals were poised to rise. The Ediacara biota is not a natural phylogenetic clade; rather, it includes soft-bodied macroscopic and likely multicellular fossils in the late Ediacaran Period, as exemplified by those from the Ediacara and Nilpena members in South Australia (Gehling et al., 2019). Phylogenetically, the Ediacara biota includes fossils that can be reasonably considered as stem-group and crown-group metazoans, but most cannot easily be assigned to any living animal phyla (Xiao and Laflamme, 2009; Erwin et al., 2011). The Ediacara biota may also include macroalgal fossils (Wan et al., 2020; Xiao et al., 2020).

The earliest-known fossils of the Ediacara biota, as represented by the ca. 575–560 Ma Avalon assemblage (Narbonne, 2005; Matthews et al., 2020), are preserved in deep-water sediments postdating the Gaskiers glaciation (Narbonne and Gehling, 2003), predating the Shuram excursion (Boag et al., 2024), and apparently recording a deep-ocean oxygenation event (Canfield et al., 2007). These temporal relationships raise the possibility that the rise of the Avalon assemblage in deep marine environments may be causally related to the decline of acanthomorphs, the Gaskiers glaciation, the Shuram excursion, and the deep-ocean oxygenation event (e.g., Boag et al., 2018), although a critical assessment of their relationships requires more precise age constraints. The Avalon assemblage is dominated by epibenthic rangeomorphs (Liu et al., 2015), modular organisms consisting of repetitive branching leaf-like units (Fig. 17C). Putative cnidarian body fossils (Liu et al., 2014a; Dunn et al., 2022) and cnidarian trace fossils have been reported from the Avalon assemblage (Liu et al., 2010); indeed, some rangeomorphs may be total-group eumetazoans or even stem-group cnidarians (Butterfield, 2020; Dunn et al., 2021). However, thus far no convincing bilaterian body fossils have been known from the Avalon assemblage. In this apparently bilaterian-free benthic marine ecosystem, multicellular organisms seem to have interacted ecologically, exhibiting evidence for resource competition and facilitation (Darroch et al., 2018; Mitchell and Butterfield, 2018).

The Avalon assemblage is succeeded by the White Sea assemblage, which has much greater taxonomic diversity, as represented by ca. 560–550 Ma macrofossils from Ediacara and Nilpena members of South Australia (Droser et al., 2017; Droser et al., 2019), the Lamtsa, Verkhovka, and Zimnegory formations in the White Sea area of Russia (Grazhdankin, 2014), and the Molyliv and Yaryshiv formations in the Polodia region in Ukraine and Moldova (Francovschi et al., 2021). Taxonomic diversity became greater in the White Sea assemblage, which consists of hold-over rangeomorphs from the Avalon assemblage, but also include many new taxa, including *Dickinsonia* (Fig. 17D), *Kimberella*, *Spriggina*, *Tribrachidium*, and *Eoandromeda* (Droser et al., 2017), the last of which also occurs in the ~ 551 Ma Miaohe Member in South China (Zhu et al., 2008). Importantly, members of the total-group bilaterians are present in the White Sea assemblage (Fedonkin and Waggoner, 1997; Evans et al., 2020), which is also supported by bilaterian scratch marks, burrows, and trails in the Ediacara Member of South Australia (Gehling et al., 2014; Gehling and Droser, 2018).

Enigmatically, a large proportion (~80 %) of taxa in the White Sea assemblage disappeared around 550 Ma (Shen et al., 2008; Evans et al., 2022), which, coupled with a decreased origination rate, resulted in the taxonomically depauperate Nama assemblage (ca. 550–538 Ma). Thus, there appears to be an extinction event separating the White Sea and Nama assemblages. The drivers of this extinction event are unclear. The survivors of this extinction event seem to have a high surface area to volume ratio, which may have facilitated oxygen uptake through diffusion in oxygen-deficient environments, favouring global oceanic anoxia as a driver (Evans et al., 2022). Indeed, there are independent geochemical data suggesting a terminal Ediacaran anoxia event (Evans et al., 2018; Tostevin et al., 2018; Zhang et al., 2018). Alternatively and additionally, ecological interactions with rising bilaterian animals may have suppressed the diversity of the Nama assemblage and eventually caused a biotic replacement of the Ediacara biota by the Cambrian fauna (Laflamme et al., 2013; Darroch et al., 2015; Cribb et al., 2019; Darroch et al., 2023).

It is important to point out that the Nama assemblage does include fossils that can be plausibly placed in the animal tree at various phylogenetic resolutions. For example, *Helicolocellus cantori* (Fig. 17E) and *Yilingia spiciformis* (Fig. 17F) from the Shibantan Member (~551–539 Ma) in South China has been interpreted, respectively, as a crown-group sponge related to the hexactinellids (Wang et al., 2024) and as a protostome related to either annelids or arthropods (Chen et al., 2019). Bilaterian trace fossils (Fig. 17G), including burrows, trails, and track ways, from the Shibantan Member were likely produced by bilaterian animals (Xiao et al., 2021), some of which probably had appendages (Chen et al., 2018) while others may have interacted with microbial mats (Meyer et al., 2014; Xiao et al., 2019). Similarly, there are abundant bilaterian trace fossils in the terminal Ediacaran Kuibis and Schwarzrand subgroups (~550–539 Ma) in Namibia (Darroch et al., 2021), and some of them may have been produced by priapulan-like animals (Turk et al., 2022). Finally, biomineralising animals are present in the Nama assemblage. These include claudinomorphs (Fig. 17H–I), *Corumbella*, and *Namacalathus*, which have been interpreted as bilaterians (Hua et al., 2005; but see Vinn and Zatoń, 2012; Schiffbauer et al., 2020; Yang et al., 2020), a cnidarian (Pacheco et al., 2015; but see Osés et al., 2022), and a lophophorate (Zhuravlev et al., 2015; but see Cunningham et al., 2017), respectively. In spite of their controversial phylogenetic placement within the animal tree, these fossils indicate that the initial evolution of animal biomineralisation had already taken place while the Ediacara biota experienced a decline.

Ultimately, the Ediacara biota disappeared almost completely at the Ediacaran-Cambrian transition, possibly representing another extinction event (Darroch et al., 2023). It is unclear whether the White Sea-Nama and Ediacaran-Cambrian extinctions represent two distinct events with different causes or two pulses of a single protracted event. Regardless, the fossil record seems to show that internal divergence of crown-group animals had already started in the Ediacaran Period or earlier, resulting in the divergence of sponges, eumetazoans, bilaterians, and probably protostomes and deuterostomes. As such, a number of animal groups must have survived the Ediacaran-Cambrian extinction, consistent with the continuity of animal taxa across the Ediacaran-Cambrian boundary (Zhu et al., 2017; Cai et al., 2019; Wood et al., 2019), even though this boundary remains an important divide in Earth history.

6.3. *Summary of the Proterozoic*

The Proterozoic was characterised by the assembly and breakup of the supercontinents Columbia (late Palaeoproterozoic) and Rodinia (Meso-Neoproterozoic). Horizontal tectonics dominated geodynamical processes. The GOE between 2.4–2.3 Ga was a major event that had enormous consequences on biomass development resulting in a spike in

oxygen production (the Lomagundi Excursion event that lasted from 2.3 to 2.1 Ga) followed by a major decrease owing to the continuing slow flow of nutrients. Massive spikes in the carbon and sulphur isotope records mirror these events. Thereafter, nutrient supply was generally abundant but periods of euxinia on the continental shelves due to overproduction occurred episodically. For much of the Proterozoic, the deep oceans remained anoxic until the Neoproterozoic and the NEO (also characterised by spikes in oxygen production and the sulphur and carbon isotope records) when the breakup of Rodinia coincided with global glaciation and the appearance of planktonic algae.

While the widespread distribution of continental shelves in the Palaeo-Mesoarchaean provided ideal habitats for phototrophic microorganisms and the buildup of massive stromatolitic formations on carbonate platforms across the globe, the Proterozoic was the golden age of giant stromatolites as cyanobacteria flourished and diversified in different environmental conditions, while non-oxygenic phototrophs continued in the background, either in non-phototrophic environments or buried in the lower layers of oxygenic cyanobacterial mats. Stromatolites declined in the Neoproterozoic even before the rise of algae, protistans and metazoans, likely because of their own success in producing too much O_2; stromatolites develop best when CO_2 is present in the atmosphere (Monty, 1974; Riding, 2005). Nevertheless, eukaryotes contributed to this decline well into the Palaeozoic, resulting in their becoming relegated to protected marginal marine and peritidal environments (Awramik and Sprinkle, 1999).

It is in this era that eukaryotes appeared. The fossil record of early eukaryotes is murky in the Neoarchaean, but becomes increasingly clear in the Palaeoproterozoic and increasingly recognisable in the Meso-Neoproterozoic. Three stages of early eukaryote evolution can be recognised. Stage I (?Neoarchaean–Mesoproterozoic) records the origin of eukaryotes and the evolution of stem group eukaryotes that eventually vanished in Earth history. Stage II (Mesoproterozoic–Neoproterozoic transition) represents the diversification of crown-group eukaryotes that have survived to the present. Stage III (Ediacaran) is characterised by the radiation of multicellular eukaryotes, including early animals and biomineralising animals. The evolutionary history of eukaryotes is intricately linked with the biogeodynamic evolution of the Earth system.

Apart from carbonate, silica and iron oxides, fossiliferous material is also preserved with phosphate. This mineral is one of the most stable fossilising minerals (Summons et al., 2011) and permitted study of superb morphological features, for example in the Weng'an biota of the Doushantuo Formation (~600 Ma) (Fig. 17A, B; Xiao et al., 2014b; Xiao et al., 2014a). With the advent of larger multicellular organisms, trace fossils made their appearance in the Neoproterozoic (Fig. 17G).

7. Conclusions and perspectives

The Precambrian, covering 80 % of the history of the Earth, saw the appearance of life, its early metabolic diversification, the appearance of anoxygenic and oxygenic photosynthesis, cellular differentiation, and the appearance of eukaryotes including, towards the Neoproterozoic, animals. The majority of the most important evolutionary changes occurred in this time period. It was also a time when the Earth itself was changing, evolution in the geodynamical regimes fuelling the formation and destruction of continental crust, as well as changes in the composition and stability of the latter. While the geosphere dominated the biosphere for most of the Hadean and Archaean, the biosphere increased in importance from the Neoarchaean throughout the whole of the Proterozoic, particularly since the GOE. This led to reciprocal feedback mechanisms whereby burial of reduced carbon and carbonates removed CO_2 from the atmosphere, while increased oxygenic phototrophy pumped oxygen into the atmosphere. Global glaciations triggered by the disposition and breakup of supercontinents greatly contributed to the flow of nutrients, the rise in atmospheric oxygen and subsequent spurts in the evolution of life.

We have attempted to summarise the parallel evolution of geodynamics and environmental conditions with the evolution of life. This broad overview highlights aspects in the evolution of life that are still unclear and merit further investigation. The first of these is the origin of life. Given the lack of rock record and the likely specificity of the accompanying environmental constraints, we will probably never know exactly how, when or where life emerged (cf. Westall 2018, 2023b). Certainly, the finding of definitive traces of life elsewhere in the Solar System or on exoplanets will support the current understanding that life emerged in a geological scenario that would have been common on other terrestrial planets. Such a finding would perhaps improve our understanding of abiogenesis, although it is necessary to keep in mind the fact that life may emergence in different scenarios on different planets. The finding of life on Mars will be paradigm breaking: yes, life (more or less as we know it) can appear elsewhere. However, it will not necessarily tell us whether life on Earth arose in a subsurface, hydrothermal environment or closer to the surface in the photic zone, both scenarios being theoretically feasible on Mars (Westall et al., 2015b, 2018; Westall et al., 2023b). On the other hand, finding traces of life on one of the icy satellites would clearly indicate a subsurface, non-photic scenario for the emergence of life.

Secondly, the early evolution and diversification of life is a conundrum. If the geochemical indications of anoxygenic photosynthetic Fe^{2+} oxidation in the 3.7 Ga Isua BIFs (Czaja et al., 2013) and the organochemical indications of biogenicity (Hassenkam et al., 2017) are correct, the Eoarchaean sediments at Isua document life and likely phototrophs. However, photosynthesis was not the first metabolism (Martin et al., 2008; Blankenship, 2010). There are various mechanisms for evolution (Hohmann-Marriott and Blankenship, 2011) including gene duplication, gene fusion and splitting, and lateral gene transfer, perhaps, by viral vectors. The evolution of cofactors, *i.e.*, specific protein complexes and molecules, are essential for electron transport, proton translocation, and light harvesting in photosynthetic systems. Examples include FeS clusters, hemes, quinones, chlorophyll, and rhodopsins. The evolution of photosynthesis involved the co-evolution of a number of interacting factors, including photosynthetic pigments, reaction centres (RCs), light-harvesting (LH) antenna systems, electron transport pathways, and carbon fixation pathways (Blankenship, 2010). Each of these factors, in turn, were the result of their own evolutionary processes. Chlorophylls (green pigments) are essential for photosynthesis and form complexes with the photosystems used by photosynthesising organisms. They are used for harvesting light, the transfer of the light energy to the reaction centres of the photosystems, and for charge separation. Chlorophyll-based photosynthesis first evolved in Bacteria. Phototrophic organisms use two types of reaction centre complexes, Reaction centre Complex I and Reaction centre Complex II, both of which share a common ancestor (Blankenship, *op. cit.*). Anoxygenic phototrophs use either one or the other, and only oxygenic cyanobacteria use both. The evolution of oxygenic photosynthesis is crucial to the emergence of eukaryotes, probably through a process of endosymbiosis (Margulis, 1991; Archibald, 2015).

Missions to Mars are searching for biosignatures like MISS and stromatolites (among others). The surface environment on Mars was not permanently habitable as it was on Earth and it can be questioned as to how far Martian life (if it exists/existed) could have evolved. The conservative view is that primitive Martian life may have resembled primitive, non-phototrophic prokaryotes. However, the finding of evidence for phototrophs on Mars (cf. Noffke, 2015, 2021) would suggest that, in favourable circumstances, this kind of energy production developed very rapidly. Such information would be informative for understanding the evolution of life on Earth.

The development of eukaryotes and particularly animals is apparently an evolutionary event unique to the biosphere on Earth. Claims of extant or extinct eukaryotes on Mars (Rizzo et al., 2021; Joseph et al., 2022) have not been subjected to rigorous scientific evaluation. Are eukaryotes and animals inevitable once life evolves on a planet? What are the environmental and biological prerequisites for the evolution of

complex life forms such as eukaryotes? And how would eukaryotic life transform other planets? Proterozoic eukaryotes on Earth can provide some insight, but these questions cannot fully be addressed until we discover another extra-terrestrial body that hosts a biosphere.

CRediT authorship contribution statement

Frances Westall: Writing – review & editing, Writing – original draft, Conceptualization. **Shuhai Xiao:** Writing – review & editing, Writing – original draft, Conceptualization.

Declaration of competing interest

The authors declare that they have no known competing financial interests or personal relationships that could have appeared to influence the work reported in this paper.

Acknowledgments

Frances Westall thanks Robert Riding and Philip Fralick for material provided. She was supported by the CNRS, ANR and CNES to study Palaeoarchaean microfossils. Shuhai Xiao was supported by the National Science Foundation (EAR-2021207) to study Proterozoic eukaryotes.

Author contributions

Both authors contributed to the conception and writing of this manuscript.

Data availability

No data was used for the research described in the article.

References

Abell, P.I., McClory, J., Martin, A., Nisbet, E.G., 1985. Archaean stromatolites from the Ngesi Group, Belingwe greenstone belt, Zimbabwe; preservation and stable isotopes - preliminary results. Precambrian Research 27, 357–383. https://doi.org/10.1016/0301-9268(85)90094-4.

Adam, Z., 2007. Actinides and life's origins. Astrobiology 7, 852–872. https://doi.org/10.1089/ast.2006.0066.

Adam, Z.R., Skidmore, M.L., Mogk, D.W., Butterfield, N.J., 2017. A Laurentian record of the earliest fossil eukaryotes. Geology 45, 387–390. https://doi.org/10.1130/g38749.1.

Afroz, M., Fralick, P.W., Lalonde, S.V., 2023. Sedimentology and geochemistry of basinal lithofacies in the Mesoarchean (2.93 Ga) Red Lake carbonate platform, northwest Ontario, Canada. Precambrian Research 388, 106996. https://doi.org/10.1016/j.precamres.2023.106996.

Agangi, A., Hofmann, A., Ossa, F.O., Paprika, D., Bekker, 2021. A Mesoarchaean acidic volcanic lakes: A critical ecological niche in early land colonisation. Earth and Planetary Science Letters 556, 116725. https://doi.org/10.1016/j.epsl.2020.116725.

Agić, H., Moczydłowska, M., Yin, L.-M., 2015. Affinity, life cycle, and intracellular complexity of organic-walled microfossils from the Mesoproterozoic of Shanxi, China. Journal of Paleontology 89, 28–50. https://doi.org/10.1017/jpa.2014.4.

Agić, H., Moczydłowska, M., Yin, L., 2017. Diversity of organic-walled microfossils from the early Mesoproterozoic Ruyang Group, North China Craton - A window into the early eukaryote evolution. Precambrian Research 297, 101–130.

Allwood, A.C., Walter, M.R., Kamber, B.S., Marshall, C.P., Burch, I.W., 2006. Stromatolite reef from the early archaean era of Australia. Nature 441, 714–718. https://doi.org/10.1038/nature04764.

Allwood, A.C., Walter, M.R., Burch, I.W., Kamber, B.S., 2007. 3.43 billion-year-old stromatolite reef from the Pilbara Craton of Western Australia: ecosystem-scale insights to early life on Earth. Precambrian Research 158, 198–227.

Allwood, A.C., Grotzinger, J.P., Knoll, A.H., Burch, I.W., Anderson, M.S., Coleman, M.L., Kanik, I., 2009. Controls on development and diversity of Early Archean stromatolites. Proceedings of the National Academy of Sciences 106, 9548–9555. https://doi.org/10.1073/pnas.0903323106.

Allwood, A.C., Rosing, M.T., Flannery, D.T., Hurowitz, J.A., Heirwegh, C.M., 2018. Reassessing evidence of life in 3,700-million-year-old rocks of Greenland. Nature 563, 241–244. https://doi.org/10.1038/s41586-018-0610-4.

Anbar, A.D., Knoll, A.H., 2002. Proterozoic ocean chemistry and evolution: a bioinorganic bridge? Science 297.

Anbar, A.D., Duan, Y., Lyons, T.W., Arnold, G.L., Kendall, B., Creaser, R.A., Kaufman, A. J., Gordon, G.W., Scott, C., Garvin, J., Buick, R., 2007. A whiff of oxygen before the great oxidation event? Science 317 (5846), 1903–1906. https://doi.org/10.1126/science.1140325.

Anderson, R.P., McMahon, S., Macdonald, F.A., Jones, D.S., Briggs, D.E.G., 2019. Palaeobiology of latest Ediacaran phosphorites from the upper Khesen Formation, Khuvsgul Group, northern Mongolia. Journal of Systematic Palaeontology 17, 501–532. https://doi.org/10.1080/14772019.2018.1443977.

Anderson, R.P., Mughal, S., Wedlake, G.O., 2024. Proterozoic microfossils continue to provide new insights into the rise of complex eukaryotic life. R. Soc. Open Sci. 11, 240154. https://doi.org/10.1098/rsos.240154.

Archibald, J.M., 2015. Endosymbiosis and eukaryotic cell evolution. Current Biology 25, R911–R921. https://doi.org/10.1016/j.cub.2015.07.055.

Arndt, N.T., Nisbet, E.G., 2012. Processes on the young Earth and the habitats of early life. Ann. Rev. Earth Planet Sci. 40, 521–549. https://doi.org/10.1146/annurevearth-042711-105316.

Arp, G., Reimer, A., Reitner, J., 2001. Photosynthesis-induced biofilm calcification and calcium concentrations in Phanerozoic oceans. Science 292, 1701–1704.

Arrhenius, S., 1908. Worlds in the making. Harper and Row, New York.

Arts, A., 2015. Macro-and micro-structure comparison of ancient and modern iron-rich stromatolites (Doctoral dissertation). Lakehead University, Canada.

Awramik, S.M., Buchheim, H.P., 2009. A giant, late Archean lake system: the Meentheena Member (Tumbiana Formation; Fortescue Group), Western Australia. Precambrian Research 174, 215–240.

Awramik, S.M., Sprinkle, J., 1999. Proterozoic stromatolites: The first marine evolutionary biota. Historical Biology 13, 241–253. https://doi.org/10.1080/08912969909386584.

Awramik, S. M. (1991). Archaean and Proterozoic stromatolites. In Riding, R. (Ed.), Calcareous algae and stromatolites (pp. 289-304). Berlin, Heidelberg: Springer Berlin Heidelberg. Doi: 10.1007/978-3-642-52335-9 15.

Bahcall, J.N., Pinsonneault, M.H., Basu, S., 2001. Solar models: Current epoch and time dependences, neutrinos, and helio seismological properties. Astrophysical J. 555, 990. https://doi.org/10.1086/321493.

Baludikay, B.K., Storme, J.-Y., François, C., Baudet, D., Javaux, E.J., 2016. A diverse and exquisitely preserved organic-walled microfossil assemblage from the Meso-Neoproterozoic Mbuji-Mayi Supergroup (Democratic Republic of Congo) and implications for Proterozoic biostratigraphy. Precambrian Research 281, 166–184. https://doi.org/10.1016/j.precamres.2016.05.017.

Banerjee, A., Słowakiewicz, M., Saha, D., 2022. On the oxygenation of the Archaean and Proterozoic oceans. Geological Magazine 159, 212–219. https://doi.org/10.1017/S0016756820001363.

Baross, J.A., Hoffman, S.E., 1985. Submarine hydrothermal vents and associated gradient environments as sites for the origin and evolution of life. Origins of Life and Evolution of the Biosphere 15, 327–345. https://doi.org/10.1007/BF01808177.

Baumgartner, L.K., Dupraz, C., Buckley, D.H., Spear, J.R., Pace, N.R., Visscher, P.T., 2009. Microbial species richness and metabolic activities in hypersaline microbial mats: insight into biosignature formation through lithification. Astrobiology 9, 861–874.

Beghin, J., Storme, J.-Y., Blanpied, C., Gueneli, N., Brocks, J.J., Poulton, S.W., Javaux, E. J., 2017. Microfossils from the late Mesoproterozoic – early Neoproterozoic Atar/El Mreïti Group, Taoudeni Basin, Mauritania, northwestern Africa. Precambrian Research 291, 63–82. https://doi.org/10.1016/j.precamres.2017.01.009.

Behrensmeyer, A.K., Kidwell, S.M., Gastaldo, R.A., 2000. Taphonomy and paleobiology. Paleobiology 26 (S4), 103–147.

Bekker, A., Holland, H.D., 2012. Oxygen overshoot and recovery during the early Paleoproterozoic. Earth Planet. Sci. Lett. 317–318, 295–304. https://doi.org/10.1016/j.epsl.2011.12.012.

Bekker, A., Kaufman, A.J., Karhu, J.A., Beukes, N.J., Swart, Q.D., Coetzee, L.L., Eriksson, K.A., 2001. Chemostratigraphy of the Paleoproterozoic Duitschland Formation, South Africa: implications for coupled climate change and carbon cycling. American Journal of Science 301, 261–285.

Bell, E.A., Boehnke, P., Harrison, T.M., Mao, W.L., 2015. Potentially biogenic carbon preserved in a 4.1 billion-year-old zircon. Proc. Nat. Acad. Sci. 112, 14518–14521. https://doi.org/10.1073/pnas.1517557112.

Bengtson, S., Sallstedt, T., Belivanova, V., Whitehouse, M., 2017a. Three-dimensional preservation of cellular and subcellular structures suggests 1.6 billion-year-old crown-group red algae. PLOS Biology 15, e2000735.

Bengtson, S., Rasmussen, B., Ivarsson, M., Muhling, J., Broman, C., Marone, F., Stampanoni, M., Bekker, A., 2017b. Fungus-like mycelial fossils in 2.4-billion-year-old vesicular basalt. Nature Ecology & Evolution 1, 0141. https://doi.org/10.1038/s41559-017-0141.

Berbee, M.L., Strullu-Derrien, C., Delaux, P.-M., Strother, P.K., Kenrick, P., Selosse, M.-A., Taylor, J.W., 2020. Genomic and fossil windows into the secret lives of the most ancient fungi. Nature Reviews Microbiology 18, 717–730. https://doi.org/10.1038/s41579-020-0426-8.

Beukes, N.J., Lowe, D.R., 1989. Environmental control on diverse stromatolite morphologies in the 3000 Myr Pongola Supergroup, South Africa. Sedimentology 36, 383–397. https://doi.org/10.1111/j.1365-3091.1989.tb00615.x.

Beukes, N.J. (1987). Facies relations, depositional environments and diagenesis in a major early Proterozoic stromatolitic carbonate platform to basinal sequence, Campbellrand Subgroup, Transvaal Supergroup, Southern Africa. Sedimentary Geology 54, 1-5, 7, 9-46. Doi: 10.1016/0037-0738(87)90002-9.

Bhagwat, G., O'Connor, W., Grainge, I., Palanisami, T., 2021. Understanding the fundamental basis for biofilm formation on plastic surfaces: role of conditioning films. Frontiers in Microbiology 12, 687118. https://doi.org/10.3389/fmicb.2021.687118.

Blake, R.E., Chang, S.J., Lepland, A., 2010. Phosphate oxygen isotopic evidence for a temperate and biologically active Archaean ocean. Nature 464, 1029–1032. https://doi.org/10.1038/nature08952.
Blankenship, R.E., 2010. Early evolution of photosynthesis. Plant Physiology 154, 434–438. https://doi.org/10.1104/pp.110.161687.
Boag, T.H., Stockey, R.G., Elder, L.E., Hull, P.M., Sperling, E.A., 2018. Oxygen, temperature and the deep-marine stenothermal cradle of Ediacaran evolution. Proceedings of the Royal Society B (biological Sciences) 285, 20181724. https://doi.org/10.1098/rspb.2018.1724.
Boag, T.H., Busch, J.F., Gooley, J.T., Strauss, J.V., Sperling, E.A., 2024. Deep-water first occurrences of Ediacara biota prior to the Shuram carbon isotope excursion in the Wernecke Mountains, Yukon. Canada. Geobiology 22, e12597.
Borg, L.E., Carlson, R.W., 2023. The evolving chronology of moon formation. Annual Review of Earth and Planetary Sciences 51, 25–52. https://doi.org/10.1146/annurev-earth-031621-060538.
Bosco-Santos, A., Gilhooly III, W.P., Fouskas, F., Fabricio-Silva, W., Oliveira, E.P., 2020. Euxinia in the Neoarchean: The starting point for early oxygenation in a Brazilian Craton. Precambrian Research 341, 105655. https://doi.org/10.1016/j.precamres.2020.105655.
Bosco-Santos, A., Gilhooly III, W.P., de Melo-Silva, P., Fouskas, F., Bouyon, A., Motta, J. G., Baldim, M.R., Fabricio-Silva, W., Philippot, P., Oliveira, E.P., 2022. Neoarchean atmospheric chemistry and the preservation of S-MIF in sediments from the São Francisco Craton. Geoscience Frontiers 13 (5), 101250. https://doi.org/10.1016/j.gsf.2021.101250.
Bowles, A.M.C., Williamson, C.J., Williams, T.A., Lenton, T.M., Donoghue, P.C.J., 2023. The origin and early evolution of plants. Trends in Plant Science 28, 312–329. https://doi.org/10.1016/j.tplants.2022.09.009.
Braissant, O., Decho, A.W., Przekop, K.M., Gallagher, K.L., Glunk, C., Dupraz, C., Visscher, P.T., 2009. Characteristics and turnover of exopolymeric substances in a hypersaline microbial mat. FEMS Microbiology Ecology 67, 293–307.
Brando Soares, M.N., Corrêa, A.V., Zeh, A., Cabral, A.R., Pereira, L.F., do Prado, M.G.B., de Almeida, A.M., Manduca, L.G., da Silva, P.H.M., de Araújo Mabub, R.O., 2017. Geology of the Pitangui greenstone belt, Minas Gerais, Brazil: stratigraphy, geochronology and BIF geochemistry. Precambrian Res. 291, 17–41. https://doi.org/10.1016/j.precamres.2017.01.008.
Brasier, M., Green, O., Lindsay, J., Steele, A., 2004. Earth's oldest (~ 3.5 Ga) fossils and the Early Eden Hypothesis': Questioning the evidence. Origins of Life and Evolution of the Biosphere 34, 257–269.
Briggs, D.E., 1995. Experimental taphonomy. Palaios 539–550.
Brocks, J.J., Logan, G.A., Buick, R., Summons, R.E., 1999. Archean molecular fossils and the early rise of eukaryotes. Science 285 (5430), 1033–1036. https://doi.org/10.1126/science.285.5430.1033.
Brocks, J.J., Buick, R., Logan, G.A., Summons, R.E., 2003. Composition and syngeneity of molecular fossils from the 2.78 to 2.45 billion-year-old Mount Bruce Supergroup, Pilbara Craton. Western Australia. Geochimica et Cosmochimica Acta 67, 4289–4319.
Brocks, J.J., Jarrett, A.J.M., Sirantoine, E., Hallmann, C., Hoshino, Y., Liyanage, T., 2017. The rise of algae in Cryogenian oceans and the emergence of animals. Nature 548, 578–581. https://doi.org/10.1038/nature23457.
Brocks, J.J., Nettersheim, B.J., Adam, P., Schaeffer, P., Jarrett, A.J.M., Güneli, N., Liyanage, T., van Maldegem, L.M., Hallmann, C., Hope, J.M., 2023. Lost world of complex life and the late rise of the eukaryotic crown. Nature 618, 767–773. https://doi.org/10.1038/s41586-023-06170-w.
Brown, A.J., Cudahy, T.J., Walter, M.R., 2006. Hydrothermal alteration of the Panorama Formation, North Pole Dome, Pilbara Craton, Western Australia. Precambrian Research 151, 211–233. https://doi.org/10.1016/j.precamres.2006.08.014.
Brüske, A., Martin, A.N., Rammensee, P., Eroglu, S., Lazarov, M., Albut, G., Schuth, S., Aulbach, S., Schoenberg, R., Beukes, N., Hofmann, A., Nägler, T., Weyer, S., 2020. The onset of oxidative weathering traced by uranium isotopes. Precambrian Research 338, 105583. https://doi.org/10.1016/j.precamres.2019.105583.
Budin, I., Szostak, J.W., 2011. Physical effects underlying the transition from primitive to modern cell membranes. Proc. Natl. Acad. Sci. 108, 5249–5254. https://doi.org/10.1073/pnas.1100498108.
Buick, R., 1992. The antiquity of oxygenic photosynthesis: evidence from stromatolites in sulphate-deficient Archaean lakes. Science 255, 74–77. https://doi.org/10.1126/science.1153649.
Buick, R., 2007. Did the Proterozoic 'Canfield Ocean' cause a laughing gas greenhouse? Geobiology 5, 97–100.
Buick, R., 2008. When did oxygenic photosynthesis evolve? Philos. Trans. r. Soc. B-Biol. Sci. 363, 2731–2743.
Buick, R., Dunlop, J., 1990. Evaporitic sediments of Early Archaean age from the Warrawoona Group, North Pole, Western Australia. Sedimentology 37, 247–277.
Buick, R., Des Marais, D.J., Knoll, A.H., 1995. Stable isotopic compositions of carbonates from the Mesoproterozoic Bangemall Group, northwestern Australia. Chemical Geology 123, 153–171.
Burki, F., Roger, A.J., Brown, M.W., Simpson, A.G.B., 2020. The new tree of eukaryotes. Trends in Ecology & Evolution 35, 43–55. https://doi.org/10.1016/j.tree.2019.08.008.
Butterfield, N.J., 1990. Organic preservation of non-mineralizing organisms and the taphonomy of the Burgess Shale. Paleobiology 16, 272–286.
Butterfield, N.J., 2000. *Bangiomorpha pubescens* n. gen., n. sp.: Implications for the evolution of sex, multicellularity, and the Mesoproterozoic-Neoproterozoic radiation of eukaryotes. Paleobiology 26, 386–404. https://doi.org/10.1666/0094-8373(2000)026<0386:BPNGNS>2.0.CO;2.
Butterfield, N.J., 2004. A vaucheriacean alga from the middle Neoproterozoic of Spitsbergen: Implications for the evolution of Proterozoic eukaryotes and the Cambrian explosion. Paleobiology 30, 231–252.
Butterfield, N.J., 2005a. Probable Proterozoic fungi. Paleobiology 31, 165–182.
Butterfield, N.J., 2005b. Reconstructing a complex early Neoproterozoic eukaryote, Wynniatt Formation, arctic Canada. Lethaia 38, 155–169.
Butterfield, N.J., 2015. Early evolution of the Eukaryota. Palaeontology 58, 5–17. https://doi.org/10.1111/pala.12139.
Butterfield, N.J., 2020. Constructional and functional anatomy of Ediacaran rangeomorphs. Geological Magazine. https://doi.org/10.1017/S0016756820000734.
Butterfield, N.J., Knoll, A.H., Swett, K., 1994. Paleobiology of the Neoproterozoic Svanbergfjellet Formation, Spitsbergen. Fossils and Strata 34, 1–84.
Byerly, G. R., Lowe, D. R., Heubeck, C., (2019). Geologic evolution of the Barberton Greenstone Belt–a unique record of crustal development, surface processes, and early life 3.55 to 3.20 Ga. In Van Kranendonk, M. J., Bennett, V. C., & Hoffmann, J. E. (Eds) Earth's oldest rocks, 569-613. DOI: 10.1016/B978-0-444-63901-1.00024-1.
Bykova, N., LoDuca, S.T., Ye, Q., Marusin, V., Grazhdankin, D., Xiao, S., 2020. Seaweeds through time: Morphological and ecological analysis of Proterozoic and early Paleozoic benthic macroalgae. Precambrian Research 350, 105875. https://doi.org/10.1016/j.precamres.2020.105875.
Cai, Y., Xiao, S., Li, G., Hua, H., 2019. Diverse biomineralizing animals in the terminal Ediacaran Period herald the Cambrian Explosion. Geology 47, 380–384. https://doi.org/10.1130/G45949.1.Canfield, D. E. A new model for Proterozoic ocean chemistry. Nature 396, 450-453. Doi: 10.1038/24839.
Canfield, D.E., Farquhar, J., 2009. Animal Evolution, Bioturbation, and the Sulfate Concentration of the Oceans 106, 8123–8127.
Canfield, D.E., Poulton, S.W., Narbonne, G.M., 2007. Late Neoproterozoic deep-ocean oxygenation and the rise of animal life. Science 315, 92–95.
Cartier, K.M.S., 2022. The young Earth under the cool Sun. Eos 103. https://doi.org/10.1029/2022EO220089.
Catling, D.C., Zahnle, K.J., 2020. The Archean atmosphere. Science Advances 6 (9), eaax1420. https://doi.org/10.1126/sciadv.aax142.
Cavalazzi, B., Lemelle, L., Simionovici, A., Cady, S.L., Russell, M.J., Bailo, E., Canteri, R., Enrico, E., Manceau, A., Maris, A., Salomé, M., Thomassot, E., Bouden, N., Tucoulou, R., Hofmann, A., 2021. Cellular remains in a ~ 3.42-billion-year-old subseafloor hydrothermal environment. Science Advances 7, eabf3963. https://doi.org/10.1126/sciadv.abf396.
Cawood, P.A., Hawkesworth, C.J., Pisarevsky, S.A., Dhuime, B., Capitanio, F.A., Nebel, O., 2018. Geological archive of the onset of plate tectonics. Philosophical Transactions of the Royal Society of London A 376, 20170405. https://doi.org/10.1098/rsta.2017.0405.
Chan, C.S., Emerson, D., Luther III, G.W., 2016. The role of microaerophilic Fe-oxidizing micro-organisms in producing banded iron formations. Geobiology 14, 509–528.
Chen, G., Cheng, Q., Lyons, T.W., Shen, J., Agterberg, F., Huang, N., Zhao, M., 2022. Reconstructing Earth's atmospheric oxygenation history using machine learning. Nature Communications 13, 5862.
Chen, Z., Zhou, C., Yuan, X., Xiao, S., 2019. Death march of a segmented and trilobate bilaterian elucidates early animal evolution. Nature 573, 412–415. https://doi.org/10.1038/s41586-019-1522-7.
Clodoré, L., Foucher, F., Hickman-Lewis, K., Sorieul, S., Jouve, J., Réfrégiers, M., Collet, G., Petoud, S., Gratuze, B., Westall, F., 2024. MultitTechnique characterization of 3.45 Ga microfossils on Earth: A key approach to detect possible traces of life in returned samples from Mars. Astrobiology 24, 190–226. https://doi.org/10.1089/ast.2023.0089.
Cockell, C., 2000. The ultraviolet history of the terrestrial planets: implications for biological evolution. Planet Space Sci 48, 203–214. https://doi.org/10.1016/S0032-0633(99)00087-2.
Cockell, C.S., Raven, J.A., 2004. Zones of photosynthetic potential on Mars and the early Earth. Icarus 169, 300–310. https://doi.org/10.1016/j.icarus.2003.12.024.
Coffey, J.M., Flannery, D.T., Walter, M.R., George, S.C., 2013. Sedimentology, stratigraphy and geochemistry of a stromatolite biofacies in the 2.72 Ga Tumbiana Formation, Fortescue Group. Western Australia. Precambrian Research 236, 282–296. https://doi.org/10.1016/j.precamres.2013.07.021.
Cohen, P.A., Macdonald, F.A., 2015. The Proterozoic record of eukaryotes. Paleobiology 41, 610–632. https://doi.org/10.1017/pab.2015.25.
Cohen, P.A., Knoll, A.H., Kodner, R.B., 2009. Large spinose microfossils in Ediacaran rocks as resting stages of early animals. Proceedings of the National Academy of Sciences of the United States of America 106, 6519–6524.
Cohen, P.A., Kodner, R.B., 2022. The earliest history of eukaryotic life: uncovering an evolutionary story through the integration of biological and geological data. Trends in Ecology & Evolution 37, P246–P256. https://doi.org/10.1016/j.tree.2021.11.005.
Cohen, P.A., Strauss, J.V., Rooney, A.D., Sharma, M., Tosca, N., 2017. Controlled hydroxyapatite biomineralization in an ~810 million-year-old unicellular eukaryote. Sci. Adv. 3, e1700095.
Cribb, A.T., Kenchington, C.G., Koester, B., Gibson, B.M., Boag, T.H., Racicot, R.A., Mocke, H., Laflamme, M., Darroch, S.A.F., 2019. Increase in metazoan ecosystem engineering prior to the Ediacaran-Cambrian boundary in the Nama Group. Namibia. Royal Society Open Science 6, 190548. https://doi.org/10.1098/rsos.190548.
Crock, F.H.C., Orgel, L.E., 1973. Directed panspermia. Icarus 19, 341–346.
Cunningham, J.A., Liu, A.G., Bengtson, S., Donoghue, P.C.J., 2017. The origin of animals: Can molecular clocks and the fossil record be reconciled? Bioessays 39. https://doi.org/10.1002/bies.201600120.

Czaja, A.D., Beukes, N.J., Osterhourt, J.T., 2016. Sulfur-oxidizing bacteria prior to the Great Oxidation Event from the 2.52 Ga Gamohaan Formation of South Africa. Geology 44, 983–986. https://doi.org/10.1130/G38150.1.

Czaja, A.D., Johnson, C.M., Beard, B.L., Roden, E.E., Li, W. and Moorbath, S. (2013). Biological Fe oxidation controlled deposition of banded iron formation in the ca. 3770Ma Isua Supracrustal Belt (West Greenland). Earth and Planetary Science Letters 363, 192–203. https://doi. org/10. 1016/j.epsl.2012.12.025.

da Costa, F. G., Silva, A. R. C., Lima, R. B., Santos, P. A., de Souza, S. M., Chaves, C. L., and Vasquez, M. L. (2023). Possible record of Neoarchean (2.7 Ca) stromatolites in the Carajás Province, Brazil. ANAJS 19° Symposio de Geologia da Amazonia, Santarém-PA, 23-25 Aug. 2023. Economic Geology 113, 1769.

da Luz, B.R., Crowley, J.K., 2012. Morphological and chemical evidence of stromatolitic deposits in the 2.75 Ga Carajas banded iron formation. Brazil. Earth and Planetary Science Letters 355, 60–72. https://doi.org/10.1016/j.epsl.2012.08.028.

Damer, B., Deamer, D., 2020. The hot spring hypothesis for an origin of life. Astrobiology 20, 429–452. https://doi.org/10.1089/ast.2019.2045.

Darroch, S.A.F., Sperling, E.A., Boag, T.H., Racicot, R.A., Mason, S.J., Morgan, A.S., Tweedt, S., Myrow, P., Johnston, D.T., Erwin, D.H., Laflamme, M., 2015. Biotic replacement and mass extinction of the Ediacara biota. Proceedings of the Royal Society B (biological Sciences) 282, 20151003. https://doi.org/10.1098/rspb.2015.1003.

Darroch, S.A.F., Laflamme, M., Wagner, P.J., 2018. High ecological complexity in benthic Ediacaran communities. Nature Ecology & Evolution 2, 1541–1547. https://doi.org/10.1038/s41559-018-0663-7.

Darroch, S.A.F., Cribb, A.T., Buatois, L.A., Germs, G.J.B., Kenchington, C.G., Smith, E.F., Mocke, H., O'Neil, G.R., Schiffbauer, J.D., Maloney, K.M., Racicot, R.A., Turk, K.A., Gibson, B.M., Almond, J., Koester, B., Boag, T.H., Tweedt, S.M., Laflamme, M., 2021. The trace fossil record of the Nama Group, Namibia: Exploring the terminal Ediacaran roots of the Cambrian explosion. Earth Science Reviews 212, 103435. https://doi.org/10.1016/j.earscirev.2020.103435.

Darroch, S.A.F., Smith, E.F., Nelson, L.L., Craffey, M., Schiffbauer, J.D., Laflamme, M., 2023. Causes and consequences of end-Ediacaran extinction: An update. Cambridge Prisms: Extinction 1, e15.

de Vries, S.T., Nijman, W., de Boer, P.L., 2010. Sedimentary geology of the palaeoarchaean Buck Ridge (South Africa) and Kittys Gap (Western Australia) volcano-sedimentary complexes. Precambrian Research 183, 749–769. https://doi.org/10.1016/j.precamres.2010.09.005.

de Wit, M.J., Furnes, H., 2016. 3.5-Ga hydrothermal fields and diamictites in the Barberton Greenstone Belt-Paleoarchean crust in cold environments. Sci. Adv. 2, e1500368.

de Wit, M., Hart, R., Martin, A., Abbott, P., 1982. Archean abiogenic and probable biogenic structures associated with mineralized hydrothermal vent systems and regional metasomatism, with implications for greenstone belt studies. Economic Geology 77, 1783–1802. https://doi.org/10.1126/sciadv.1500368.

Delarue, F., Robert, F., Sugitani, K., Tartese, R., Duhamel, R., Derenne, S., 2018. Nitrogen isotope signatures of microfossils suggest aerobic metabolism 3.0 Gyr ago. Geochemical Perspectives Letters 7, 32–36. https://doi.org/10.7185/geochemlet.1816. hal-02330893.

Demoulin, C.F., Lara, Y.J., Cornet, L., François, C., Baurain, D., Wilmotte, A., Javaux, E. J., 2019. Cyanobacteria evolution: Insight from the fossil record. Free Radical Biology and Medicine 140, 206–223.

Dhuime, B., Hawkesworth, C.J., Cawood, P.A., Storey, C.D., 2012. A change in the geodynamics of continental growth 3 billion years ago. Science 335, 1334–1336. https://doi.org/10.1126/science.1216066.

Di Giulio, M., 2010. Biological evidence against the panspermia theory. Journal of Theoretical Biology 266 (4), 569–572.

Dietz, R.S., Fairbridge, R.W., 1968. Wave base. In: Geomorphology. Encyclopedia of Earth Science. Springer, Berlin, Heidelberg. https://doi.org/10.1007/3-540-31060-6_404.

Djokic, T., Van Kranendonk, M.J., Campbell, K.A., Walter, M.R., Ward, C.R., 2017. Earliest signs of life on land preserved in ca. 3.5 Ga hot spring deposits. Nature. Communications 8, 15263. https://doi.org/10.1038/ncomms15263.

Dodd, M.S., Papineau, D., Grenne, T., Slack, J.F., Rittner, M., Pirajno, F., O'Neill, J., Little, C.T., 2017. Evidence for early life in Earth's oldest hydrothermal vent precipitates. Nature 543, 60–64. https://doi.org/10.1038/nature21377.

Dohrmann, M., Wörheide, G., 2017. Dating early animal evolution using phylogenomic data. Scientific Reports 7, 3599. https://doi.org/10.1038/s41598-017-03791-w.

Dong, L., Xiao, S., Shen, B., Yuan, X., Yan, X., Peng, Y., 2008. Restudy of the worm-like carbonaceous compression fossils *Protoarenicola*, *Pararenicola*, and *Sinosabellidites* from early Neoproterozoic successions in North China. Palaeogeography Palaeoclimatology Palaeoecology 258, 138–161. https://doi.org/10.1016/j.palaeo.2007.05.019.

Dos Reis, M., Thawornwattana, Y., Angelis, K., Telford, M.J., Donoghue, P.C.J., Yang, Z., 2015. Uncertainty in the timing of origin of animals and the limits of precision in molecular timescales. Current Biology 25, 2939–2950. https://doi.org/10.1016/j.cub.2015.09.066.

Dreher, C.L., Schad, M., Robbins, L.J., Konhauser, K.O., Kappler, A., Joshi, P., 2021. Microbial processes during deposition and diagenesis of Banded Iron Formations. PalZ 95, 593–610. https://doi.org/10.1007/s12542-021-00598-z.

Droser, M.L., Tarhan, L.G., Gehling, J.G., 2017. The rise of animals in a changing environment: Global ecological innovation in the late Ediacaran. Annual Review of Earth and Planetary Sciences 45, 593–617. https://doi.org/10.1146/annurev-earth-063016-015645.

Droser, M.L., Gehling, J.G., Tarhan, L.G., Evans, S.D., Hall, C.M.S., Hughes, I.V., Hughes, E.B., Dzaugis, M.E., Dzaugis, M.P., Dzaugis, P.W., Rice, D., 2019. Piecing together the puzzle of the Ediacara Biota: Excavation and reconstruction at the Ediacara National Heritage site Nilpena (South Australia). Palaeogeography Palaeoclimatology Palaeoecology 513, 132–145. https://doi.org/10.1016/j.palaeo.2017.09.007.

Du, R., Tian, L., 1986. The Macroalgal Fossils of the Qingbaikou Period in the Yanshan Range. Hebei Science and Technology Press, Shijiazhuang, p. 114.

Dunn, F.S., Liu, A.G., Grazhdankin, D.V., Vixseboxse, P., Flannery-Sutherland, J., Green, E., Harris, S., Wilby, P.R., Donoghue, P.C.J., 2021. The developmental biology of *Charnia* and the eumetazoan affinity of the Ediacaran rangeomorphs. Science. Advances 7, eabe0291. https://doi.org/10.1126/sciadv.abe0291.

Dunn, F.S., Kenchington, C.G., Parry, L.A., Clark, J.W., Kendall, R.S., Wilby, P.R., 2022. A crown-group cnidarian from the Ediacaran of Charnwood Forest, UK. Nature Ecology & Evolution 6, 1095–1104. https://doi.org/10.1038/s41559-022-01807-x.

Efremov, I.A., 1940. Taphonomy: a new branch of paleontology. Pan-American Geology. 74, 81–93.

Eickmann, B., Hofmann, A., Wille, M., Bui, T.H., Wing, B.A., Schoenberg, R., 2018. Isotopic evidence for oxygenated Mesoarchaean shallow oceans. Nature Geoscience 11, 133–138. https://doi.org/10.1038/s41561-017-0036-x.

Eme, L., Sharpe, S.C., Brown, M.W., Roger, A.J., 2014. On the age of eukaryotes: evaluating evidence from fossils and molecular clocks. Cold Spring Harbor Perspectives in Biology 6, a016139.

Eme, L., Spang, A., Lombard, J., Stairs, C.W., Ettema, T.J.G., 2017. Archaea and the origin of eukaryotes. Nature Review Microbiology 15, 711–723. https://doi.org/10.1038/nrmicro.2017.133.

Eme, L., Tamarit, D., Caceres, E.F., Stairs, C.W., Anda, V.D., Schön, M.E., Seitz, K.W., Dombrowski, N., Lewis, W.H., Homa, F., Saw, J.H., Lombard, J., Nunoura, T., Li, W.-J., Hua, Z.-S., Chen, L.-X., Banfield, J.F., St John, E., Reysenbach, A.-L., Stott, M.B., Schramm, A., Kjeldsen, K.U., Teske, A.P., Baker, B.J., Ettema, T.J.G., 2023. Inference and reconstruction of the heimdallarchaeial ancestry of eukaryotes. Nature 618, 992–999. https://doi.org/10.1038/s41586-023-06186-2.

Eriksson, P.G., Altermann, W., 1998. An overview of the geology of the Transvaal Supergroup dolomites (South Africa). Environmental Geology 36, 179–188. https://doi.org/10.1007/s002540050334.

Eroglu, S., van Zuilen, M.A., Taubald, H., Drost, K., Wille, M., Swanner, E.D., Beukes, N. J., Schoenberg, R., 2017. Depth-dependent δ13C trends in platform and slope settings of the Campbellrand-Malmani carbonate platform and possible implications for Early Earth oxygenation. Precambrian Research 302, 122–139. https://doi.org/10.1016/j.precamres.2017.09.018.

Erwin, D.H., Laflamme, M., Tweedt, S.M., Sperling, E.A., Pisani, D., Peterson, K.J., 2011. The Cambrian conundrum: Early divergence and later ecological success in the early history of animals. Science 334, 1091–1097.

Ettwig, K.F., Butler, M.K., Le Paslier, D., Pelletier, E., Mangenot, S., Kuypers, M.M.M., Schreiber, F., Dutilh, B.E., Zedelius, J., de Beer, D., Gloerich, J., Wessels, H.J.C.T., van Alen, T., Luesken, F., Wu, M.L., van de Pas-Schoonen, K.T., Op den Camp, H.J. M., Janssen-Megens, E.M., Francoijs, K.J., Stunnenberg, H., Weissenbach, J., Jetten, M.S.M., Strous, M., 2010. Nitrite-driven anaerobic methane oxidation by oxygenic bacteria. Nature 464, 543–558. https://doi.org/10.1038/nature08883.

Evans, S.D., Diamond, C.W., Droser, M.L., Lyons, T.W., 2018. Dynamic oxygen and coupled biological and ecological innovation during the second wave of the Ediacara Biota. Emerging Topics in Life Sciences 2, 223–233. https://doi.org/10.1042/ETLS20170148.

Evans, S.D., Hughes, I.V., Gehling, J.G., Droser, M.L., 2020. Discovery of the oldest bilaterian from the Ediacaran of South Australia. Proceeding of the National Academy of Sciences of the United State of America 117, 7845–7850. https://doi.org/10.1073/pnas.2001045117.

Evans, S.D., Tu, C., Rizzo, A., Surprenant, R.L., Boan, P.C., McCandless, H., Marshall, N., Xiao, S., Droser, M.L., 2022. Environmental drivers of the first major animal extinction across the Ediacaran White Sea-Nama transition. Proceeding of the National Academy of Sciences of the United State of America 119. https://doi.org/10.1073/pnas.2207475119 e2207475119.

Fairchild, T.R., Sanchez, E.A., Pacheco, M.L.A., de Moraes Leme, J., 2012. Evolution of Precambrian life in the Brazilian geological record. International Journal of Astrobiology 11, 309–323. https://doi.org/10.1017/S1473550412000183.

Falkowski, P.G., Katz, M.E., Knoll, A.H., Quigg, A., Raven, J.A., Schofield, O., Taylor, F.J. R., 2004. The evolution of modern eukaryotic phytoplankton. Science 305, 354–360.

Fang, H., Tang, D., Zhou, L., Jiang, G., Shi, X., Liang, L., Zhuo, X., Longfei, S., Xie, B., 2024. Mineralogy-based stepwise dissolution of dolomitic limestone reveals high iodine content in water-column precipitated calcite and well–oxygenated shallow seawater during the~ 1.57 Ga oxygenation event. Chemical Geology 654, 122052. https://doi.org/10.1016/j.chemgeo.2024.122052.

Farquhar, J., Peters, M., Johnston, D.T., Strauss, H., Masterson, A., Masterton, A., Wiechert, M., Kaufman, A.J., 2007. Isotopic evidence for Mesoarchaean anoxia and changing atmospheric sulphur chemistry. Nature 449, 706–709. https://doi.org/10.1038/nature06202.

Fedo, C.M., Myers, J.S., Appel, P.W., 2001. Depositional setting and paleogeographic implications of earth's oldest supracrustal rocks, the > 3.7 Ga Isua Greenstone belt. West Greenland. Sedimentary Geology 141, 61–77.

Fedonkin, M.A., Waggoner, B.M., 1997. The late Precambrian fossil *Kimberella* is a mollusc-like bilaterian organism. Nature 388, 868–871.

Field, E.K., Kato, S., Findlay, A.J., MacDonald, D.J., Chiu, B.K., Luther III, G.W., Chan, C. S., 2016. Planktonic marine iron oxidizers drive iron mineralization under low-oxygen conditions. Geobiology 14, 499–508.

Fischer, W.W., Schroder, S., Lacassie, J.P., Beukes, N.J., Goldberg, T., Strauss, H., Horstmann, U.E., Schrag, D.P., Knoll, A.H., 2009. Isotopic constraints on the Late Archean carbon cycle from the Transvaal Supergroup along the western margin of the Kaapvaal Craton, South Africa. Precambrian Research 169, 15–27. https://doi.org/10.1016/j.precamres.2008.10.010.

Flannery, D. T. (2010). Timing the origin of cyanobacteria: sedimentology and stromatolites of the 2.72 Ga Tumbiana formation (Doctoral dissertation, UNSW Sydney). Doi: 10.26190/unsworks/23566.
Flemming, B.W., 2024. The concept of wave base: fact and fiction. Geo-Marine Letters 44 (3), 1–9.
Fouquet, Y., Pelleter, E., Konn, C., Chazot, G., Dupré, S., Alix, A.S., Chéron, S., Donval, J.-P., Guyader, V., Etoubleau, J., Charlou, J.-L., Labanieh, S., Scalabrin, C., 2018. Volcanic and hydrothermal processes in submarine calderas: The Kulo Lasi example (SW Pacific). Ore Geology Reviews 99, 314–343.
Fralick, P.W., Ramsay, B., Afroz, M., Lalonde, S.V., and Riding, R. (2024). Chapter 6.4.6 Earth's first major carbonate platforms. In, ed. by M. Homann, Archean Earth, Elsevier, in press.
Fralick, P., Riding, R., 2015. Steep Rock Lake: Sedimentology and geochemistry of an Archean carbonate platform. Earth Sci. Rev. 15, 132–175. https://doi.org/10.1016/j.earscirev.2015.10.006.
François, C., Debaille, V., Paquette, J.L., Baudet, D., Javaux, E., 2018. The earliest evidence for modern-style plate tectonics recorded by HP–LT metamorphism in the Paleoproterozoic of the Democratic Republic of the Congo. Scientific Reports 8, 15452. https://doi-org.inc.bib.cnrs.fr/10.1038/s41598-018-33823-y.
Francovschi, I., Grădinaru, E., Li, H., Shumlyanskyy, L., Ciobotaru, V., 2021. U-Pb geochronology and Hf isotope systematics of detrital zircon from the late Ediacaran Kalyus Beds (East European Platform): palaeogeographic evolution of southwestern Baltica and constraints on the Ediacaran biota. Precambrian Research 355, 106062. https://doi.org/10.1016/j.precamres.2020.106062.
Frei, R., Bridgwater, D., Rosing, M., Stecher, O., 1999. Controversial Pb-Pb and Sm-Nd isotope results in the early Archean Isua (West Greenland) oxide iron formation: Preservation of primary signatures versus secondary disturbances. Geochimica Cosmochimica Acta 63, 473–488. https://doi.org/10.1016/S0016-7037(98)00290-7.
Frei, R., Gaucher, C., Poulton, S.W., Canfield, D.E., 2009. Fluctuations in Precambrian atmospheric oxygenation recorded by chromium isotopes. Nature 461, 250–1223. https://doi.org/10.1038/nature08266.
French, K.L., Hallmann, C., Hope, J.M., Schoon, P.L., Zumberge, J.A., Hoshino, Y., Peters, C.A., George, S.C., Love, G.D., Brocks, J.J., Buick, R., Summons, R.E., 2015. Reappraisal of hydrocarbon biomarkers in Archean rocks. Proceedings of the National Academy of Sciences 112, 5915–5920. https://doi-org.inc.bib.cnrs.fr/10.1073/pnas.1419563112.
Gehling, J.G., Droser, M.L., 2018. Ediacaran scavenging as a prelude to predation. Emerging Topics in Life Sciences 2, 213–222. https://doi.org/10.1042/ETLS20170166.
Gehling, J.G., Runnegar, B.N., Droser, M.L., 2014. Scratch traces of large Ediacara bilaterian animals. Journal of Paleontology 88, 284–298.
Gehling, J.G., García-Bellido, D.C., Droser, M.L., Tarhan, M.L., Runnegar, B., 2019. Ediacaran-Cambrian transition: sedimentary facies versus extinction. Estudios Geológicos 75, e099.
Gehling, J.G., Narbonne, G.M., 2007. Spindle-shaped Ediacara fossils from the Mistaken Point assemblage, Avalon Zone, Newfoundland. Canadian Journal of Earth Sciences 44, 367–387.
Gibson, T.M., Shih, P.M., Cumming, V.M., Fischer, W.W., Crockford, P.W., Hodgskiss, M. S.W., Wörndle, S., Creaser, R.A., Rainbird, R.H., Skulski, T.M., Halverson, G.P., 2018. Precise age of *Bangiomorpha pubescens* dates the origin of eukaryotic photosynthesis. Geology 46, 135–138. https://doi.org/10.1130/G39829.1.
Glass, J.B., Wolfe-Simon, F., Anbar, A.D., 2009. Coevolution of metal availability and nitrogen assimilation in cyanobacteria and algae. Geobiology 7, 100–123.
Gnilovskaya, M.B., Veis, A.F., Bekker, A.Y., Olovyanishnikov, V.G., Raaben, M.E., 2000. Pre-Ediacarian fauna from Timan (Annelidomorphs of the late Riphean). Stratigraphy and Geological Correlation 8, 327–352.
Godfrey, L.V., Falkowski, P.G., 2009. The cycling and redox state of nitrogen in the Archaean ocean. Nature Geoscience 2, 725–729. https://doi.org/10.1038/ngeo633.
Golubkova, Y.E., Zaitseva, T.S., Kuznetsov, A.B., Dovzhikova, E.G., Maslov, A.V., 2015. Microfossils and Rb-Sr age of glauconite in the key section of the upper Proterozoic of the northeastern part of the Russian Plate (Keltmen-1 Borehole). Doklady Earth Sciences 462, 547–551. https://doi.org/10.1134/S1028334X15060045.
Gourier, D., Binet, L., Calligaro, T., Capelli, S., Vezin, H., Bréhéret, J.G., Hickman-Lewis, K., Gautret, P., Foucher, F., Campbell, K.A., Westall, F., 2019. Extraterrestrial organic matter preserved in 3.33 Ga sediments from Barberton. South Africa. Geochimica et Cosmochimica Acta 258, 207–225.
Govind, A.V., Behera, K., Dash, J.K., Balakrishnan, S., Bhutani, R., Managave, S., Srinivasan, R., 2021. Trace element and isotope Geochemistry of Neoarchean carbonate rocks from the Dharwar craton, southern India: Implications for depositional environments and mantle influence on ocean chemistry. Precambrian Research 357, 106137. https://doi.org/10.1016/j.precamres.2021.106137.
Grassineau, N.V., Abell, P., Appel, P.W.U., Lowry, D. and Nisbet, E.G. (2006). Early life signatures in sulfur and carbon isotopes from Isua, Barberton, Wabigoon (Steep Rock), and Belingwe Greenstone Belts (3.8 to 2.7 Ga). In: S.E. Kesler and H. Ohmoto, (Editors), Evolution of Early Earth's Atmosphere, Hydrosphere, and Biosphere – Constraints from Ore Deposits: Geological Society of America Memoir 198, 33-52. Doi: 10.1130/2006.1198(02).
Grassineau, N.V., Nisbet, E.G., Bickle, M.J., Fowler, C.M.R., Lowry, D., Mattey, D.P., Abell, P., Martin, A., 2001. Antiquity of the biological sulphur cycle: evidence from sulphur and carbon isotopes in 2700 million-year-old rocks of the Belingwe Belt, Zimbabwe. Proceedings of the Royal Society of London B 268, 113–119. https://doi.org/10.1098/rspb.2000.1338.
Grey, K., 2005. Ediacaran palynology of Australia. Memoirs of the Association of Australasian Palaeontologists 31, 1–439.
Grey, K., Awramik, S.M., 2020. Handbook for the Study and Description of Microbialites. Geological Survey of Western Australia 147, 278 p.
Grosch, E.G., Hazen, R.M., 2015. Microbes, mineral evolution, and the rise of microcontinents—origin and coevolution of life with early earth. Astrobiology 15, 922–939.
Grotzinger, J.P., Ingersoll, R.V., 1992. Proterozoic sedimentary basins. In: Schopf, J.W., Klein, C. (Eds.), The Proterozoic Biosphere. Cambridge Univ. Press, pp. 47–50. https://doi.org/10.1017/CBO9780511601064.
Grotzinger, J.P., Fike, D.A., Fischer, W.W., 2011. Enigmatic origin of the largest-known carbon isotope excursion in Earth's history. Nature Geoscience 4, 285–292. https://doi.org/10.1038/NGEO1138.
Gumsley, A.P., Chamberlain, K.R., Bleeker, W., Söderlund, U., De Kock, M.O., Larsson, E. R., Bekker, A., 2017. Timing and tempo of the Great Oxidation Event. Proceedings of the National Academy of Sciences 114, 1811–1816. https://doi.org/10.1073/pnas.1608824114.
Halla, J., Noffke, N., Reis, H., Awramik, S., Bekker, A., Brasier, A., Callefo, F., Choudhury, A., Duda, J.-P., Fedo, C., Galante, D., Haddock, J., Haines, P., Hinnov, L., Hofmann, A., Homann, M., Huston, D., Johnson, S., Kah, L., Kaufman, A., Kovalick, A., Kuchenbecker, M., Köykkä, J., Lowe, D., Nhleko, N., Reno, B., Sanchez, E., Shukla, Y., Smith, A., Van Zuilen, M., Westall, F., Whitehouse, M., 2024. Ratification of the base of the ICS Geological Time Scale: the Global Standard Stratigraphic Age (GSSA) for the Hadean lower boundary. Episodes Journal of International Geoscience. https://doi.org/10.18814/epiiugs/2024/024002.
Halliday, A.N., 2000. Terrestrial accretion rates and the origin of the Moon. Earth & Planetary Science Letters 176, 17–30. https://doi.org/10.1016/S0012-821X(99)00317-9.
Han, T.-M., Runnegar, B., 1992. Megascopic eukaryotic algae from the 2.1 billion-year-old Negaunee Iron-Formation. Michigan. Science 257, 232–235.
Harrison, T.M., 2009. The Hadean crust: evidence from> 4 Ga zircons. Annual Review of Earth and Planetary Sciences 37, 479–505. https://doi.org/10.1146/annurev.earth.031208.100151.
Hassenkam, T., Andersson, M., Dalby, K., Mackenzie, D., Rosing, M., 2017. Elements of Eoarchean life trapped in mineral inclusions. Nature 548, 78–81. https://doi.org/10.1038/nature23261.
Haugaard, R., White, S., Jørgensen, T. R., Frieman, B., Meek, D., Zhou, X., Mathieu, L. and Ayer, J. (2023). Sedimentary processes, provenance, and tectonic control on fluvial sandstone geochemistry during Superior craton stabilization. In: Laurentia: Turning Points in the Evolution of a Continent, (Eds. S. J. Whitmeyer, M. L. Williams, D. A. Kellett, and B. Tikoff) Geological Society of America. DOI: 10.1130/2022.1220(02).
Hawkesworth, C.J., Cawood, P.A., Dhuime, B., 2020. The evolution of the continental crust and the onset of plate tectonics. Frontiers in Earth Science 8, 326. https://doi.org/10.3389/feart.2020.00326.
Hazen, R.M., 2005. Genesis: The Scientific Quest for Life's Origins. National Academy Press, Washington, D.C., p. 368
Hermann, T.N., 1990. Organic World Billion Year Ago. Nauka, Leningrad, p. 49.
Hermann, T.N., Podkovyrov, V.N., 2010. A discovery of Riphean heterotrophs in the Lakhanda Group of Siberia. Paleontological Journal 44, 374–383.
Heubeck, C., 2009. An early ecosystem of Archean tidal microbial mats (Moodies Group, South Africa, ca. 3.2 Ga). Geology 37, 931–934. https://doi.org/10.1130/G30101A.1.
Heubeck, C., 2019. The Moodies Group—a high-resolution archive of Archaean surface processes and basin-forming mechanisms. The Archaean Geology of the Kaapvaal Craton, Southern Africa 133–169. https://doi.org/10.1007/978-3-319-78652-0_6.
Hickman, A.H., 2012. Review of the Pilbara Craton and Fortescue Basin, Western Australia: Crustal evolution providing environments for early life. Island Arc 21, 1–31. https://doi.org/10.1111/j.1440-1738.2011.00783.x.
Hickman, A.H., 2023. Fortescue Group: The Neoarchean Breakup of the Pilbara Craton. In: Archean Evolution of the Pilbara Craton and Fortescue Basin. Modern Approaches in Solid Earth Sciences. Springer, Cham, p. 24. https://doi.org/10.1007/978-3-031-18007-1_12.
Hickman-Lewis, K., Cavalazzi, B., Foucher, F., Westall, F., 2018. Most Ancient Evidence for Life in the Barberton Greenstone Belt: Microbial Mats and Biofabrics of the ~3.47 Ga Middle Marker Horizon. Precambrian Research 312, 45–67. https://doi.org/10.1016/j.precamres.2018.04.007.
Hickman-Lewis, K., Westall, F., 2021. A southern African perspective on the co-evolution of early life and environments. South African Journal of Geology 124, 225–252. https://doi.org/10.25131/sajg.124.0016.
Hickman-Lewis, K., Gautret, P., Arbaret, L., Sorieul, S., De Wit, R., Foucher, F., Cavalazzi, B., Westall, F., 2019. Mechanistic morphogenesis of organosedimentary structures growing under geochemically stressed conditions: keystone to the interpretation of some Archaean stromatolites? Geosciences 9, 359. https://doi.org/10.3390/geosciences9080359.
Hickman-Lewis, K., Cavalazzi, B., Sorieul, S., Gautret, P., Foucher, F., Whitehouse, M.J., Jeon, H., Georgelin, T., Cockell, C.S., Westall, F., 2020a. Metallomics in deep time and the influence of ocean chemistry on the metabolic landscapes of Earth's earliest ecosystems. Scientific Reports 10, 4965. https://doi.org/10.1038/s41598-020-61774-w.
Hickman-Lewis, K., Gourcerol, B., Westall, F., Manzini, D., Cavalazzi, B., 2020b. Reconstructing Palaeoarchaean microbial biomes flourishing in the presence of emergent landmasses using trace and rare earth element systematics. Precambrian Research 342, 105689.
Hoffman, P.F., Abbot, D.S., Ashkenazy, Y., Benn, D.I., Brocks, J.J., Cohen, P.A., Cox, G. M., Creveling, J.R., Donnadieu, Y., Erwin, D.H., Fairchild, I.J., Ferreira, D., Goodman, J.C., Halverson, G.P., Jansen, M.F., Le Hir, G., Love, G.D., Macdonald, F. A., Maloof, A.C., Partin, C.A., Ramstein, G., Rose, B.E.J., Rose, C.V., Sadler, P.M.,

Tziperman, E., Voigt, A., Warren, S.G., 2017. Snowball Earth climate dynamics and Cryogenian geology-geobiology. Science Advances 3, e1600983.
Hofmann, H.J., 1985. The mid-Proterozoic Little Dal macrobiota, Mackenzie Mountains, north-west Canada. Palaeontology 28, 331–354.
Hofmann, H.J., 1999. Global distribution of the Proterozoic sphaeromorph acritarch Valeria lophostriata (Jankauskas). Acta Micropalaeontologica Sinica 16, 215–224.
Hofmann, A., and Wilson, A. H. (2007). Chapter 5.5 Silicified Basalts, Bedded Cherts and Other Sea Floor Alteration Phenomena of the 3.4 Ga Nondweni Greenstone Belt, South Africa. In M. Kranendonk, H. Smithies, & V. Bennett (Eds.), Earth's Oldest Rocks (pp. 571-605). (Developments in Precambrian Geology; Vol. 15). Doi: 10.1016/S0166-2635(07)15055-6.
Hofmann, H., Chen, J., 1981. Carbonaceous megafossils from the Precambrian (1800 Ma) near Jixian, northern China. Canadian Journal of Earth Sciences 18, 443–447.
Hofmann, H.J., Grey, K., Hickman, A.H., Thorpe, R., 1999. Origin of 3.45 Ga coniform stromatolites in Warrawoona Group, Western Australia. Geological Society of America Bulletin 111, 1256–1262. https://doi.org/10.1130/0016-7606(1999)111<1256:oogcsi>2.3.co;2.
Hofmann, A., Harris, C., 2008. Silica alteration zones in the Barberton greenstone belt: A window into subseafloor processes 3.5–3.3 Ga ago. Chemical Geology 257, 221–239. https://doi.org/10.1016/j.chemgeo.2008.09.015.
Hohmann-Marriott, M.F., Blankenship, R.E., 2011. Evolution of photosynthesis. Annual Review of Plant Biology 62, 515–548. https://doi.org/10.1146/annurev-arplant-042110-103811.
Holland, H.D., 1994. Early Proterozoic atmosphere change. In: Bengtson, S. (Ed.), Early Life on Earth. Columbia University Press, New York, pp. 237–244.
Holland, H.D., 2002. Volcanic gases, black smokers, and the Great Oxidation Event. Geochim Cosmochim Acta 66, 3811–3826. https://doi.org/10.1016/S0016-7037(02)00950-X.
Holligan, P.M., Fernández, E., Aiken, J., Balch, W.M., Boyd, P., Burkill, P.H., Finch, M., Groom, S.B., Malin, G., Muller, K., Purdie, D.A., Robinson, C., Trees, C.C., Turner, S. M., van der Wal, P., 1993. A biogeochemical study of the coccolithophore, *Emiliania huxleyi*, in the North Atlantic. Global Biogeochemical Cycles 7, 879–900. https://doi.org/10.1029/93GB01731.
Homann, M., 2019. Earliest life on earth: evidence from the Barberton Greenstone Belt. South Africa. Earth-Science Reviews 196, 102888. https://doi.org/10.1016/j.earscirev.2019.102888.
Homann, M., Heubeck, C., Airo, A., Tice, M.M., 2015. Morphological adaptations of 3.22 Ga-old microbial communities to Archean coastal habitats (Moodies Group, Barberton Greenstone Belt, South Africa). Precambrian Research 266, 47–64. https://doi.org/10.1016/j.precamres.2015.04.018.
Homann, M., Heubeck, C., Bontognali, T.R.R., Bouvier, A.S., Baumgartner, L.P., Airo, A., 2016. Evidence for cavity-dwelling microbial life in 3.22 Ga tidal deposits. Geology 44, 51–54. https://doi.org/10.1130/G37272.1.
Howard, C.M., Sheldon, N.D., Smith, S.Y., Noffke, N., 2024. Interpreting an Archaean paleoenvironment through 3D imagery of microbialites. Geobiology 22, e12601.
Hren, M.T., Lowe, D.R., Tice, M.M., Byerly, G., Chamberlain, C.P., 2006. Stable isotope and rare earth element evidence for recent ironstone pods within the Archean Barberton greenstone belt, South Africa. Geochimica et Cosmochimica Acta 70, 1457–1470. https://doi.org/10.1016/j.gca.2005.11.016.
Hribovšek, P., Olesin Denny, E., Dahle, H., Mall, A., Øfstegaard Viflot, T., Boonnawa, C., Reeves, E.P., Steen, H., Stokke, R., 2023. Putative novel hydrogen-and iron-oxidizing sheath-producing Zetaproteobacteria thrive at the Fåvne deep-sea hydrothermal vent field. mSystems 8 (6), e00543–e623. https://doi.org/10.1128/msystems.00543-23.
Hua, H., Chen, Z., Yuan, X., Zhang, L., Xiao, S., 2005. Skeletogenesis and asexual reproduction in the earliest biomineralizing animal *Cloudina*. Geology 33, 277–280.
Hua, H., Chen, Z., Yuan, X., 2007. The advent of mineralized skeletons in Neoproterozoic Metazoa: new fossil evidence from the Gaojiashan Fauna. Geological Journal 42, 263–279.
Hubert, A., 2015. Chemical and mineralogical signatures of oxygenic photosynthesis in Archean and Paleoproterozoic sediments. University of Orléans. PhD thesis.
Hug, L.A., Baker, B.J., Anantharaman, K., Brown, C.T., Probst, A.J., Castelle, C.J., Butterfield, C.N., Hernsdorf, A.W., Amano, Y., Ise, K., Suzuki, Y., Dudek, N., Relman, D.A., Finstad, K.M., Amundson, R., Thomas, B.C., Banfield, J.F., 2017. A new view of the tree of life. Nature Microbiology 1, 16048. https://doi.org/10.1038/nmicrobiol.2016.48.
Huntley, J.W., Xiao, S., Kowalewski, M., 2006. 1.3 billion years of acritarch history: An empirical morphospace approach. Precambrian Research 144, 52–68.
Jacobson, S.A., Morbidelli, A., Raymond, S.N., O'Brien, D.P., Walsh, K.J., Rubie, D.C., 2014. Highly siderophile elements in Earth's mantle as a clock for the Moon-forming impact. Nature 508, 84–87. https://doi.org/10.1038/nature13172.
Javaux, E.J., 2007. The early eukaryotic fossil record. In: Jékely, G. (Ed.), Eukaryotic Membranes and Cytoskeleton: Origins and Evolution. Landes Bioscience and Springer Science & Business Media, New York, NY, pp. 1–19.
Javaux, E.J., 2011. Evolution of early eukaryotes in Precambrian oceans. In: Gargaud, M., López-García, P., Martin, H. (Eds.), Origins and Evolution of Life: an Astrobiological Perspective. Cambridge University Press, Cambridge, pp. 414–449.
Javaux, E.J., 2019. Challenges in evidencing the earliest traces of life. Nature 572, 451–460. https://doi.org/10.1038/s41586-019-1436-4.
Javaux, E.J., Knoll, A.H., 2017. Micropaleontology of the lower Mesoproterozoic Roper Group, Australia, and implications for early eukaryotic evolution. Journal of Paleontology 91, 199–229. https://doi.org/10.1017/jpa.2016.124.
Javaux, E.J., Lepot, K., 2018. The Paleoproterozoic fossil record: implications for the evolution of the biosphere during Earth's middle-age. Earth-Science Reviews 176, 68–86. https://doi.org/10.1016/j.earscirev.2017.10.001.
Javaux, E.J., Marshall, C.P., Bekker, A., 2010. Organic-walled microfossils in 3.2-billion-year-old shallow-marine siliciclastic deposits. Nature 463, 934–938. https://doi.org/10.1038/nature08793.
Jing, Y., Chen, Z.-Q., Anderson, R.P., Wang, X., Zheng, Z., Feng, X., 2022. Microscopic and geochemical analyses of the Tonian Longfengshan biota from the Luotuoling Formation (Hebei Province, North China) with taphonomic implications. Precambrian Research 382, 106899. https://doi.org/10.1016/j.precamres.2022.106899.
Johnson, C.M., Zheng, X.Y., Djokic, T., Van Kranendonk, M.J., Czaja, A.D., Roden, E.E., Beard, B.L., 2022. Early Archean biogeochemical iron cycling and nutrient availability: New insights from a 3.5 Ga land-sea transition. Earth-Science Reviews 228, 103992. https://doi.org/10.1016/j.earscirev.2022.103992.
Johnston, D.T., Wolfe-Simon, F., Pearson, A., and Knoll, A.H. (2009). Anoxygenic photosynthesis modulated Proterozoic oxygen and sustained Earth's middle age. Proceedings of the National Academy of Sciences U. S. A. 106, 16925–16929.
Jørgensen, B.B., Boetius, A., 2007. Feast and famine—microbial life in the deep-sea bed. Nature Reviews Microbiology 5, 770–781. https://doi.org/10.1038/nrmicro1745.
Joseph, R., Gibson, C., Wolowski, K., Bianciardi, G., Kidron, G.J., del Gaudio, R., Armstrong, R.A., Suamanarathna, A.R., Cantasano, N., Duvall, D., Schild, R., 2022. Mars: Evolution of life in the oceans? Episodes of global warming, flooding, rivers, lakes, and chaotic orbital obliquity. Journal of Astrobiology 13, 14–126.
Kamber, B.S., 2015. The evolving nature of terrestrial crust from the Hadean, through the Archaean, into the Proterozoic. Precambrian Research 258, 48–82. https://doi.org/10.1016/j.precamres.2014.12.007.
Kamber, B.S., Bolhar, R., Webb, G.E., 2004. Geochemistry of late Archaean stromatolites from Zimbabwe: evidence for microbial life in restricted epicontinental seas. Precambrian Research 132, 379–399. https://doi.org/10.1016/j.precamres.2004.03.006.
Kamber, B.S., Webb, G.E., Gallagher, M., 2014. The rare earth element signal in Archaean microbial carbonate: information on ocean redox and biogenicity. Journal of the Geological Society 171, 745–763. https://doi.org/10.1144/jgs2013-110.
Kamber, B.S., Whitehouse, M.J., 2007. Microscale sulphur isotope evidence for sulphur cycling in the late Archean shallow ocean. Geobiology 5, 5–17. https://doi.org/10.1111/j.1472-4669.2006.00091.x.
Kanaparthi, D. Westall, F., Lampe, M., Zhu, B., Boesen, T., Scheu, B., Klingl, A., Schwille, P., and Lueders, T. (2024). On the nature of the earliest known lifeforms. eLife. Doi: 10.7554/eLife.98637.1.
Kappler, A., Pasquero, C., Konhauser, K.O., Newman, D.K., 2005. Deposition of banded iron formations by anoxygenic phototrophic Fe (II)-oxidizing bacteria. Geology 33, 865–868. https://doi.org/10.1130/G21658.1.
Karhu, J.A., Holland, H.D., 1996. Carbon isotopes and the rise of atmospheric oxygen. Geology 24, 867–870. https://doi.org/10.1130/0091-7613(1996)024<0867:CIATRO>2.3.CO;2.
Kasting, J.F., Liu, S.C., Donahue, T.M., 1979. Oxygen levels in the prebiological atmosphere. Journal of Geophysical Research: Oceans 84, 3097–3107. https://doi.org/10.1029/JC084iC06p03097.
Kazmierczak, J., Altermann, W., Kremer, B., Kempe, S., Eriksson, P.G., 2009. Mass occurrence of benthic coccoid cyanobacteria and their role in the production of Neoarchean carbonates of South Africa. Precambrian Research 173, 79–92. https://doi.org/10.1016/j.precamres.2009.02.002.
Keeling, P.J., Burki, F., 2019. Progress towards the Tree of eukaryotes. Current Biology 29, R808–R817. https://doi.org/10.1016/j.cub.2019.07.031.
Kminek, G., Bada, J.L., Pogliano, K., Ward, J., 2003. Radiation dependent limit for the viability of bacterial spores in halite fluid inclusions and on Mars. Radiation Research 159, 722–729. https://doi.org/10.1667/0033-7587(2003)159[0722:rlftvo]2.0.co;2.
Knauth, P.L., 2005. Temperature and salinity history of the Precambrian ocean: implications for the course of microbial evolution. Palaeogeography, Palaeoclimatology, Palaeoecology 219, 53e69. https://doi.org/10.1016/j.palaeo.2004.10.014.
Knoll, A.H., 1992. The early evolution of eukaryotes: A geological perspective. Science 256, 622–627.
Knoll, A.H., 2011. The multiple origins of complex multicellularity. Annual Review of Earth and Planetary Sciences 39, 217–239. https://doi.org/10.1146/annurev.earth.031208.100209.
Knoll, A.H., 2014. Paleobiological perspectives on early eukaryotic evolution. Cold Spring Harbor Perspectives in Biology 6, a016121.
Knoll, A.H., Javaux, E.J., Hewitt, D., Cohen, P., 2006. Eukaryotic organisms in Proterozoic oceans. Philosophical Transactions of the Royal Society of London B Biological Sciences 361, 1023–1038.
Konhauser, K.O., Amskold, L., Lalonde, S.V., Posth, N.R., Kappler, A., Anbar, A., 2007. Decoupling photochemical Fe (II) oxidation from shallow-water BIF deposition. Earth and Planetary Science Letters 258 (1–2), 87–100.
Konhauser, K.O., Pecoits, E., Lalonde, S.V., Papineau, D., Nisbet, E.G., Barley, M.E., Arndt, N.T., Zahnle, K., Kamber, B.S., 2009. Oceanic nickel depletion and a methanogen famine before the great oxidation event. Nature 458, 750–753.
Korenaga, J., 2021. Hadean geodynamics and the nature of early continental crust. Precambrian Research 359, 106178. https://doi.org/10.1016/j.precamres.2021.106178.
Krissansen-Totton, J., Arney, G. N., and Catling, D. C. (2018), Constraining the climate and ocean pH of the early Earth with a geological carbon cycle model. Proceedings of the National Academy of Sciences U.S.A. 115, 4105–4110. https://doi-org.inc.bib.cnrs.fr/10.1073/pnas.1721296115.
Laflamme, M., Darroch, S.A.F., Tweedt, S.M., Peterson, K.J., Erwin, D.H., 2013. The end of the Ediacara biota: Extinction, biotic replacement, or Cheshire Cat? Gondwana Research 23, 558–573.

Lahr, D.J.G., Kosakyan, A., Lara, E., Mitchell, E.A.D., Morais, L., Porfirio-Sousa, A.L., Ribeiro, G.M., Tice, A.K., Pánek, T., Kang, S., Brown, M.W., 2019. Phylogenomics and morphological reconstruction of Arcellinida testate amoebae highlight diversity of microbial eukaryotes in the Neoproterozoic. Current Biology 29, 991–1001. https://doi.org/10.1016/j.cub.2019.01.078.

Lamb, D.M., Awramik, S.M., Zhu, S., 2007. Paleoproterozoic compression-like structures from the Changzhougou Formation, China: Eukaryotes or clasts? Precambrian Research 154, 236–247. https://doi.org/10.1016/j.precamres.2006.12.012.

Lamb, D.M., Awramik, S.M., Chapman, D.J., Zhu, S., 2009. Evidence for eukaryotic diversification in the ~1800 million-year-old Changzhougou Formation, North China. Precambrian Research 173, 93–104.

Lan, Z., Kamo, S.L., Roberts, N.M.W., Sano, Y., Li, X.-H., 2022. A Neoarchean (ca. 2500 Ma) age for jaspilite-carbonate BIF hosting purported micro-fossils from the Eoarchean (≥3750 Ma) Nuvvuagittuq supracrustal belt (Québec, Canada). Precambrian Research 377, 106728. https://doi.org/10.1016/j.precamres.2022.106728.

Lane, N., Allen, J.F., Martin, W., 2010. How did LUCA make a living? Chemiosmosis in the origin of life. BioEssays 32, 271–280. https://doi.org/10.1002/bies.200900131.

Lantink, M.L., Davies, J.H., Ovtcharova, M., and Hilgen, F.J. (2022). Milankovitch cycles in banded iron formations constrain the Earth–moon system 2.46 billion years ago. Proceedings of the National Academy of Sciences USA119 (40), e2117146119. DOI: 10.1073/pnas.2117146119.

Ledevin, M., 2019. Archean cherts: Formation processes and paleoenvironments. Earth's Oldest Rocks: Amsterdam, Elsevier 913–944. https://doi.org/10.1016/B978-0-444-63901-1.00037-X.

Lenton, T.M., Daines, S.J., 2016. Matworld - the biogeochemical effects of early life on land. New Phytologist. https://doi.org/10.1111/nph.14338.

Lepot, K., 2020. Signatures of early microbial life from the Archean (4 to 2.5 Ga) eon. Earth-Science Reviews 209, 103296.

Lepot, K., Benzerara, K., Brown Jr, G.E., Philippot, P., 2008. Microbially influenced formation of 2,724-million-year-old stromatolites. Nature Geoscience 1, 118–121. https://doi.org/10.1038/ngeo107.

Li, Z.X., Bogdanova, S.V., Collins, A.S., Davidson, A., De Waele, B., Ernst, R.E., Fitzsimons, I.C.W., Fuck, R.A., Gladkochub, D.P., Jacobs, J., Karlstrom, K.E., Lu, S., Natapov, L.M., Pease, V., Pisarevsky, S., Thrane, K., Vernikovsky, V., 2008. Assembly, configuration, and break-up history of Rodinia: A synthesis. Precambrian Research 160, 179–210.

Li, G., Chen, L., Pang, K., Zhou, G., Han, C., Yang, L., Lv, W., Wu, C., Wang, W., Yang, F., 2020. An assemblage of macroscopic and diversified carbonaceous compression fossils from the Tonian Shiwangzhuang Formation in western Shandong. North China. Precambrian Research 346, 105801. https://doi.org/10.1016/j.precamres.2020.105801.

Li, M., Liu, P., Yin, C., Tang, F., Gao, L., Chen, S., 2012. Acritarchs from the Baicaoping Formation (Ruyang Group) of Henan. Acta Palaeontologica Sinica 51, 76–87.

Li, Z., Ma, X., Li, S., An, W., Li, Q., Dong, Y., Zhang, Y., 2023. Mesoproterozoic-Neoproterozoic chronostratigraphic framework and provenance analysis in the southeastern North China Craton and its tectonic significance. Geological Journal 58, 3096–3120. https://doi.org/10.1002/gj.4754.

Liu, P., Xiao, S., Yin, C., Chen, S., Zhou, C., and Li, M. (2014). Ediacaran acanthomorphic acritarchs and other microfossils from chert nodules of the upper Doushantuo Formation in the Yangtze Gorges area, South China. Journal of Paleontology 72 (supplement to No 1), 1-139. Doi: 10.1666/13-009.

Liu, A.G., McIlroy, D., Brasier, M.D., 2010. First evidence for locomotion in the Ediacara biota from the 565 Ma Mistaken Point Formation, Newfoundland. Geology 38, 123–126. https://doi.org/10.1130/G30368.1.

Liu, A.G., Matthews, J.J., Menon, L.R., McIlroy, D., Brasier, M.D., 2014a. *Haootia quadriformis* n. gen., n. sp., interpreted as a muscular cnidarian impression from the late Ediacaran period (approx. In: 560 Ma). Proceedings of the Royal Society B (biological Sciences), p. 281. https://doi.org/10.1098/rspb.2014.1202.

Liu, A.G., Kenchington, C.G., Mitchell, E.G., 2015. Remarkable insights into the paleoecology of the Avalonian Ediacaran macrobiota. Gondwana Research 27, 1355–1380. https://doi.org/10.1016/j.gr.2014.11.002.

Liu, P., Moczydłowska, M., 2019. Ediacaran microfossils from the Doushantuo Formation chert nodules in the Yangtze Gorges area, South China, and new biozones. Fossils and Strata 65, 1–172. https://doi.org/10.1002/9781119564195.

Loron, C.C., Rainbird, R.H., Turner, E.C., Greenman, J.W., Javaux, E.J., 2019a. Organic-walled microfossils from the late Mesoproterozoic to early Neoproterozoic lower Shaler Supergroup (Arctic Canada): Diversity and biostratigraphic significance. Precambrian Research 321, 349–374. https://doi.org/10.1016/j.precamres.2018.12.024.

Loron, C.C., François, C., Rainbird, R.H., Turner, E.C., Borensztajn, S., Javaux, E.J., 2019b. Early fungi from the Proterozoic era in Arctic Canada. Nature 570, 232–235. https://doi.org/10.1038/s41586-019-1217-0.

Loron, C.C., Halverson, G.P., Rainbird, R.H., Skulski, T., Turner, E.C., Javaux, E.J., 2021. Shale-hosted biota from the Dismal Lakes Group in Arctic Canada supports an early Mesoproterozoic diversification of eukaryotes. Journal of Paleontology 95, 1113–1137. https://doi.org/10.1017/jpa.2021.45.

Lowe, D.R., 1999. Petrology and sedimentology of cherts and related silicified sedimentary rocks in the Swaziland Supergroup, Geologic Evolution of the Barberton Greenstone Belt, South Africa. Geological Society of America Special Paper 29, 83–114. https://doi.org/10.1016/j.earscirev.2020.103296.

Lowe, D.R., Byerly, G.R., 2018. The terrestrial record of Late Heavy Bombardment. New Astronomy Reviews 81, 39–61. https://doi.org/10.1016/j.newar.2018.03.002.

Lowe, D.R., Byerly, G.R., 2020. The non-glacial and non-cratonic origin of an early Archean felsic volcaniclastic unit, Barberton Greenstone Belt. South Africa. Precambrian Research 341, 105647. https://doi.org/10.1016/j.precamres.2020.105647.

Lowe, D.R., Ibarra, D.E., Drabon, N., Chamberlain, C.P., 2020. Constraints on surface temperature 3.4 billion years ago based on triple oxygen isotopes of cherts from the Barberton Greenstone Belt, South Africa, and the problem of sample selection. American Journal of Science 320, 790–814. https://doi.org/10.2475/11.2020.02.

Lyons, T.W., Reinhard, C.T., Planavsky, N.J., 2014. The rise of oxygen in Earth's early ocean and atmosphere. Nature 506, 307–315. https://doi.org/10.1038/nature13068.

Lyons, T.W., Diamond, C.W., Planavsky, N.J., Reinhard, C.T., Li, C., 2021. Oxygenation, life, and the planetary system during Earth's middle history: An overview. Astrobiology 21, 906–923. https://doi.org/10.1089/ast.2020.2418.

Lyu, D., Deng, Y., Wang, X., Ye, Y., Pang, K., Miao, L., Luo, Z., Zhang, F., Lu, Y., Deng, S., Wang, H., Zhang, S., 2022. New chronological and paleontological evidence for Paleoproterozoic eukaryote distribution and stratigraphic correlation between the Yanliao and Xiong'er basins. North China Craton. Precambrian Research 371, 106577. https://doi.org/10.1016/j.precamres.2022.106577.

Maher, K.A., Stevenson, D.J., 1988. Impact frustration of the origin of life. Nature 331, 612–614. https://doi.org/10.1038/331612a0.

Marchi, S., Drabon, N., Schulz, T., Schaefer, L., Nesvorny, D., Bottke, W.F., Koeberl, C., Lyons, T., 2021. Delayed and variable late Archaean atmospheric oxidation due tohigh collision rates on Earth. Nature Geoscience 14, 827–831. https://doi.org/10.1038/s41561-021-00835-9.

Margulis, L., 1991. Symbiosis in Evolution: Origins of Cell Motility: Origins of Cell Motility. In: Evolution of Life: Fossils, Molecules, and Culture. Tokyo, Springer Japan, pp. 305–324.

Marin-Carbonne, J., Chaussidon, M., Robert, F., 2012. Micrometer-scale chemical and isotopic criteria (O and Si) on the origin and history of Precambrian cherts: implications for paleo-temperature reconstructions. Geochimica et Cosmochimica Acta 92, 129–147. https://doi.org/10.1016/j.gca.2012.05.040.

Martin, W., Baross, J., Kelley, D., Russell, M.J., 2008. Hydrothermal vents and the origin of life. Nature Reviews Microbiology 6, 805–814. https://doi.org/10.1038/nrmicro1991.

Martin, A., Nisbet, E.G., Bickle, M.J., 1980. Archaean stromatolites of the Belingwe greenstone belt, Zimbabwe (Rhodesia). Precambrian Research 13, 337–362. https://doi.org/10.1016/0301-9268(80)90049-2.

Marty, B., Avice, G., Bekaert, D.V., Broadley, M.W., 2018. Salinity of the Archaean oceans from analysis of fluid inclusions in quartz. Comptes Rendus Geoscience 350, 154–163. https://doi.org/10.1016/j.crte.2017.12.002.

Mason, T.R., von Brunn, V., 1977. 3-Gyr-old stromatolites from South Africa. Nature 266, 47–49. https://doi-org.inc.bib.cnrs.fr/10.1038/266047a0.

Matthews, J.J., Liu, A.G., Yang, C., McIlroy, D., Levell, B., Condon, D.J., 2020. A chronostratigraphic framework for the rise of the Ediacaran macrobiota: New constraints from Mistaken Point Ecological Reserve, Newfoundland. Geological Society of America Bulletin 133, 612–624. https://doi.org/10.1130/B35646.1.

Maynard Smith, J., Szathmary, E., 1997. The Major Transitions in Evolution. Oxford University Press, Oxford, p. 346.

McIntyre, T., Fralick, P., 2017. Sedimentology and geochemistry of the 2930 Ma Red Lake-Wallace Lake carbonate platform, Western Superior Province. Canada. the Depositional Record 3), 258–287. https://doi.org/10.1002/dep2.36.

McMahon, S., 2019. Earth's earliest and deepest purported fossils may be iron-mineralized chemical gardens. Proceedings of the Royal Society B 286 (1916), 20192410.

McMahon, S., Ivarsson, M., Wacey, D., Saunders, M., Belivanova, V., Muirhead, D., Knoll, P., Steinbock, O., Frost, D.A., 2021. Dubiofossils from a Mars-analogue subsurface palaeoenvironment: The limits of biogenicity criteria. Geobiology 19, 473–488. https://doi.org/10.1111/gbi.12445.

Meyer, M., Xiao, S., Gill, B.C., Schiffbauer, J.D., Chen, Z., Zhou, C., Yuan, X., 2014. Interactions between Ediacaran animals and microbial mats: Insights from *Lamonte trevallis*, a new trace fossil from the Dengying Formation of South China. Palaeogeography Palaeoclimatology Palaeoecology 396, 62–74. https://doi.org/10.1016/j.palaeo.2013.12.026.

Miao, L., Moczydłowska, M., Zhu, S., Zhu, M., 2019. New record of organic-walled, morphologically distinct microfossils from the late Paleoproterozoic Changcheng Group in the Yanshan Range, North China. Precambrian Research 321, 172–198. https://doi.org/10.1016/j.precamres.2018.11.019.

Miao, L., Moczydłowska, M., Zhu, M., 2021. A diverse organic-walled microfossil assemblage from the Mesoproterozoic Xiamaling Formation. North China. Precambrian Research 360, 106235. https://doi.org/10.1016/j.precamres.2021.106235.

Miao, L., Yin, Z., Li, G., Zhu, M., 2024a. First report of *Tappania* and associated microfossils from the late Paleoproterozoic Chuanlinggou Formation of the Yanliao Basin. North China. Precambrian Research 400, 107268. https://doi.org/10.1016/j.precamres.2023.107268.

Miao, L., Yin, Z., Knoll, A.H., Qu, Y., Zhu, M., 2024b. 1.63-billion-year-old multicellular eukaryotes from the Chuanlinggou Formation in North China. Science. Advances 10, eadk3208. https://doi.org/10.1126/sciadv.adk3208.

Mißbach, H., Duda, J.P., van den Kerkhof, A.M., Lüders, V., Pack, A., Reitner, J., Thiel, V., 2021. Ingredients for microbial life preserved in 3.5 billion-year-old fluid inclusions. Nature. Communications 12, 1101. https://doi-org.inc.bib.cnrs.fr/10.1038/s41467-021-21323-z.

Mitchell, E.G., Butterfield, N.J., 2018. Spatial analyses of Ediacaran communities at Mistaken Point. Paleobiology 44, 40–57. https://doi.org/10.1017/pab.2017.35.

Mitchell, R., Evans, D.A.D., 2023. The balanced billion. GSA Today 34 (2), 10–11.

Moczydłowska, M., Nagovitsin, K.E., 2012. Ediacaran radiation of organic-walled microbiota recorded in the Ura Formation, Patom Uplift, East Siberia. Precambrian Research 198–199, 1–24.
Moczydłowska, M., Willman, S., 2009. Ultrastructure of cell walls in ancient microfossils as a proxy to their biological affinities. Precambrian Research 173, 27–38.
Mojzsis, S.J., Brasser, R., Kelly, N.M., Abramov, O., Werner, S.C., 2019. Onset of giant planet migration before 4480 million years ago. Astrophysics Journal 881, 44. https://doi.org/10.3847/1538-4357/ab2c03.
Monty, C., 1974. Precambrian background and Phanerozoic history of stromatolitic communities, an overview. Annales De La Société Géologique De Belgique 90, 55–99.
Morais, L., Fairchild, T.R., Lahr, D.J.G., Rudnitzki, I.D., Schopf, J.W., Garcia, A.K., Kudryavtsev, A.B., Romero, G.R., 2017. Carbonaceous and siliceous Neoproterozoic vase-shaped microfossils (Urucum Formation, Brazil) and the question of early protistan biomineralization. Journal of Paleontology 91, 393–406. https://doi.org/10.1017/jpa.2017.16.
Morton, R.A. (1988). Nearshore responses to great storms. In H.E. Clifton (Ed.) Sedimentologic consequences of convulsive geologic events. Geological Society of America Special Paper, 229, 7-22. DOI: Doi: 10.1130/SPE229.
Mukhopadhyay, J., 2020. Archean banded iron formations of India. Earth-Science Reviews 201, 102927. https://doi.org/10.1016/j.earscirev.2019.102927.
Mulder, J.A., Nebel, O., Gardiner, N.J., Cawood, P.A., Wainwright, A.N., Ivanic, T.J., 2021. Crustal rejuvenation stabilised Earth's first cratons. Nature Communications 12, 3535. https://doi.org/10.1038/s41467-021-23805-6.
Nagovitsin, K.E., 2001. New late Riphean composite microfossils from the Yenisei Ridge. Paleontological Journal 35, 225–232.
Nagovitsin, K., 2009. *Tappania*-bearing association of the Siberian platform: Biodiversity, stratigraphic position and geochronological constraints. Precambrian Research 173, 137–145. https://doi.org/10.1016/j.precamres.2009.02.005.
Nagovitsin, K.E., Rogov, V.I., Marusin, V.V., Karlova, G.A., Kolesnikov, A.V., Bykova, N. V., Grazhdankin, D.V., 2015. Revised Neoproterozoic and Terreneuvian stratigraphy of the Lena-Anabar Basin and north-western slope of the Olenek Uplift, Siberian Platform. Precambrian Research 270, 226–245. https://doi.org/10.1016/j.precamres.2015.09.012.
Narbonne, G.M., 2005. The Ediacara Biota: Neoproterozoic origin of animals and their ecosystems. Annual Review of Earth and Planetary Sciences 33, 421–442.
Narbonne, G.M., Gehling, J.G., 2003. Life after snowball: The oldest complex Ediacaran fossils. Geology 31, 27–30.
Neveu, M., Hays, L.E., Voytek, M.A., New, M.H., Schulte, M.D., 2018. The ladder of life detection. Astrobiology 18, 1375–1402. https://doi.org/10.1089/ast.2017.1773.
Nijman, W., Kloppenburg, A., de Vries, S.T., 2017. Archaean basin margin geology and crustal evolution: An east Pilbara traverse. Journal of the Geological Society 174, 1090–1112. https://doi.org/10.1144/jgs2016-127.
Nisbet E.G. and Fowler, C.M.R. (2014). The Early History of Life. In: H.D. Holland and K. K. Turekian (Editors), Treatise on Geochemistry, Second Edition, vol. 10, 1-42. Oxford: Elsevier. ISBN: 0080999476, 9780080999470.
Nisbet, E.G., Grassineau, N.V., Howe, C.J., Abell, P.I., Regelous, M., Nisbet, R.E.R., 2007. The age of Rubisco: the evolution of oxygenic photosynthesis. Geobiology 5, 311–335. https://doi.org/10.1111/j.1472-4669.2007.00127.x.
Noffke, N., 2009. The criteria for the biogeneicity of microbially induced sedimentary structures (MISS) in Archean and younger, sandy deposits. Earth-Science Reviews 96, 173–180. https://doi.org/10.1016/j.earscirev.2008.08.002.
Noffke, N., 2015. Ancient sedimentary structures in the< 3.7 Ga Gillespie Lake Member, Mars, that resemble macroscopic morphology, spatial associations, and temporal succession in terrestrial microbialites. Astrobiology 15, 169–192. https://doi.org/10.1089/ast.2014.1218.
Noffke, N., 2021. Microbially induced sedimentary structures in clastic deposits: implication for the prospection for fossil life on Mars. Astrobiology 21, 866–892. https://doi.org/10.1089/ast.2021.0011.
Noffke, N., Awramik, S.M., 2013. Stromatolites and MISS—differences between relatives. Geological Society of America Today 23, 4–9.
Noffke, N., Eriksson, K.A., Hazen, R.M., Simpson, E.L., 2006. A new window into early Archaean life: microbial mats in Earth's oldest siliciclastic tidal deposits (3.2 Ga Moodies Group, South Africa). Geology 34, 253–256. https://doi.org/10.1130/G22246.1.
Noffke, N., Beukes, N., Hazen, R.M., Swift, D., 2008. An actualistic perspective into Archean worlds—(cyano-)bacterially induced sedimentary structures in the siliciclastic Nhlazatse Section, 2.9 Ga Pongola Supergroup. South Africa. Geobiology 6, 5–20. https://doi.org/10.1111/j.1472-4669.2007.00118.x.
Noffke, N., Christian, D., Wacey, D., Hazen, R.M., 2013. Microbially induced sedimentary structures recording an ancient ecosystem in the ca. 3.48 billion-year-old Dresser Formation, Pilbara. Western Australia. Astrobiology 13, 1103–1124. https://doi.org/10.1089/ast.2013.1030.
Nutman, A.P., Bennett, V.C., Friend, C.R., Van Kranendonk, M.J., Chivas, A.R., 2016. Rapid emergence of life shown by discovery of 3,700-million-year-old microbial structures. Nature 537, 535–538. https://doi.org/10.1038/nature19355.
Nutman, A.P., Bennett, V.C., Friend, C.R., 2017. Seeing through the magnetite: Reassessing Eoarchean atmosphere composition from Isua (Greenland)≥ 3.7 Ga banded iron formations. Geoscience Frontiers 8, 1233–1240. https://doi.org/10.1016/j.gsf.2017.02.008.
Nutman, A.P., Bennett, V.C., Friend, C.R., Van Kranendonk, M.J., Rothacker, L., Chivas, A.R., 2019. Cross-examining Earth's oldest stromatolites: Seeing through the effects of heterogeneous deformation, metamorphism and metasomatism affecting Isua (Greenland)~ 3700 Ma sedimentary rocks. Precambrian Research 331, 105347. https://doi.org/10.1016/j.precamres.2019.105347.
Oehler, D.Z., Robert, F., Walter, M.R., Sugitani, K., Meibom, A., Mostefaoui, S., Gibson, E. K., 2010. Diversity in the Archean biosphere: new insights from NanoSIMS. Astrobiology 10, 413–424. https://doi.org/10.1089/ast.2009.0426.
Oehler, D.Z., Walsh, M.M., Sugitani, K., Liu, M.C., House, C.H., 2017. Large and robust lenticular microorganisms on the young Earth. Precambrian Research 296, 112–119. https://doi.org/10.1016/j.precamres.2017.04.031.
Olson, J.M., Blankenship, R.E., 2004. Thinking about the evolution of photosynthesis. Photosynthesis Research 80, 373–386. https://doi.org/10.1098/rsob.180246.
O'Neill, C., Debaille, V., Griffin, W., 2013. Deep earth recycling in the Hadean and constraints on surface tectonics. American Journal of Science 313, 912–932. https://doi.org/10.2475/09.2013.04.
Onstott, T.C., Phelps, T.J., Kieft, T., Colwell, F.S., Balkwill, D.L., Fredrickson, J.K., Brockman, F.J., 1999. A global perspective on the microbial abundance and activity in the deep subsurface. Enigmatic Microorganisms and Life in Extreme Environments 487–500. https://doi.org/10.1099/mic.0.001172.
Onstott, T.C., Ehlmann, B.L., Sapers, H., Coleman, M., Ivarsson, M., Marlow, J.J., Neubeck, A., Niles, P., 2019. Paleo-rock-hosted life on Earth and the search on Mars: a review and strategy for exploration. Astrobiology 19, 1230–1262. https://doi.org/10.1089/ast.2018.1960.
Orange, F., Westall, F., Disnar, J.R., Prieur, D., Bienvenu, N., Le Romancer, M., Défarge, C., 2009. Experimental silicification of the extremophilic Archaea *Pyrococcus abyssi* and *Methanocaldococcus jannaschii*: applications in the search for evidence of life in early Earth and extraterrestrial rocks. Geobiology 7 (4), 403–418. https://doi.org/10.1111/j.1472-4669.2009.00212.x.
Orange, F., Disnar, J.R., Gautret, P., Westall, F., Bienvenu, N., Lottier, N., Prieur, D., 2013. Preservation and evolution of organic matter during experimental fossilisation of the hyperthermophilic Archaea Methanocaldococcus jannaschii. Origins of Life & Evolution of Biosphere 42, 587–609.
Oren, A., 2002. Diversity of halophilic microorganisms: environments, phylogeny, physiology, and applications. Journal of Industrial Microbiology and Biotechnology 28, 56–63. https://doi.org/10.1038/sj/jim/7000176.
Orpen, J.L., Wilson, J.F., 1981. Stromatolites at !3,500 Myr and a greenstone granite unconformity in the Zimbabwean Archaean. Nature 291, 218–220. https://doi-org.inc.bib.cnrs.fr/10.1038/291218a0.
Osés, G.L., Wood, R., Romero, G.R., Prado, G.M.E.M., Bidola, P., Herzen, J., Pfeiffer, F., Stampar, S.N., Pacheco, M.L.A.F., 2022. Ediacaran *Corumbella* Has a Cataphract Calcareous Skeleton with Controlled Biomineralization. iScience, 25, 105676. https://doi.org/10.1016/j.isci.2022.105676.
Ossa, F.O., Hofmann, A., Vidal, O., Kramers, J.D., Belyanin, G., Cavalazzi, B., 2016. Unusual manganese enrichment in the Mesoarchean Mozaan Group, Pongola Supergroup, South Africa. Precambrian Research 281, 414–433. https://doi.org/10.1016/j.precamres.2016.06.009.
Ouyang, Q., Guan, C., Zhou, C., Xiao, S., 2017. Acanthomorphic acritarchs of the Doushantuo Formation from an upper slope section in northwestern Hunan Province, South China, with implications for early-middle Ediacaran biostratigraphy. Precambrian Research 298, 512–529. https://doi.org/10.1016/j.precamres.2017.07.005.
Ouyang, Q., Zhou, C., Xiao, S., Guan, C., Chen, Z., Yuan, X., Sun, Y., 2021. Distribution of Ediacaran acanthomorphic acritarchs in the lower Doushantuo Formation of the Yangtze Gorges area, South China: evolutionary and stratigraphic implications. Precambrian Research 353, 106005. https://doi.org/10.1016/j.precamres.2020.106005.
Pacheco, M.L.A.F., Galante, D., Rodrigues, F., Leme, J.D.M., Bidola, P., Hagadorn, W., Stockmar, M., Herzen, J., Rudnitzki, I.D., Pfeiffer, F., Marques, A.C., 2015. Insights into the skeletonization, lifestyle, and affinity of the unusual Ediacaran fossil Corumbella. PLoS. ONE 10, e0114219.
Pang, K., Tang, Q., Schiffbauer, J.D., Yao, J., Yuan, X., Wan, B., Chen, L., Ou, Z., Xiao, S., 2013. The nature and origin of nucleus-like intracellular inclusions in Paleoproterozoic eukaryote microfossils. Geobiology 11, 499–510. https://doi.org/10.1111/gbi.12053.
Pang, K., Tang, Q., Yuan, X., Wan, B., Xiao, S., 2015. A biomechanical analysis of the early eukaryotic fossil Valeria and new occurrence of organic-walled microfossils from the Paleo-Mesoproterozoic Ruyang Group. Palaeoworld 24, 251–262. https://doi.org/10.1016/j.palwor.2015.04.002.
Pang, K., Tang, Q., Wan, B., Yuan, X., 2020. New insights on the palaeobiology and biostratigraphy of the acritarch *Trachyhystrichosphaera aimika*: A potential late Mesoproterozoic to Tonian index fossil. Palaeoworld 29, 476–489. https://doi.org/10.1016/j.palwor.2020.02.003.
Papineau, D., She, Z., Dodd, M.S., Iacoviello, F., Slack, J.F., Hauri, Eshearing, P., Little, C., 2022. Metabolically diverse primordial microbial communities in Earth's oldest seafloor hydrothermal jasper. Science Advances 8, eabm2296. https://doi.org/10.1126/sciadv.abm2296.
Parfrey, L.W., Lahr, D.J.G., Knoll, A.H., Katz, L.A., 2011. Estimating the timing of early eukaryotic diversification with multigene molecular clocks. Proceedings of the National Academy of Sciences of the United States of America 108, 13624–13629.
Parkes, R.J., Cragg, B., Roussel, E., Webster, G., Weightman, A., Sass, H., 2014. A review of prokaryotic populations and processes in sub-seafloor sediments, including biosphere: geosphere interactions. Marine Geology 352, 409–425. https://doi.org/10.1016/j.margeo.2014.02.009.
Pascal, R., Pross, A., Sutherland, J.D., 2013. Towards an evolutionary theory of the origin of life based on kinetics and thermodynamics. Open Biology 130, 156. https://doi.org/10.1098/rsob.130156.
Pavlov, A.A., Kasting, J.F., Eigenbrode, J.L., Freeman, K.H., 2001. Organic haze in Earth's early atmosphere: Source of low-^{13}C Late Archean kerogens? Geology 29 (11), 1003–1006. https://doi.org/10.1130/0091-7613(2001)029<1003:OHIESE>2.0.CO;2.

Peng, Y., Bao, H., Yuan, X., 2009. New morphological observations for Paleoproterozoic acritarchs from the Chuanlinggou Formation, North China. Precambrian Research 168, 223–232.
Peng, Y., Kusky, T., Wang, L., Luan, Z., Wang, C., Liu, X., Zhong, Y., Evans, N.J., 2022. Passive margins in accreting Archaean archipelagos signal continental stability promoting early atmospheric oxygen rise. Nature Communications 13, 7821. https://doi-org.inc.bib.cnrs.fr/10.1038/s41467-022-35559-w.
Peters, S.E., Loss, D.P., 2012. Storm and fair-weather wave base: A relevant distinction? Geology 40, 511–514.
Peters, S.E., Husson, J.M., Wilcots, J., 2017. The rise and fall of stromatolites in shallow marine environments. Geology 45, 487–490. https://doi.org/10.1130/G38931.1.
Pflug, H.D., Jaeschke-Boyer, H., 1979. Combined structural and chemical analysis of 3,800-Myr-old microfossils. Nature 280, 483–486. https://doi.org/10.1038/280483a0.
Pirajno, F. and Huston, D.L. (2019). Paleoarchean (3.6e3.2 Ga) Mineral Systems in the Context of Continental Crust Building and the Role of Mantle Plumes. In Van Kranendonk, M. J., Bennett, V. C., & Hoffmann, J. E. (Eds) Earth's oldest rocks, 187-208. DOI: 10.1016/B978-0-444-63901-1.00009-5.
Porfirio-Sousa, A.L., Tice, A.K., Morais, L., Ribeiro, G.M., Blandenier, Q., Dumack, K., Eglit, Y., Fry, N.W., Souza, M.B.G.E., Henderson, T., Kleitz-Singleton, F., Singer, D., Brown, M.W., and Lahr, D.J.G. (2023). Amoebozoan testate amoebae illuminate the diversity of heterotrophs and the complexity of ecosystems throughout geological time. bioRxiv. Doi: 10.1101/2023.11.08.566222.
Porter, S.M., 2016. Tiny vampires in ancient seas: evidence for predation via perforation in fossils from the 780–740 million-year-old Chuar Group, Grand Canyon, USA. Proceedings of the Royal Society of London, Series b: Biological Sciences 283, 20160221. https://doi.org/10.1098/rspb.2016.0221.
Porter, S.M., 2020. Insights into eukaryogenesis from the fossil record. Interface Focus 10, 20190105. https://doi.org/10.1098/rsfs.2019.0105.
Porter, S.M., Riedman, L.A., 2016. Systematics of organic-walled microfossils from the ca. 780–740 Ma Chuar Group, Grand Canyon. Arizona. Journal of Paleontology 90, 815–853. https://doi.org/10.1017/jpa.2016.57.
Porter, S.M., Riedman, L.A., 2019. Ancient fossilized amoebae find their home in the tree. Current Biology 29, R200–R223. https://doi.org/10.1016/j.cub.2019.02.003.
Porter, S.M., Riedman, L.A., 2023. Frameworks for interpreting the early fossil record of eukaryotes. Annual Review of Microbiology 77, 173–191. https://doi.org/10.1146/annurev-micro-032421-113254.
Porter, S.M., Meisterfeld, R., Knoll, A.H., 2003. Vase-shaped microfossils from the Neoproterozoic Chuar Group, Grand Canyon: A classification guided by modern testate amoebae. Journal of Paleontology 77, 409–429.
Posth, N.R., Hegler, F., Konhauser, K.O., Kappler, A., 2008. Alternating Si and Fe deposition caused by temperature fluctuations in Precambrian oceans. Nature Geoscience 1, 703e708. https://doi.org/10.1016/j.gca.2019.08.031.
Posth, N.R., Canfield, D.E., Kappler, A., 2014. Biogenic Fe (III) minerals: from formation to diagenesis and preservation in the rock record. Earth-Science Reviews 135, 103–121. https://doi.org/10.1016/j.earscirev.2014.03.012.
Poulton, S.W., Fralick, P.W., Canfield, D.E., 2010. Spatial variability in oceanic redox structure 1.8 billion years ago. Nature Geoscience 3, 486–490. https://doi.org/10.1038/ngeo889.
Prasad, B., Uniyal, S.N., Asher, R., 2005. Organic-walled microfossils from the Proterozoic Vindhyan Supergroup of Son Valley, Madhya Pradesh, India. Palaeobotanist 54, 13–60.
Pu, J.P., Bowring, S.A., Ramezani, J., Myrow, P., Raub, T.D., Landing, E., Mills, A., Hodgin, E., Macdonald, F.A., 2016. Dodging snowballs: Geochronology of the Gaskiers glaciation and the first appearance of the Ediacaran biota. Geology 44, 955–958. https://doi.org/10.1130/G38284.1.
Qu, Y., Zhu, S., Whitehouse, M., Engdahl, A., McLoughlin, N., 2018. Carbonaceous biosignatures of the earliest putative macroscopic multicellular eukaryotes from 1630 Ma Tuanshanzi Formation, north China. Precambrian Research 304, 99–109. https://doi.org/10.1016/j.precamres.2017.11.004.
Rasmussen, B., Muhling, J.R., Suvorova, A., Krapež, B., 2017. Greenalite precipitation linked to the deposition of banded iron formations downslope from a late Archean carbonate platform. Precambrian Research, 290: 49–62. doi.org/10. 1016/j.precamres.
Rasmussen, B., J.R. Muhling, and W.W. Fischer. (2019). Evidence from laminated chert in banded iron formations for deposition by gravitational settling of iron-silicate muds. Geology, 47, 167–170. https://doi.org/10.1130/G45560.1.
Rasmussen, B., Fletcher, I.R., Brocks, J.J., Kilburn, M.R., 2008. Reassessing the first appearance of eukaryotes and cyanobacteria. Nature 455, 1101–1104.
Reid, R.P., Visscher, P.T., Decho, A.W., Stolz, J.F., Bebout, B.M., Dupraz, C., Macintyre, I.G., Paerl, H.W., Pinckney, J.L., Prufert-Bebout, L., Steppe, T.F., DesMarais, D.J., 2000. The role of microbes in accretion, lamination and early lithification of modern marine stromatolites. Nature 406, 989–992.
Retallack, G.J., Schmitz, M.D., 2023. Archean (3.3 Ga) paleosols and paleoenvironments of Western Australia. PLoS ONE 18 (9), e0291074.
Retallack, G.J., Krinsley, D.H., Fischer, R., Razink, J.J., Langworthy, K.A., 2016. Archean coastal-plain paleosols and life on land. Gondwana Research 40, 1–20. https://doi.org/10.1016/j.gr.2016.08.003.
Rickaby, R.E.M., 2015. Goldilocks and the three inorganic equilibria: how Earth's chemistry and life coevolve to be nearly in tune. Philosophical Transactions of the Royal Society A 373, 20140188. https://doi.org/10.1098/rsta.2014.0188.
Riding, R., 1999. The term stromatolite: towards an essential definition. Lethaia 32, 321–330.
Riding, R., 2000. Microbial carbonates: the geological record of calcified bacterial–algal mats and biofilms. Sedimentology 47, 179–214.
Riding, R., 2005. Phanerozoic reefal microbial carbonate abundance: Comparisons with metazoan diversity, mass extinction events, and seawater saturation state. Revista Española De Micropaleontología 37, 23–39.
Riding, R., 2008. Abiogenic, microbial and hybrid authigenic carbonate crusts: components of Precambrian stromatolites. Geologia Croatica 61, 73–103. https://doi.org/10.4154/gc.2008.10.
Riding, R., Fralick, P., Liang, L., 2014. Identification of an Archean marine oxygen oasis. Precambrian Research 251, 232–237.
Riding, R., Liang, L., Fralick, P., 2022. Oxygen-induced chemocline precipitation between Archean Fe-rich and Fe-poor carbonate seas. Precambrian Research 383, 106902. https://doi.org/10.1016/j.precamres.2014.06.017.
Riedman, L.A., Porter, S.M., Halverson, G.P., Hurtgen, M.T., Junium, C.K., 2014. Organic-walled microfossil assemblages from glacial and interglacial Neoproterozoic units of Australia and Svalbard. Geology 42, 1011–1014.
Riedman, L.A., Porter, S.M., Calver, C.R., 2017. Vase-shaped microfossil biostratigraphy with new data from Tasmania, Svalbard, Greenland, Sweden and the Yukon. Precambrian Research 319, 19–36. https://doi.org/10.1016/j.precamres.2017.09.019.
Riedman, L.A., Porter, S.M., Lechte, M.A., dos Santos, A., Halverson, G.P., 2023. Early eukaryotic microfossils of the late Palaeoproterozoic Limbunya Group, Birrindudu Basin, northern Australia. Papers in Palaeontology 9, e1538.
Rizzo, V., Armstrong, R., Hua, H., Cantasano, N., Nicolò, T., Giorgio, B., 2021. Life on Mars: Clues, evidence or proof? Solar Planets and Exoplanets, Intechopen, pp. 1–38.
Robbins, L.J., Fakhraee, M., Smith, A.J., Bishop, B.A., Swanner, E.D., Peacock, C.L., Wang, C.L., Planavsky, N.J., Reintard, C., Croawe, S.A., Lyons, T.W., 2023. Manganese oxides, Earth surface oxygenation, and the rise of oxygenic photosynthesis. Earth-Science Reviews 239, 104368. https://doi.org/10.1016/j.earscirev.2023.104368.
Roberge, A., Bolcar, M. R., and France, K. C. (2019). Telling the story of life in the cosmos: the LUVOIR telescope concepts. In UV/Optical/IR Space Telescopes and Instruments: Innovative Technologies and Concepts IX (Vol. 11115, pp. 155-169). SPIE. DOI: 10.1117/12.2530475.
Robert, F., Chaussidon, M., 2006. A palaeotemperature curve for the Precambrian oceans based on silicon isotopes in cherts. Nature 443, 969–972. https://doi.org/10.1038/nature05239.
Roberts, N. M. W., Van Kranendonk, M., Parman, S., Shirey, S. and Clift, P. D. (eds) 2015. Continent Formation Through Time. Geological Society, London, Special Publications, 389, 1–16.
Roberts, N.M., Hernández-Montenegro, J.D., Palin, R.M., 2024. Garnet stability during crustal melting: Implications for chemical mohometry and secular change in arc magmatism and continent formation. Chemical Geology 659, 122142. https://doi.org/10.1016/j.chemgeo.2024.122142.
Rodriguez, L. E., Altair, T., Hermis, N. Y., Jia, T. Z., Roche, T. P., Steller, L. H., and Weber, J. M. (2024). Chapter 4: A Geological and Chemical Context for the Origins of Life on Early Earth. Astrobiology, 24(S1), S-76. DOI: 10.1089/ast.2021.0139.
Rooney, A.D., Cantine, M.D., Bergmann, K.D., Gómez-Pérez, I., Baloushi, B.A., Boag, T.H., Busch, J.F., Sperling, E.A., Strauss, J.V., 2020. Calibrating the Coevolution of Ediacaran Life and Environment 117, 16824–16830. https://doi.org/10.1073/pnas.2002918117.
Rosing, M.T., Frei, R., 2004. U-rich Archaean sea-floor sediments from Greenland–indications of> 3700 Ma oxygenic photosynthesis. Earth and Planetary Science Letters 217, 237–244. https://doi.org/10.1016/S0012-821X(03)00609-5.
Rosing, M.T., Rose, N.M., Bridgwater, D., Thomsen, H.S., 1996. Earliest part of Earth's stratigraphic record: A reappraisal of the ca 3.7 Ga Isua (Greenland) supracrustal sequence. Geology 24, 43–46. https://doi.org/10.34194/ggub.v180.5092.
Ruiz, J., 2017. Heat flow evolution of the Earth from paleomantle temperatures: Evidence for increasing heat loss since~ 2.5 Ga. Physics of the Earth and Planetary Interiors 269, 165–171. https://doi.org/10.1016/j.pepi.2017.06.001.
Russell, M.J., Hall, A.J., 1997. The emergence of life from iron monosulphide bubbles at a submarine hydrothermalredox and pH front. Journal of the Geological Society of London 154, 377–402. https://doi.org/10.1144/gsjgs.154.3.0377.
Sagan, C., Mullen, G., 1972. Earth and Mars: Evolution of atmospheres and surface temperatures. Science 177, 52–56. https://doi.org/10.1126/science.177.4043.52.
Sagan, C., Pollack, J.B., 1974. Differential transmission of sunlight on Mars: biological implications. Icarus 21, 490–495. https://doi.org/10.1016/0019-1035(74)90151-1.
Sánchez-Baracaldo, P., Ridgwell, A., Raven, J.A., 2014. A Neoproterozoic transition in the marine nitrogen cycle. Current Biology 24, 652–657. https://doi.org/10.1016/j.cub.2014.01.041.
Sánchez-Baracaldo, P., Bianchini, G., Wilson, J.D., Knoll, A.H., 2022. Cyanobacteria and biogeochemical cycles through Earth history. Trends in Microbiology 30, 143–157. https://doi.org/10.1016/j.tim.2021.05.008.
Sasselov, D.D., Grotzinger, J.P., Sutherland, J.D., 2020. The origin of life as a planetary phenomenon. Science Advances 6, eaax3419. https://doi.org/10.1126/sciadv.aax3419.
Schidlowski, M., 2001. Carbon isotopes as biogeochemical recorders of life over 3.8 Ga of Earth history: evolution of a concept. Precambrian Research 106, 117–134. https://doi.org/10.1016/S0301-9268(00)00128-5.
Schiffbauer, J.D., Selly, T., Jacquet, S.M., Merz, R.A., Nelson, L.L., Strange, M.A., Cai, Y., Smith, E.F., 2020. Discovery of bilaterian-type through-guts in cloudinomorphs from the terminal Ediacaran Period. Nature Communications 11, 205. https://doi.org/10.1038/s41467-019-13882-z.
Schneider, D.A., Bickford, M.E., Cannon, W.F., Schulz, K.J., Hamilton, M.A., 2002. Age of volcanic rocks and syndepositional iron formations, Marquette Range Supergroup: Implications for the tectonic setting of Paleoproterozoic iron formations of the Lake Superior region. Canadian Journal of Earth Sciences 39, 999–1012.

Schopf, J.W., Kudryavtsev, A.B., Czaja, A.D., Tripathi, A.B., 2007. Evidence of Archean life: stromatolites and microfossils. Precambrian Research 158, 141–155. https://doi.org/10.1016/j.precamres.2007.04.009.
Schreiber, U., Locker-Grütjen, O., Mayer, C., 2012. Hypothesis: Origin of life in deep-reaching tectonic faults. Origins of Life and Evolution of Biosphere 42, 47–54. https://doi.org/10.1007/s11084-012-9267-4.
Schröder, S., Beukes, N.J., Sumner, D.Y., 2008. Microbialite-sediment interactions on the slope of the Campbellrand carbonate platform (Neoarchean, South Africa). Precambrian Research 169, 68–79. https://doi.org/10.1016/j.precamres.2008.10.014.
Sforna, M.C., Loron, C.C., Demoulin, C.F., François, C., Cornet, Y., Lara, Y.J., Grolimund, D., Sanchez, D.F., Medjoubi, K., Somogyi, A., Addad, A., Fadel, A., Compère, P., Baudet, D., Brocks, J.J., Javaux, E.J., 2022. Intracellular bound chlorophyll residues identify 1 Gyr-old fossils as eukaryotic algae. Nature Communications 13, 146. https://doi.org/10.1038/s41467-021-27810-7.
Sharma, M., Shukla, Y., 2009. Taxonomy and affinity of Early Mesoproterozoic megascopic helically coiled and related fossils from the Rohtas Formation, the Vindhyan Supergroup, India. Precambrian Research 193, 105–122.
Sharma, M., Mishra, S., Dutta, S., Banerjee, S., Shukla, Y., 2009. On the affinity of *Chuaria-Tawuia* complex: A multidisciplinary study. Precambrian Research 173, 123–136. https://doi.org/10.1016/j.precamres.2009.04.003.
Shen, B., Dong, L., Xiao, S., Kowalewski, M., 2008. The Avalon explosion: Evolution of Ediacara morphospace. Science 319, 81–84.
Siahi, M., Hofmann, A., Hegner, E., Master, S., 2016. Sedimentology and facies analysis of Mesoarchaean stromatolitic carbonate rocks of the Pongola Supergroup, South Africa. Precambrian Research 278, 244–264. https://doi.org/10.1016/j.precamres.2016.03.004.
Siahi, M., Hofmann, A., Master, S., Wilson, A., Mayr, C., 2018. Trace element and stable (C, O) and radiogenic (Sr) isotope geochemistry of stromatolitic carbonate rocks of the Mesoarchaean Pongola Supergroup: Implications for seawater composition. Chemical Geology 476, 389–406. https://doi.org/10.1016/j.chemgeo.2017.11.036.
Singh, V.K., Sharma, M., 2014. Morphologically complex organic-walled microfossils (OWM) from the late Palaeoproterozoic - early Mesoproterozoic Chitrakut Formation, Vindhyan Supergroup, central India and their implications on the antiquity of eukaryotes. Journal of the Palaeontological Society of India 59, 89–102.
Singh, V.K., Sharma, M., Sergeev, V.N., 2019. A new record of acanthomorphic acritarch Tappania Yin from the early Mesoproterozoic Saraipali Formation, Singhora Group, Chhattisgarh Supergroup, India and its biostratigraphic significance. Journal of Geological Society of India 94, 471–479. https://doi.org/10.1007/s12594-019-1343-1.
Sleep, N.H., 2010. The Hadean-Archaean environment. Cold Spring Harbor Perspectives in Biology 2, a002527. https://doi.org/10.1101/cshperspect.a002527.
Sleep, N. H., Zahnle, K. J., and Lupu, R. E. (2014). Terrestrial aftermath of the moon-forming impact. Philosophical Trans.actions of the Royal Society London A 372 (2024), 20130172. doi:10.1098/rsta.2013.0172.
Spencer, J., 2019. The faint young sun problem revisited. Geological Society of America Today 29 (12). https://doi.org/10.1130/GSATG403A.1.
Spencer, C.J., 2020. Continuous continental growth as constrained by the sedimentary record. American Journal of Science 320, 373–401.
Sprigg, R.C., 1947. Early Cambrian (?) jellyfishes from the Flinders Ranges, South Australia. Transaction of the Royal Society of South Australia 71, 212–224.
Stal, L. J. and Caumette, P. (Eds.). (2013). Microbial mats: structure, development and environmental significance (Vol. 35). Springer Science & Business Media.
Stal, L. J. (2012). Cyanobacterial mats and stromatolites. In Ecology of cyanobacteria II: their diversity in space and time (pp. 65-125). Dordrecht: Springer Netherlands. Doi: 10.1007/978-94-007-3855-3 4.
Steiner, M., 1994. Die neoproterozoischen Megaalgen Südchinas. Berliner Geowissenschaftliche Abhandlungen (e) 15, 1–146.
Steinhoefel, G., Horn, I., von Blanckenburg, F., 2009. Micro-scale tracing of Fe and Si isotope signatures in banded iron formation using femtosecond laser ablation. Geochimica et Cosmochimica Acta 73, 5343e5360. https://doi.org/10.1016/j.gca.2009.05.037.
Steinmann, L., Spiess, V., Sacchi, M., 2018. Post-collapse evolution of a coastal caldera system: Insights from a 3D multichannel seismic survey from the Campi Flegrei caldera (Italy). Journal of Volcanology and Geothermal Research 349, 83–98.
Stern, R.J., 2018. The evolution of plate tectonics. Philosophical Transactions of the Royal Society a: Mathematical, Physical and Engineering Sciences 376 (2132), 20170406. https://doi.org/10.1098/rsta.2017.0406.
Stiller, J.W., Schreiber, J., Yue, J., Guo, H., Ding, Q., Huang, J., 2014. The evolution of photosynthesis in chromist algae through serial endosymbioses. Nature Communications 5, 5764. https://doi.org/10.1038/ncomms6764.
Strassert, J.F.H., Irisarri, I., Williams, T.A., Burki, F., 2021. A molecular timescale for eukaryote evolution with implications for the origin of red algal-derived plastids. Nature Communications 12, 1879. https://doi.org/10.1038/s41467-021-22044-z.
Strother, P.K., Brasier, M.D., Wacey, D., Timpe, L., Saunders, M., Wellman, C.H., 2021. A possible billion-year-old holozoan with differentiated multicellularity. Current Biology 31, 2658–2665.e2. https://doi.org/10.1016/j.cub.2021.03.051.
Strother, P.K., Wellman, C.H., 2021. The Nonesuch Formation Lagerstätte: a rare window into freshwater life one billion years ago. Journal of the Geological Society 178. https://doi.org/10.1144/jgs2020-133 jgs2020-133.
Stüeken, E.E., Buick, R., 2018. Environmental control on microbial diversification and methane production in the Mesoarchean. Precambrian Research 304, 64–72, 10.1016/j.precamres.2017.11.003. Doi: 10.1016/j.earscirev.2016.07.007.
Stüeken, E.E., Kipp, M.A., Koehler, M.C., Buick, R., 2016. The evolution of Earth's biogeochemical nitrogen cycle. Earth Science Reviews 160, 220–239.
Stüeken, E.E., Som, S.M., Claire, M., Rugheimer, S., Scherf, M., Sproß, L., Tsoi, N., Ueno, Y., Lammer, H., 2020. Mission to planet Earth: the first two billion years. Space Science Reviews 216, 1–37. https://doi.org/10.1007/s11214-020-00652-3.
Stüeken, E.E., Kuznetsov, A.B., Vasilyeva, I.M., Krupenin, M.T., Bekker, A., 2021. Transient deep-water oxygenation recorded by rare Mesoproterozoic phosphorites. South Urals. Precambrian Research 360, 106242. https://doi.org/10.1016/j.precamres.2021.106242.
Sugitani, K., 2009. Palynology of Archean microfossils (c.3.0 Ga) from the Mount Grant area, Pilbara Craton, Western Australia: further evidence of biogenicity. Precambrian Research 173, 60–69. https://doi.org/10.1016/j.precamres.2009.02.003.
Sugitani, K., Mimura, K., and Walter, M. R. (2011). Farrel Quartzite microfossils in the Goldsworthy Greenstone Belt, Pilbara Craton, Western Australia: additional evidence for a diverse and evolved biota on the Archean Earth. Stromatolites: Interaction of microbes with sediments, 115-132. DOI: 10.1007/978-94-007-0397-1_6.
Sugitani, K., Mimura, K., Suzuki, K., Nagamine, K., Sugisaki, R., 2003. Stratigraphy and sedimentary petrology of an Archean volcanic–sedimentary succession at Mt. Goldsworthy in the Pilbara Block, Western Australia: implications of evaporite (nahcolite) and barite deposition. Precambrian Research 120, 55–79. https://doi.org/10.1016/S0301-9268(02)00145-6.
Sugitani, K., Grey, K., Allwood, A., Nagaoka, T., Mimura, K., Minami, M., Marchall, C., van Kanendonk, M., Walter, M.R., 2007. Diverse microstructures from Archaean chert from the Mount Goldsworthy-Mount Grant area, Pilbara Craton, Western Australia: microfossils, dubiofossils, or pseudofossils? Precambrian Research 158, 228–262. https://doi.org/10.1016/j.precamres.2007.03.006.
Sugitani, K., Grey, K., Nagaoka, T., Mimura, K., 2009. Three-dimensional morphological and textural complexity of Archean putative microfossils from the northeastern Pilbara Craton: indications of biogenicity of large (> 15 μ m) spheroidal and spindle-like structures. Astrobiology 9, 603–615. https://doi.org/10.1089/ast.2008.0268.
Sugitani, K., Mimura, K., Takeuchi, M., Lepot, K., Ito, S., Javaux, E.J., 2015. Early evolution of large micro-organisms with cytological complexity revealed by microanalyses of 3.4 Ga organic-walled microfossils. Geobiology 13, 507–521. https://doi.org/10.1111/gbi.1214.
Sugitani, K., Kohama, T., Mimura, K., Takeuchi, M., Senda, R., Morimoto, H., 2018. Speciation of paleoarchean life demonstrated by analysis of the morphological variation of lenticular microfossils from the Pilbara Craton, Australia. Astrobiology 18, 1057–1070. https://doi.org/10.1089/ast.2017.1799.
Sugitani, K. (2019). Early Archean (Pre-3.0 Ga) cellularly preserved microfossils and microfossil-like structures from the Pilbara Craton, Western Australia—a review. Earth's oldest rocks, 1007-1028. ISBN: 9780444639011.
Summons, R.E., Lincoln, S.A., 2012. Biomarkers: informative molecules for studies in geobiology. Fundamentals of Geobiology 269–296. https://doi.org/10.1002/9781118280874.ch15.
Summons, R.E., Amend, J.P., Bish, D., Buick, R., Cody, G.D., Des Marais, D.J., Dromart, G., Eigenbrod, J.L., Knoll, A.H., Sumner, D.Y., 2011. Preservation of Martian organic and environmental records: final report of the Mars Biosignature Working Group. Astrobiology 11, 157–181. https://doi.org/10.1089/ast.2010.0506.
Sumner, D.Y., 2000. Microbial vs environmental influences on the morphology of Late Archean fenestrate microbialites. In: Riding, R.E., Awramik, S.M. (Eds.), Microbial Sediments. Springer, Berlin Heidelberg, pp. 307–314. https://doi.org/10.1007/978-3-662-04036-2_33.
Tang, Q., Pang, K., Yuan, X., Wan, B., Xiao, S., 2015. Organic-walled microfossils from the Tonian Gouhou Formation, Huaibei region, North China Craton, and their biostratigraphic implications. Precambrian Research 266, 296–318. https://doi.org/10.1016/j.precamres.2015.05.025.
Tang, Q., Pang, K., Yuan, X., Xiao, S., 2020. A one-billion-year-old multicellular chlorophyte. Nature Ecology & Evolution 4, 543–549. https://doi.org/10.1038/s41559-020-1122-9.
Tang, Q., Pang, K., Li, G., Chen, L., Yuan, X., Sharma, M., Xiao, S., 2021. The Proterozoic macrofossil *Tawuia* as a coenocytic eukaryote and a possible macroalga. Palaeoecology Palaeoclimatology Palaeoecology 576, 110485. https://doi.org/10.1016/j.palaeo.2021.110485.
Tartèse, R., Chaussidon, M., Gurenko, A., Delarue, F., Robert, F., 2017. Warm Archean oceans reconstructed from oxygen isotope composition of early-life remnants. Geochemistry Perspectives Letters 3, 55–65. https://doi.org/10.7185/geochemlet.1706.
Tehrany, M.G., Lammer, H., Selsis, F., Ribas, I., Guinan, E.F., Hanslmeier, A., 2002. The particle and radiation environment of the early Sun. In *Solar Variability: From Core to Outer*. Frontiers Vol. 506, 209–212. http://adsabs.harvard.edu/full/2002ESASP.506.209T.
Templeton, A., Benzerara, K., 2015. Emerging frontiers in geomicrobiology. Elements 11, 423–429.
Tice, M.M., 2009. Environmental controls on photosynthetic microbial mat distribution and morphogenesis on a 3.42 Ga clastic-starved platform. Astrobiology 9, 989–1000. https://doi.org/10.1089/ast.2008.0330.
Tice, M.M., Lowe, D.R., 2004. Photosynthetic microbial mats in the 3,416-Myr-old ocean. Nature 431, 549–552. https://doi.org/10.1038/nature02888.
Tingle, K.E., Porter, S.M., Raven, M.R., Czaja, A.D., Webb, S.M., Bloeser, B., 2023. Organic preservation of vase-shaped microfossils from the late Tonian Chuar Group, Grand Canyon, Arizona, USA. Geobiology 21, 290–309. https://doi.org/10.1111/gbi.12544.
Tostevin, R., Clarkson, M.O., Gangl, S., Shields, G.A., Wood, R.A., Bowyer, F., Penny, A. M., Stirling, C.H., 2018. Uranium isotope evidence for an expansion of anoxia in terminal Ediacaran oceans. Earth and Planetary Science Letters 506, 104–112. https://doi.org/10.1016/j.epsl.2018.10.045.

Trower, E.J.T., Lowe, D.R., Zentner, D., Fischer, W.W., 2014. Primary silica granules-A new mode of Paleoarchean sedimentation. Geology 42, 283e286. https://doi.org/10.1130/G35187.1.

Trower, E.J., Lowe, D.R., 2016. Sedimentology of the~ 3.3 Ga upper Mendon Formation, Barberton Greenstone Belt. South Africa. Precambrian Research 281, 473–494. https://doi.org/10.1016/j.precamres.2016.06.003.

Turk, K.A., Maloney, K.M., Laflamme, M., Darroch, S.A.F., 2022. Paleontology and ichnology of the late Ediacaran Nasep-Huns transition (Nama Group, southern Namibia). Journal of Paleontology 96, 753–769. https://doi.org/10.1017/jpa.2022.31.

Ueno, Y., Yamada, K., Yoshida, N., Maruyama, S., Isozaki, Y., 2006. Evidence from fluid inclusions for microbial methanogenesis in the early Archaean era. Nature 440, 516–519. https://doi.org/10.1038/nature04584.

Ueno, Y., Ono, S., Rumble, D., Maruyama, S., 2008. Quadruple sulfur isotope analysis of ca. 3.5 Ga Dresser Formation: New evidence for microbial sulfate reduction in the early Archean. Geochimica et Cosmochimica Acta 72, 5675–5691. https://doi.org/10.1016/j.gca.2008.08.026.

Van den Boorn, S.H.J.M., Van Bergen, M.J., Vroon, P.Z., De Vries, S.T., Nijman, W., 2010. Silicon isotope and trace element constraints on the origin of~ 3.5 Ga cherts: implications for Early Archaean marine environments. Geochimica et Cosmochimica Acta 74, 1077–1103. https://doi.org/10.1016/j.gca.2009.09.009.

Van Kranendonk, M.J., 2010. Two types of Archean continental crust: Plume and plate tectonics on early Earth. American Journal of Science 310, 1187–1209. https://doi.org/10.2475/10.2010.01.

Van Kranendonk, M. J., Djokic, T., Poole, G., Tadbiri, S., Steller, L., and Baumgartner, R. (2018). Depositional setting of the fossiliferous, c. 3480 Ma Dresser Formation, Pilbara Craton: A review. Earth's Oldest Rocks (2nd edition): Amsterdam, Elsevier, 985-1006. DOI: 10.1016/B978-0-444-63901-1.00040-X.

van Kranendonk, M.J., Pirajno, F., 2004. Geochemistry of metabasalts and hydrothermal alteration zones associated with c. 3450 Ga chert and barite deposits: implications for the geological setting of the Warrawoona Group, Pilbara Craton. Australia. Geochemistry Exploration and Environmental Analysis 4, 253–278. https://doi.org/10.1144/1467-7873/04-205.

Van Kranendonk, M.J., Baumgartner, R., Djokic, T., Ota, T., Steller, L., Garbe, U., Nakamura, E., 2021. Elements for the origin of life on land: A deep-time perspective from the Pilbara Craton of Western Australia. Astrobiology 21, 39–59. https://doi.org/10.1089/ast.2019.2107.

van Zuilen, M.A., Lepland, A., Arhenius, G., 2002. Reassessing the Evidence for the Earliest Traces of Life. Nature 418, 627–630.

Vinn, O., Zatoń, M., 2012. Inconsistencies in proposed annelid affinities of early biominera-lized organism Cloudina (Ediacaran): structural and ontogenetic evidences. Carnets De Géologie [note-Books on Geology] CG2012_A03, 39–47.

Visscher, P.T., Stolz, J.F., 2005. Microbial mats as bioreactors: populations, processes, and products. In: Geobiology: Objectives, Concepts, Perspectives. Elsevier, pp. 87–100.

Vorobeva, N.G., Sergeev, V.N., Petrov, P., Yu, 2015. Kotuikan Formation assemblage: A diverse organic-walled microbiotain the Mesoproterozoic Anabar succession, northern Siberia. Precambrian Research 256, 201–222.

Wacey, D., 2009. Early life on earth: a practical guide. Springer, Netherlands, Dordrecht, 10.1007/978-1-4020-9389-0.

Wacey, D., Kilburn, M.R., Saunders, M., Cliff, J., Brasier, M.D., 2011. Microfossils of sulphur-metabolizing cells in 3.4-billion-year-old rocks of Western Australia. Nature Geoscience 4, 698–702.

Wacey, D., Noffke, N., Saunders, M., Guagliardo, P., Pyle, D.M., 2018. Volcanogenic pseudo-fossils from the~ 3.48 Ga dresser formation, Pilbara. Western Australia. Astrobiology 18, 539–555. https://doi.org/10.1089/ast.2017.1734.

Walsh, M.W., 1992. Microfossils and possible microfossils from the early Archean Onverwacht Group, Barberton Mountain Land, South Africa. Precambrian Research 54, 271–293. https://doi.org/10.1016/0301-9268(92)90074-x.

Walsh MM, Lowe DR (1999) Modes of accumulation of carbonaceous matter in the early Archean: a petrographic and geochemical study of the carbonaceous cherts of the Swaziland Supergroup. In: Lowe DR, Byerly GR (eds) Geological evolution of the Barberton Greenstone Belt, South Africa, vol 329. Geological Society of America, Special Publications, pp 115–132. Doi: 10.1130/0-8137-2329-9.115.

Walter, M.R., Du, R., Horodyski, R.J., 1990. Coiled carbonaceous megafossils from the middle Proterozoic of Jixian (Tianjin) and Montana. American Journal of Science 290-A, 133–148.

Wan, B., Yuan, X., Chen, Z., Guan, C., Pang, K., Tang, Q., Xiao, S., 2016. Systematic description of putative animal fossils from the early Ediacaran Lantian Formation of South China. Palaeontology 59. https://doi.org/10.1111/pala.12242.

Wan, B., Chen, Z., Yuan, X., Pang, K., Tang, Q., Guan, C., Wang, X., Pandey, S.K., Droser, M.L., Xiao, S., 2020. A tale of three taphonomic modes: the Ediacaran fossil *Flabellophyton* preserved in limestone, black shale, and sandstone. Gondwana Research 84, 296–314. https://doi.org/10.1016/j.gr.2020.04.003.

Wang, X., Liu, A.G., Chen, Z., Wu, C., Liu, Y., Wan, B., Pang, K., Zhou, C., Yuan, X., Xiao, S., 2024. A late Ediacaran crown-group sponge animal. Nature 630, 905–911. https://doi.org/10.1038/s41586-024-07520-y.

Wang, R., Yin, Z., Shen, B., 2023. A late Ediacaran ice age: The key node in the Earth system evolution. Earth-Science Reviews 247, 104610. https://doi.org/10.1016/j.earscirev.2023.104610.

Westall, F. and Cavalazzi, B. (2011). Biosignatures in rocks. Encyclopedia of Geobiology (Eds.) V. Thiel, J. Reitner, Springer, Berlin, 189-201. Doi: 10.1007/978-1-4020-9212-1_36.

Westall, F. and Hickman-Lewis, K. (2018). Fossilisation of bacteria and implications for the search for early life on Earth and astrobiology missions to Mars. In Handbook of Astrobiology (Ed. Kolb, V.). CSC Press, pp. 609–631. Doi: 10.1201/b22230.

Westall, F., Campbell, K.A., Bréhéret, J.G., Foucher, F., Gautret, P., Hubert, A., Sorieul, S., Grassineau, N., Guido, D.M., 2015a. Archean (3.33 Ga) microbe-sediment systems were diverse and flourished in a hydrothermal context. Geology 43, 615–618. https://doi.org/10.1130/G36646.1.

Westall, F., Brack, A., Fairén, A.G., Schulte, M.D., 2023a. Setting the geological scene for the origin of life and continuing open questions about its emergence. Frontiers in Astronomy and Space Science 9, 1095701. https://doi.org/10.3389/fspas.2022.1095701.

Westall, F., Purvis, G., Sano N., Sherrif, J., Clodoré, L., Foucher, F., Milojevic, T., The frequency of (elusive) life in the Universe. In review.

Westall, F., Folk, R.L., 2003. Exogenous carbonaceous microstructures in Early Archaean cherts and BIFs from the Isua greenstone belt: Implications for the search for life in ancient rocks. Precambrian Research 126, 313–330. https://doi.org/10.1016/S0301-9268(03)00102-5.

Westall, F., de Ronde, C.E.J., Southam, G., Grassineau, N., Colas, M., Cockell, C., Lammer, H., 2006. Implications of a 3.472-3.333 Ga-old subaerial microbial mat from the Barberton greenstone belt, South Africa for the UV environmental conditions on the early Earth. Philosophical Transactions of the Royal Society of London Series b. 361, 1857–1875. https://doi.org/10.1098/rstb.2006.1896.

Westall, F., Cavalazzi, B., Lemelle, L., Marrocchi, Y., Rouzaud, J.N., Simionovici, A., Salomé, M., Mostefaoui, S., Andreazza, C., Foucher, F., Toporski, J., Jauss, A., Thiel, V., Southam, G., MacLean, L., Wirick, S., Hofmann, A., Meibom, A., Robert, F., Défarge, C., 2011a. Implications of in situ calcification for photosynthesis in a ~3.3 Ga-old microbial biofilm from the Barberton greenstone belt. South Africa. Earth Planet. Sci. Lett. 310, 468–479. https://doi.org/10.1016/j.epsl.2011.08.029.

Westall, F., Foucher, F., Cavalazzi, B., de Vries, S.T., Nijman, W., Pearson, V., Verchovsky, A., Wright, I., Rouzaud, J.-N., Marchesini, D., Anne, S., 2011b. Volcaniclastic habitats for early life on Earth and Mars: a case study from~ 3.5 Ga-old rocks from the Pilbara, Australia. Planetary and Space Science 59 (10), 1093–1106. https://doi.org/10.1016/j.pss.2010.09.006.

Westall, F., Foucher, F., Bost, N., Bertrand, M., Loizeau, D., Vago, J.L., Kminek, G., Gaboyer, F., Campbell, K.A., Bréhéret, J.-B., Gautret, P., Cockell, C.S., 2015b. Biosignatures on Mars: what, where and how? Implications for the search for Martian life. Astrobiology 15, 998–1029. https://doi.org/10.1017/S1473550421000264.

Westall, F., Hickman-Lewis, K., Hinman, N., Gautret, P., Campbell, K.A., Bréhéret, J.-G., Foucher, F., Hubert, A., Sorieul, S., Kee, T.P., Dass, A.V., Georgelin, T., Brack, A., 2018. A hydrothermal-sedimentary context for the origin for life. Astrobiology 18, 259–293. https://doi.org/10.1089/ast.2017.1680.

Westall, F., Höning, D., Avice, G., Gentry, D., Gerya, T., Gillmann, C., Izenberg, N., Way, M.J., Wilson, C., 2023b. The habitability of Venus. Space Science Reviews 219, 17. https://doi.org/10.1007/s11214-023-00960-4.

Westall, F., de Vries, S.T., Nijman, W., Rouchon, V., Orberger, B. Pearson, V., Watson, J., Verchovsky, A., Wright, I., Rouzaud, J.-N., Marchesini, D., and Anne, S. (2006b). The 3.466 Ga Kitty's Gap Chert, an Early Archaean microbial ecosystem. In Processes on the Early Earth (W.U. Reimold & R. Gibson, Eds.), Geological Society of America Spececial Publicaltion, 405, 105-131. Doi: 10.1130/2006.2405(07).

Wilde, S.A., Valley, J.W., Peck, W.H., Graham, C.M., 2001. Evidence from detrital zircons for the existence of continental crust and oceans on the Earth 4.4 Gyr ago. Nature 409, 175–178. https://doi.org/10.1038/35051550.

Wilmeth, D.T., Corsetti, F.A., Beukes, N.J., Awramik, S.A., Petryshyn, V., Spear, J.R., Celestian, A.J., 2019. Neoarchean (2.7 Ga) lacustrine stromatolite deposits in the Hartbeesfontein Basin, Ventersdorp Supergroup, South Africa: Implications for oxygen oases. Precambrian Research 320, 291–302. https://doi.org/10.1130/G49894.1.

Wilson, A.H., Groenwald, B., Palmer, C., 2013. Volcanic and volcaniclastic rocks of the Mesoarchaean Pongola Supergroup in South Africa and Swaziland: distribution, physical characteristics, stratigraphy and correlations. South African Journal of Geology 116, 119–168. https://doi.org/10.2113/gssajg.116.1.119.

Wilson, A.H., Versfeld, J.A., 1994. The early Archaean Nondweni greenstone belt, southern Kaapvaal Craton, South Africa, Part I. Stratigraphy, sedimentology, mineralization and depositional environment. Precambrian Research 67, 243–276.

Woese, C.R., Kandler, O., Wheelis, M.L., 1990. Towards a natural system of organisms: proposal for the domains Archaea, Bacteria, and Eucarya. Proceedings of the National Academy of Sciences, USA 87, 4576–4579.

Wood, R., Liu, A.G., Bowyer, F., Wilby, P.R., Dunn, F.S., Kenchington, C.G., Hoyal Cuthill, J.F., Mitchell, E.G., Penny, A., 2019. Integrated records of environmental change and evolution challenge the Cambrian Explosion. Nature Ecology & Evolution 3, 528–538. https://doi.org/10.1038/s41559-019-0821-6.

Xiao, S., 2013. Written in stone: The fossil record of early eukaryotes. In: Trueba, G., Montúfar, C. (Eds.), Evolution from the Galapagos: Social and Ecological Interactions in the Gapalagos Islands 2. Springer, New York, pp. 107–124.

Xiao, S., 2022. Extinctions, morphological gaps, major transitions, stem groups, and the origin of major clades, with a focus on early animals. Acta Geologica Sinica 96, 1821–1829. https://doi.org/10.1111/1755-6724.15027.

Xiao, S., Dong, L., 2006. On the morphological and ecological history of Proterozoic macroalgae. In: Xiao, S., Kaufman, A.J. (Eds.), Neoproterozoic Geobiology and Paleobiology. Springer, Dordrecht, the Netherlands, pp. 57–90.

Xiao, S., Knoll, A.H., Kaufman, A.J., Yin, L., Zhang, Y., 1997. Neoproterozoic fossils in Mesoproterozoic rocks? Chemostratigraphic resolution of a biostratigraphic conundrum from the North China Platform. Precambrian Research 84, 197–220. https://doi.org/10.1016/S0301-9268(97)00029-6.

Xiao, S., Zhang, Y., Knoll, A.H., 1998. Three-dimensional preservation of algae and animal embryos in a Neoproterozoic phosphorite. Nature 391, 553–558.

Xiao, S., Knoll, A.H., Yuan, X., Pueschel, C.M., 2004. Phosphatized multicellular algae in the Neoproterozoic Doushantuo Formation, China, and the early evolution of florideophyte red algae. American Journal of Botany 91, 214–227.
Xiao, S., Laflamme, M., 2009. On the eve of animal radiation: Phylogeny, ecology and evolution of the Ediacara biota. Trends in Ecology & Evolution 24, 31–40.
Xiao, S., Narbonne, G.M., 2020. The Ediacaran Period. In: Gradstein, F.M., Ogg, J.G., Schmitz, M.D., Ogg, G.M. (Eds.), Geologic Time Scale 2020 (volume 1). Elsevier, Oxford, pp. 521–561.
Xiao, S., Zhou, C., Liu, P., Wang, D., Yuan, X., 2014a. Phosphatized acanthomorphic acritarchs and related microfossils from the Ediacaran Doushantuo Formation at Weng'an (South China) and their implications for biostratigraphic correlation. Journal of Paleontology 88, 1–67. https://doi.org/10.1666/12-157R.
Xiao, S., Muscente, A.D., Chen, L., Zhou, C., Schiffbauer, J.D., Wood, A.D., Polys, N.F., Yuan, X., 2014b. The Weng'an biota and the Ediacaran radiation of multicellular eukaryotes. National Science Review 1, 498–520. https://doi.org/10.1093/nsr/nwu061.
Xiao, S., Tang, Q., Hughes, N.C., McKenzie, N.R., Myrow, P.M., 2016. Biostratigraphic and detrital zircon age constraints on the basement of the Himalayan Foreland Basin: Implications for a Proterozoic link to the Lesser Himalaya and cratonic India. Terra Nova 28, 419–426. https://doi.org/10.1111/ter.12235.
Xiao, S., Chen, Z., Zhou, C., Yuan, X., 2019. Surfing in and on microbial mats: Oxygen-related behavior of a terminal Ediacaran bilaterian animal. Geology 47, 1054–1058. https://doi.org/10.1130/G46474.1.
Xiao, S., Gehling, J.G., Evans, S.D., Hughes, I.V., Droser, M.L., 2020. Probable benthic macroalgae from the Ediacara Member. South Australia. Precambrian Research 350, 105903. https://doi.org/10.1016/j.precamres.2020.105903.
Xiao, S., Chen, Z., Pang, K., Zhou, C., Yuan, X., 2021. The Shibantan Lagerstätte: Insights into the Proterozoic-Phanerozoic transition. Journal of the Geological Society of London 178. https://doi.org/10.1144/jgs2020-135 jgs2020-135.
Xiao, S., Jiang, G., Ye, Q., Ouyang, Q., Banerjee, D.M., Singh, B.P., Muscente, A.D., Zhou, C., Hughes, N.C., 2022. Systematic paleontology, acritarch biostratigraphy, and $\delta^{13}C$ chemostratigraphy of the early Ediacaran Krol A Formation, Lesser Himalaya, northern India. Journal of Paleontology 97. https://doi.org/10.1017/jpa.2022.7.
Xu, D., Qin, Z., Wang, X., Li, J., Shi, X., Tang, D., Liu, J., 2023. Extensive sea-floor oxygenation during the early Mesoproterozoic. Geochimica et Cosmochimica Acta 354, 186–196.
Yan, Y., 1982. *Scizofusa* from the Chuanlinggou Formation of Changcheng System in Jixian County. Bulletin of the Tianjin Institute of Geology and Mineral Resources 6, 1–7.
Yan, Y., 1985. Preliminary research on microflora from Chuanlinggou Formation of Changcheng System in Jixian County. Bulletin of Tianjin Institute of Geology and Mineral Resources 12, 137–168.
Yan, Y., 1989. Shale-facies algal filaments from Chuanlinggou Formation in Jixian County. Bulletin of the Tianjin Institute of Geology and Mineral Resources 21, 149–162.
Yan, Y., 1995a. Shale facies microfloras from lower Changcheng System in Kuancheng, Hebei, and comparison with those of neighboring areas. Acta Micropalaeontologica Sinica 12, 349–373.
Yan, Y., 1995b. Discovery and preliminary study of megascopic algae (1700 Ma) from the Tuanshanzi Formation in Jixian, China. Acta Micropalaeontologica Sinica 12, 107–126.
Yan, Y., Liu, Z., 1993. Significance of eucaryotic organisms in the microfossil flora of the Changcheng System. Acta Micropalaeontologica Sinica 10, 167–180.
Yan, Y., Liu, Z., 1997. Tuanshanzian macroscopic algae of 1700 Ma b. p. from Changcheng System of Jixian, China. Acta Palaeontologica Sinica 36, 18–41.
Yang, B., Steiner, M., Schiffbauer, J.D., Selly, T., Wu, X., Zhang, C., Liu, P., 2020. Ultrastructure of Ediacaran cloudinids suggests diverse taphonomic histories and affinities with non-biomineralized annelids. Scientific Reports 10, 535. https://doi.org/10.1038/s41598-019-56317-x.
Ye, Q., Tong, J., Xiao, S., Zhu, S., An, Z., Tian, L., Hu, J., 2015. The survival of benthic macroscopic phototrophs on a Neoproterozoic snowball Earth. Geology 43, 507–510. https://doi.org/10.1130/G36640.1.
Yin, L., 1997. Acanthomorphic acritarchs from Meso-Neoproterozoic shales of the Ruyang Group, Shanxi, China. Review of Palaeobotany and Palynology 98, 15–25. https://doi.org/10.1016/S0034-6667(97)00022-5.
Yin, L., Yuan, X., Meng, F., Hu, J., 2005. Protists of the Upper Mesoproterozoic Ruyang Group in Shanxi Province, China. Precambrian Research 141, 49–66. https://doi.org/10.1016/j.precamres.2005.08.001.
Yin, L., Zhu, M., Knoll, A.H., Yuan, X., Zhang, J., Hu, J., 2007. Doushantuo embryos preserved inside diapause egg cysts. Nature 446, 661–663.
Yin, L., Meng, F., Kong, F., Niu, C., 2020. Microfossils from the Paleoproterozoic Hutuo Group, Shanxi, North China: Early evidence for eukaryotic metabolism. Precambrian Research 342, 105650. https://doi.org/10.1016/j.precamres.2020.105650.
Yirgu, G., Ferguson, D.J., Barnie, T.D., Oppenheimer, C., 2014. Recent volcanic eruptions in the Afar rift, northeastern Africa, and implications for volcanic risk management in the region. Extreme natural hazards, disaster risks and societal implications. Cambridge University Press, Cambridge, pp. 200–213.
Yuan, X., Chen, Z., Xiao, S., Zhou, C., Hua, H., 2011. An early Ediacaran assemblage of macroscopic and morphologically differentiated eukaryotes. Nature 470, 389–392. https://doi.org/10.1038/nature09810.
Yuan, X., Wan, B., Guan, C., Chen, Z., Zhou, C., Xiao, S., Wang, W., Pang, K., Tang, Q., Hua, H., 2016. The Lantian Biota. Shanghai Science and Technology Press, Shanghai.
Zahnle, K.J., 2006. Earth's earliest atmosphere. Elements 2, 217–222. https://doi.org/10.2113/gselements.2.4.217.
Zahnle, K.J., Lupu, R., Dobrovolskis, A., Sleep, N.H., 2015. The tethered moon. Earth Planetary Science Letters 427, 74–82. https://doi.org/10.1016/j.epsl.2015.06.058.
Zawaski, M.J., Kelly, N.M., Orlandini, O.F., Nichols, C.I., Allwood, A.C., Mojzsis, S.J., 2020. Reappraisal of purported ca. 3.7 Ga stromatolites from the Isua Supracrustal Belt (West Greenland) from detailed chemical and structural analysis. Earth and Planetary Science Letters 545, 116409. https://doi.org/10.1016/j.epsl.2020.116409.
Zhang, F., Xiao, S., Kendall, B., Romaniello, S.J., Cui, H., Meyer, M., Gilleaudeau, G.J., Kaufman, A.J., Anbar, A.D., 2018. Extensive marine anoxia during the terminal Ediacaran Period. Science Advances 4. https://doi.org/10.1126/sciadv.aan8983.
Zhou, C., Xie, G., McFadden, K., Xiao, S., Yuan, X., 2007. The diversification and extinction of Doushantuo-Pertatataka acritarchs in South China: Causes and biostratigraphic significance. Geological Journal 42, 229–262.
Zhu, S., Chen, H., 1995. Megascopic multicellular organisms from the 1700-million-year-old Tuanshanzi Formation in the Jixian area, North China. Science 270, 620–622.
Zhu, M., Gehling, J.G., Xiao, S., Zhao, Y.-L., Droser, M., 2008. Eight-armed Ediacara fossil preserved in contrasting taphonomic windows from China and Australia. Geology 36, 867–870.
Zhu, S., Sun, S., Huang, X., He, Y., Zhu, G., Sun, L., Zhang, K., 2000. Discovery of carbonaceous compressions and their multicellular tissues from the Changzhougou Formation (1800 Ma) in the Yanshan Range, North China. Chinese Science Bulletin 45, 841–846.
Zhu, T.F., Szostak, J.W., 2009. Coupled growth and division of model protocell membranes. Journal of the American Chemical Society 131, 5705–5713. https://doi.org/10.1021/ja900919c.
Zhu, M., Zhuravlev, A.Y., Wood, R.A., Zhao, F., Sukhov, S.S., 2017. A deep root for the Cambrian Explosion: Implications of new bio- and chemostratigraphy from the Siberian Platform. Geology 45, 459–462. https://doi.org/10.1130/G38865.1.
Zhuravlev, A., Yu, Wood, R.A., Penny, A.M., 2015. Ediacaran skeletal metazoan interpreted as a lophophorate. Proceedings of the Royal Society B (biological Sciences) 282, 20151860. https://doi.org/10.1098/rspb.2015.1860.